COMMUNICATION-BASED ADAPTIVE OVERCURRENT PROTECTION FOR DISTRIBUTION SYSTEMS WITH DISTRIBUTED GENERATORS

by

Mohamad Sulaiman

A Thesis Presented to the Faculty of the

American University of Sharjah

College of Engineering

in Partial Fulfillment

of the Requirements

for the Degree of

Master of Science in

Electrical Engineering

Sharjah, United Arab Emirates

May 2012

Approval Signatures

We, the undersigned, approve the Master's Thesis of Mohamad Sulaiman.

Thesis Title: Communication-Based Adaptive Overcurrent Protection for Distribution Systems with Distributed Generators

Signature	Date of Signature
____________________________	________________
Dr. Ahmed Osman-Ahmed Associate Professor Department of Electrical Engineering Thesis Advisor	
____________________________	________________
Dr. Mohamed Hassan Associate Professor Department of Electrical Engineering Thesis Co-Advisor	
____________________________	________________
Dr. Ayman El-Hag Associate Professor Department of Electrical Engineering Thesis Committee Member	
____________________________	________________
Dr. Abdulrahman Al-Ali Professor Department of Computer Science & Engineering Thesis Committee Member	
____________________________	________________
Dr. Mohamed El-Tarhuni Head, Department of Electrical Engineering	
____________________________	________________
Dr. Hany El Kadi Associate Dean, College of Engineering	
____________________________	________________
Dr. Yousef Al-Assaf Dean of College of Engineering	
____________________________	________________
Dr Khaled Assaleh Director of Graduate Studies	

Acknowledgments

First of all, thanks to Allah for guiding me throughout my master thesis journey. It is with immense gratitude that I acknowledge my thesis advisors Dr. Ahmed Osman and Dr. Mohamed Hassan, who showed me continuous guidance and support throughout this work. I consider myself grateful to have such advisors who patiently helped me while working on this thesis. Also, I would like to thank my examiners Dr. Ayman El-Hag and Dr. Abdulrahman Al-Ali, who guided me to supplement the thesis. Finally, I express my deepest gratitude to my parents, brothers, and sisters for their nonstop support during my master studies.

To my parents, brothers, and sisters for

their love and faith in me

Abstract

Traditional distribution systems are designed with a radial structure. As a result, their protection systems are designed and set based on one utility source feeding the whole system. Nowadays, Distributed Generators (DG) are increasingly connected to distribution systems to meet the load demand and increase the reliability of the system. With the additionally connected sources, the system is no longer radial. Moreover, during a fault condition, the fault is fed from all the sources connected to the power system. Therefore, the fault current level is different compared with the radial system. The DGs affect the operation of the protection relays in distribution feeders as they reduce the reach of the relays. This is due to the fact that DGs increase the equivalent impedance of the feeder which decreases the fault current. Furthermore, protective relays on the main feeder must see fault currents in forward or reverse directions, and they have to detect the fault direction. Another important problem is that DGs can get disconnected from the grid due to disturbances or for maintenance. Consequently, a new configuration for the system results and, if a fault occurs, a different fault current level flows. Therefore, one setting for the protective relays cannot respond to the continuously changing system configuration. Thus, relays have to be adaptively coordinated for each new system configuration to achieve correct fault clearance operation.

In this thesis, a communication-based adaptive protection system is proposed. The proposed system operates during islanding and normal connection operation modes. Linear optimization is used for overcurrent relay setting. DNP3 communication protocol is chosen to facilitate the communication between the various devices in the adaptive protection system. Centralized and decentralized adaptive protection schemes are investigated. In each scheme, two simultaneous algorithms are executed. The first algorithm works when the system configuration is changed due to the disconnection or reconnection of a DG. While the other algorithm operates when faults are detected to speed up fault clearance. A backup scheme is developed to operate in case of communication failure between the various devices in the adaptive protection system. The proposed schemes are tested for different types of faults, different system configurations, and during communication failure. The obtained results show that the proposed adaptive overcurrent protection system is able to respond to system changes accordingly to ensure reliable protection operation and fast response during fault occurrences.

Search Terms: Adaptive Protection, Overcurrent Relays, Distributed Generators, Relay Communication

Table of Contents

Abstract **6**

List of Figures **10**

List of Tables **12**

Abbreviations **13**

1 Introduction **15**

1.1 Protection in Power Distribution Systems 17
1.2 Types of Protection Systems 18
1.2.1 Fuses 18
1.2.2 Protective Relays 18
1.2.2.1 Differential Relays 19
1.2.2.2 Distance Relays 20
1.2.2.3 Overcurrent Relays 20
1.2.3 Conventional Overcurrent Relay Coordination 22
1.2.4 Overcurrent Relay Coordination Using Linear and Nonlinear Optimization 23
1.3 Problem Statement 24
1.4 Thesis Objectives and Contribution 25
1.5 Thesis Outline 26

2 Literature Review **27**

2.1 Non-communication Based ADPS 27
2.2 Communication-based ADPS 31
2.3 Multi-Agent Systems 34

3 Proposed Adaptive Protection System **39**

3.1 Communication Network 39
3.1.1 DNP3 40
3.1.2 Fiber Optic Communication 41
3.2 Proposed Adaptive Protection Strategy 42
3.2.1 Centralized Adaptive Protection System (CAPS) 42
3.2.2 Decentralized Adaptive Protection System (DAPS) 45
3.2.2.1 Proposed MAS 45
3.2.2.2 Operation of the Proposed DAPS 47
3.3 Backup Adaptive Protection System 48
3.4 Differences Between The Proposed Work and Existing Solutions 50

4 Results 52
4.1 System Model . . . 52
4.2 Communication Time Delay . . . 56
4.2.1 Centralized Adaptive Protection System (CAPS) . . . 56
4.2.2 Decentralized Adaptive Protection System (DAPS) . . . 59
4.2.3 DNP3 Processing Time . . . 60
4.2.4 Internet Communication Delay . . . 60
4.3 Simulation of the Proposed Adaptive Protection Systems . . . 61
4.3.1 Centralized Adaptive Protection System (CAPS) . . . 62
4.3.1.1 CHP Plant is Disconnected from the Power Distribution System . . . 62
4.3.1.2 SLG Fault at Line 8-9 with CHP Disconnected . . . 63
4.3.1.3 SLG Fault at Line 8-9 with All Generators Connected 64
4.3.1.4 LL Fault at Line 8-9 with All Generators Connected . 65
4.3.1.5 SLG Fault at Line 11-12 with All Generators Connected 67
4.3.1.6 DLG Fault at Line 8-9 with WTG1 Disconnected . . 68
4.3.1.7 DLG Fault at Line 11-12 with CHP Disconnected . . 70
4.3.1.8 SLG Fault at Line 8-9 with All WTGs Disconnected . 71
4.3.1.9 SLG Fault at Line 8-9 with TG Disconnected (Islanded Mode) . . . 71
4.3.1.10 SLG Fault at Line 11-12 with TG Disconnected (Islanded Mode) . . . 72
4.3.2 Decentralized Adaptive Protection System (DAPS) . . . 74
4.3.2.1 CHP Plant is Disconnected from the Power Distribution System . . . 75
4.3.2.2 SLG Fault at Line 8-9 with CHP Disconnected . . . 76
4.3.2.3 SLG Fault at Line 8-9 with All Generators Connected 77
4.3.2.4 LL Fault at Line 8-9 with All Generators Connected . 79
4.3.2.5 SLG Fault at Line 11-12 with All Generators Connected 79
4.3.2.6 DLG Fault at Line 8-9 with WTG1 Disconnected . . 80
4.3.2.7 DLG Fault at Line 11-12 with CHP Disconnected . . 82
4.3.2.8 SLG Fault at Line 8-9 with All WTGs Disconnected . 82
4.3.2.9 SLG Fault at Line 8-9 with TG Disconnected (Islanded Mode) . . . 83
4.3.2.10 SLG Fault at Line 11-12 with TG Disconnected (Islanded Mode) . . . 84
4.4 Backup Technique . . . 85

5 Conclusions and Future Work 89

References 91

A System Model in PSCAD 95

B Linear Optimization 97

C Negative Sequence Impedance Directional Element 99

Vita 101

List of Figures

1.1 Typical radial system. 15
1.2 Relay reach with and without a DG. 17
1.3 Typical time-current characteristic of a fuse. 18
1.4 Differential protection. 20
1.5 Simple Mho function. 21
1.6 Different types of TDS curves. 22
1.7 Relay coordination example. 22
1.8 Relay characteristic curves for different TDS values. 24

2.1 Typical ADPS hardware architecture. 28
2.2 Adaptive protection system using voltage and frequency measurement. . 29
2.3 Adaptive distance relay protection system. 30
2.4 Adaptive distance relay protection system. 31
2.5 Adaptive protection system when wind farms are connected to the power distribution system. 32
2.6 Adaptive PMU protection system. 33
2.7 Deliberative Agent. 36
2.8 Reactive Agent. 36
2.9 Hybrid Agent. 36
2.10 Structure of a relay agent. 37
2.11 Adaptive protection MAS architecture. 38

3.1 CAPS's communication topology. 43
3.2 CAPS's faulted section identification. 44
3.3 Flowchart of the CAPS. 45
3.4 DAPS's communication topology. 46
3.5 Proposed MAS. 46
3.6 DAPS's faulted section identification. 47
3.7 Flowchart of the DAPS. 48
3.8 Flowchart of the backup adaptive protection system. 49

4.1 System Model. 52
4.2 Transformer model. 54
4.3 Multiple run module. 55
4.4 Fault module. 55
4.5 RTP and COMTRADE recorder. 56
4.6 CAPS communication model. 58
4.7 DAPS communication model. 59
4.8 Disruption in intranet communication. 60
4.9 Internet communication network. 61

4.10 Fault current at relay R4 for a SLG fault on line 8-9 when all generators are connected. 66
4.11 Upstream and downstream TDS curves for a SLG fault on line 8-9 with all generators connected. 66
4.12 Fault current at relay R7 for a SLG fault on line 11-12 when all generators are connected. 69
4.13 Upstream and downstream TDS curves for a SLG fault on line 11-12 with all generators connected. 69
4.14 Downstream looking relays' TDS curves for a SLG fault at line 8-9 with all WTGs disconnected. 72
4.15 Upstream and downstream TDS curves for a SLG fault on line 8-9 with TG disconnected (islanded mode). 73
4.16 Upstream and downstream TDS curves for a SLG fault on line 11-12 with TG disconnected (islanded mode). 74
4.17 Upstream and downstream TDS curves for a SLG fault on line 8-9 with all generators connected. 78
4.18 Fault current for a SLG fault on line 8-9 when all generators are connected. 78
4.19 Upstream and downstream TDS curves for a SLG fault on line 11-12 with all generators connected. 81
4.20 Upstream and downstream TDS curves for a SLG fault on line 8-9 with TG disconnected (islanded mode). 84
4.21 Upstream and downstream TDS curves for a SLG fault at line 11-12 with TG disconnected (islanded mode). 86

A.1 PSCAD system model buses 5-8. 95
A.2 PSCAD system model buses 9-11. 95
A.3 PSCAD system model buses 12-14. 96
A.4 PSCAD WTG model 96
A.5 PSCAD CHP model 96

List of Tables

3.1 DNP3 processing delay. 40
3.2 DNP3 hardware specifications. 40

4.1 Transmission grid data. 53
4.2 Line data for the modeled system. 53
4.3 Generators data. 53
4.4 Load and generation data. 54
4.5 Transformer model data. 55
4.6 Fiber simulation parameters. 56
4.7 RTT delay calculation. 61
4.8 Centralized: CHP is disconnected. 63
4.9 Centralized: SLG fault at line 8-9 with CHP disconnected. 64
4.10 Centralized: SLG fault at line 8-9 with all generators connected. 65
4.11 Centralized: LL fault at line 8-9 with all generators connected. 67
4.12 Centralized: SLG fault at line 11-12 with all generators connected. . . . 68
4.13 Centralized: DLG fault at line 8-9 with WTG1 disconnected. 70
4.14 Centralized: DLG fault at line 11-12 with CHP disconnected. 70
4.15 Centralized: SLG fault at line 8-9 with all WTGs disconnected. 71
4.16 Centralized: SLG fault at line 8-9 with TG disconnected (islanded mode). 72
4.17 Centralized: SLG fault at line 11-12 with TG disconnected (islanded mode). 73
4.18 Decentralized: CHP is disconnected. 75
4.19 Decentralized: SLG fault at line 8-9 with CHP disconnected. 76
4.20 Decentralized: SLG fault at line 8-9 with all generators connected. . . . 77
4.21 Decentralized: LL fault at line 8-9 with all generators connected. 79
4.22 Decentralized: SLG fault at line 11-12 with all generators connected. . . 80
4.23 Decentralized: DLG fault at line 8-9 with WTG1 disconnected. 81
4.24 Decentralized: DLG fault at line 11-12 with CHP disconnected. 82
4.25 Decentralized: SLG fault at line 8-9 with all WTGs disconnected. . . . 83
4.26 Decentralized: SLG Fault at Line 8-9 with TG Disconnected (Islanded Mode). 83
4.27 Decentralized: SLG fault at line 11-12 with TG disconnected (islanded mode). 85
4.28 Backup: varying DG connection during normal operation. 86
4.29 Backup: varying DG connection during normal operation. 87
4.30 Backup: varying DG connection during islanded operation. 87
4.31 Backup: varying DG connection during islanded operation. 88

B.1 Model A type CO induction relay. 97

Abbreviations

A/D	Analog-to-digital
ADPS	Adaptive Distribution Protection System
ADUV	Accelerated Directional Under Voltage
ANN	Artificial Neural Networks
AOC	Accelerated Overcurrent
CAPS	Centralized Adaptive Protection System
CB	Circuit Breaker
CHP	Combined Heat and Power
COMTRADE	Common format for Transient Data Exchange for power systems
CRU	Central Relaying Unit
CT	Current Transformer
CVT	Capacitor Voltage Transformer
DAPS	Decentralized Adaptive Protection System
DG	Distributed Generator
DLG	Double-Line to Ground
DNP3	Distributed Network Protocol 3.0
DUV	Directional Under Voltage
FFT	Fast Fourier Transform
GVD	Group Velocity Dispersion
LL	Line-to-Line
LP	Linear Programming
MAS	Multi-Agent System
MINLP	Mixed Integer Non-Linear Programming
NLP	Non-Linear Programming
OC	Overcurrent
PCC	Point of Common Coupling
PMU	Phasor Measurement Unit

PT	Potential Transformer
RAM	Random-access Memory
ROM	Read-only Memory
RTP	Real Time Playback
RTT	Round-Trip Time
SCADA	Supervisory Control and Data Acquisition
SLG	Single-Line to Ground
TCC	Time-Current Curve
TDS	Time Dial Setting
TG	Transmission Grid
WTG	Wind Turbine Generators

Chapter 1

Introduction

Traditional distribution systems are designed to allow power flow in one direction from the substation to the loads, as shown in Figure 1.1. The protection schemes for radial systems are designed and coordinated based on this assumption. The relays are coordinated in an upstream fashion, with sections farther away from the substation isolating first, until the fault is cleared [1].

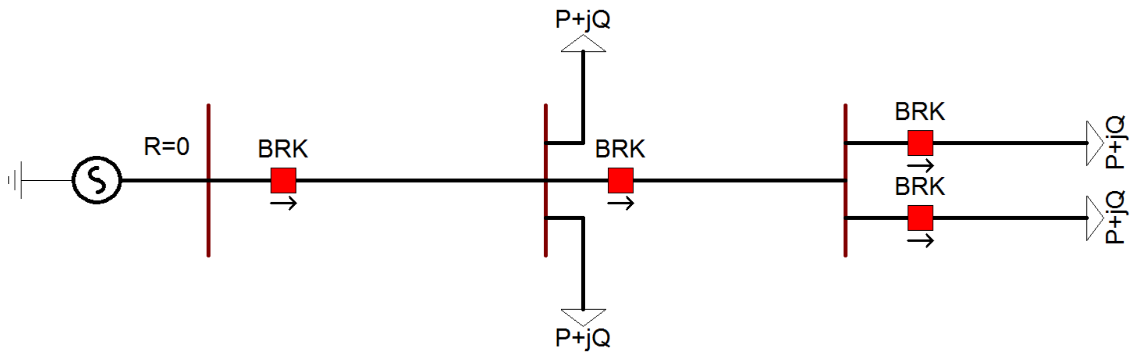

Figure 1.1: Typical radial system.

Recently, more power distribution systems are moving from being centralized regulated systems to decentralized systems because Distributed Generators (DG) are increasingly connected. When a DG is connected to the power distribution system, power flows bi-directionally and hence the system is no longer a radial system. DGs provide several advantages when connected to a power distribution system. First, DGs can be connected near the load to reduce the energy lost in transmitting electric power. Second, DGs decrease the size and number of power lines constructed. Also, they allow operating the system in island mode [2].

DGs can be classified into three main categories. First, different types of DGs exist based on the driving energy, and they include solar panels, wind turbines, fuel cells, small-scale hydro, tidal and wave generators, and micro-turbines [3]. Second, DGs are classified into four classes based on the level of generated power, which are micro (1W $<$ 5kW), small (5kW $<$ 5MW), medium (5MW $<$ 50MW), or large (50MW $<$ 300MW) [4]. Third, two DG classes exist based on the type of connection, inverter interfaced DGs that produce DC voltage and need inverters to change the DC power to AC power, and traditional rotating machine DGs that produce AC power and are directly connected to the system [5, 6].

One of the main problem that arise when DGs are connected to distribution systems is islanding. Islanding refers to the case in which a DG continues to supply a location while the main grid is disconnected. The main concern on the occurence of islanding is the danger posed on utility workers who might think that the system is offline due to fault clearance; however, this part of the system is still energized due to the connected DG. Another problem with islanding is synchronization, i.e., the voltage magnitudes, the frequency of the voltages, and the phase angle of the voltages should be synchronized between the generator and the main grid. If this is not properly performed, reconnecting the main grid might damage the DG rotor [7]. As a result, the commonly followed procedure is to automatically disconnect all DGs on the medium voltage and low voltage utility distribution networks in case of tripping of a circuit breaker [8].

Islanding is categorized into two types, intentional islanding and non-intentional islanding. In the event of a network failure, intentional islanding of DGs can be utilized during the presence of critical load to increase the overall reliability of the power distribution system. To achieve intentional islanding, certain conditions should be satisfied. First, the DG power must be sufficient to satisfy the needs of loads in the island. Second, the DG protection should be reset for island operation due to changes in the system conditions and currents flowing [9]. Furthermore, the DG interface control is responsible for maintaining both the voltage and the frequency on the islanded part of the network within the permissible operating levels.

Another disadvantage of DGs is their impact on the fault current and existing protection systems. DGs reduce the reach of relays by increasing the equivalent impedance of the feeder which in turn decreases the fault current [5]. Figure 1.2 shows the reach of an overcurrent relay with and without a DG connected to the power distribution system. If a fault occurs at bus 6, relay R might attribute the fault to be outside its zone when in fact it is within the relay's protection zone.

Several system operating conditions arise when DGs are connected to power distribution systems:

- All the DGs are connected and the system is operating in the normal operation mode.

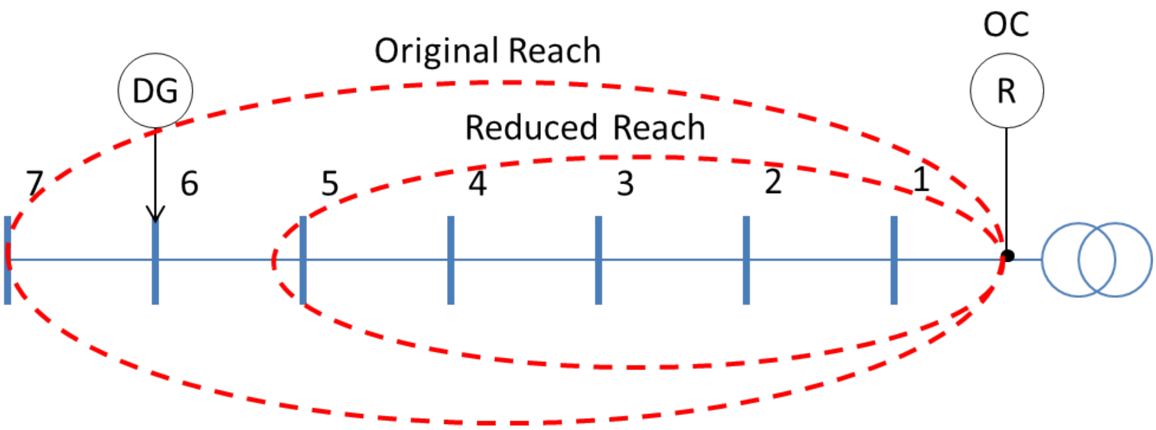

Figure 1.2: Relay reach with and without a DG.

- Part of the DGs is disconnected due to maintenance or due to a previously isolated fault.
- The main grid is disconnected, and the system is operating in island mode.

The variations in the configuration of power distribution systems are not taken into account in conventional protection systems. Moreover, the introduction of DGs changes the system from being radial, and therefore the relays must detect the direction of the fault. This chapter discusses the importance of implementing protection systems in power distribution systems and the different types of protection systems used.

1.1 Protection in Power Distribution Systems

In power distribution systems, protection systems are installed with the assumption that the system is radial. The main role of protection systems is to maintain the stability of the system by isolating only the sections that are under fault, while leaving the rest of the network in operation. This can be achieved by properly coordinating the protection devices.

After the operation of a protection system, continuity of power can be increased by avoiding the use of radial systems, where additional generators are incorporated into the power distribution system. When a fault occurs, one or more of the generators might get disconnected from the power system during fault clearance. But in a non-radial system, a protection system allows the load to be supplied through another generator connected to the power distribution system. Several protection systems are used in power distribution systems, namely, fuses, differential relays, distance relays, and overcurrent relays.

1.2 Types of Protection Systems

1.2.1 Fuses

Fuses are considered as one of the simplest protective devices. They are characterized by being inexpensive, and do not require any Current Transformers (CT) to operate. When the current in the fuse increases beyond a certain limit, the fuse link melts and a gap is formed which constitutes an open circuit. A typical fuse time-current characteristics is shown in Figure 1.3 [10]. Fuses operate at distribution level voltages of 5.5, 8.3, 15.5, 23.0, 27.0, and 38.0 kV [11]. The disadvantages of fuses are their fixed characteristics and the need to be replaced after every fault clearance.

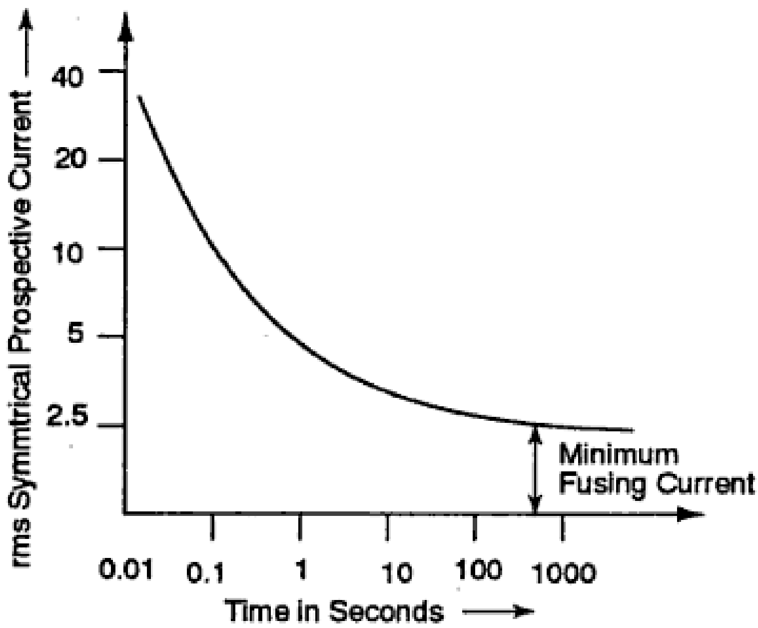

Figure 1.3: Typical time-current characteristic of a fuse.

1.2.2 Protective Relays

Protective relays are another way for protecting power systems and are required to operate circuit breakers above 600 V. By definition, a protective relay is a device which, when energized by suitable currents, voltages, or both, responds to the magnitude and phase relationship to indicate or isolate an abnormally operating condition.

Relays have adjustable settings and are used to actuate the opening of circuit breakers under various fault conditions [12]. The following sections present the basic principle and operation of differential, distance, and overcurrent relays.

1.2.2.1 Differential Relays

In differential protection, two sets of three-phase CTs are used to compare the currents on both sides of the protected equipment. During normal conditions, both currents are equal and the current through the relay is zero. If an internal fault occurs, an unbalance between the two measured currents forms, which causes a current to appear at the installed relay. The relay is activated if the unbalance in the currents exceeds a certain threshold. Differential protection cannot detect faults outside the protected equipment. During an external fault, the current in both CTs increases while having the same direction of flow. As a result, the current through the relay is zero. A commonly used differential relay is the percentage differential type [13]. Figure 1.4 shows the arrangement of CTs in a percentage differential relay. The differential current required to operate this relay is a variable quantity, and is affected by the restraining coil. The differential current in the operating coil is proportional to the difference between I_1 and I_2, and the equivalent current in the restraining coil is proportional to

$$\frac{I_1 + I_2}{2}. \tag{1.1}$$

The differential relay operates if the differential current exceeds the restraining current. The principle of operation is given by

$$(I_1 - I_2) > N\left(\frac{I_1 + I_2}{2}\right), \tag{1.2}$$

where N is the number of turns in the restraining coil [13]. The setting of the differential relay should take into account the error that may result if unidentical CTs are used. Differential relays are not desirable protection for distribution power lines because they do not provide backup protection to adjacent lines.

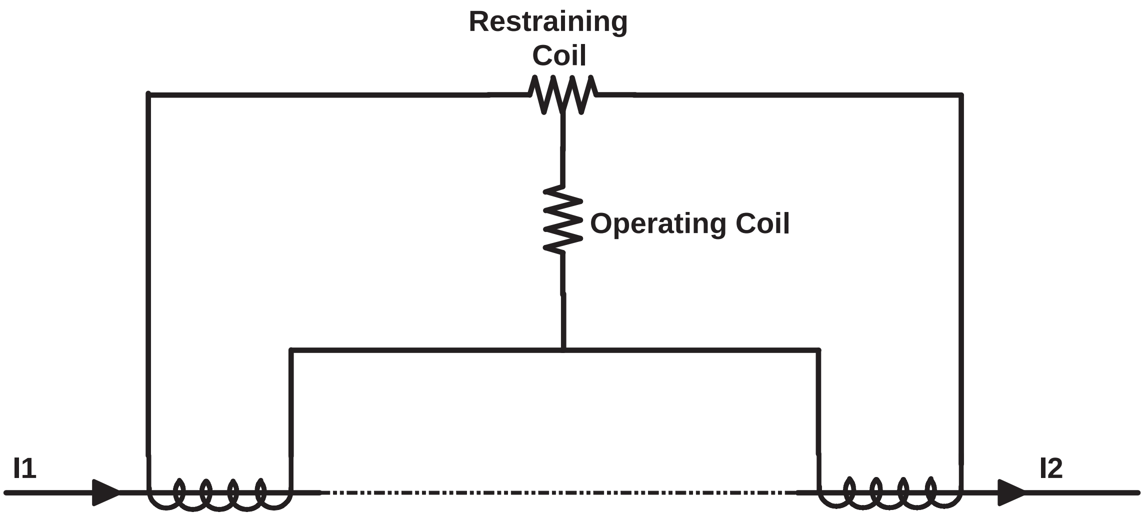

Figure 1.4: Differential protection.

1.2.2.2 Distance Relays

Distance relays are another type of protective relays. They estimate the distance to the fault from the relay location by calculating the ratio of the voltage to the current [14]. The calculated ratio is called the apparent impedance seen by the relay. The apparent impedance is determined by calculating the ratio of the operating quantity to the ratio of the polarizing quantity. If the calculated value falls within the characteristics of the relay, the relay trips [15]. If the fault impedance is zero, then distance relays do not malfunction. If a fault impedance or load current exists prior to fault occurrence, this might cause distance relays to either over-reach or under-reach [16, 17]. Under-reach occurs when the fault impedance is large, which causes the calculated impedance value to be large. As a result, a distance relay attributes the fault outside its zone when in fact it is within the relay's protection zone [17]. A typical characteristics for a distance relay, known as Mho characteristics, is shown in Figure 1.5. Distance relays provide backup protection for adjacent lines as shown in the characteristics in Figure 1.5 and they are mostly used for transmission system protection.

1.2.2.3 Overcurrent Relays

The third type of protective relays is an overcurrent relay. While overcurrent relays are one of the first developed protection systems, they are still widely used in many applications [14]. Overcurrent relays are characterized by their lower cost when

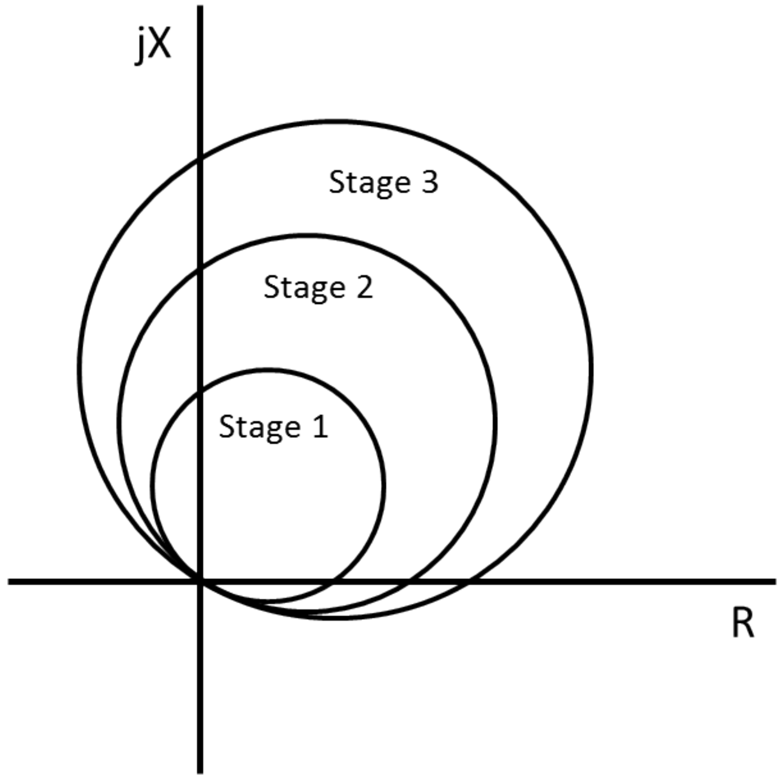

Figure 1.5: Simple Mho function.

compared to other protection systems. They also provide a large range of characteristics [18]. An overcurrent relay has several taps which determine the operating current level. Also, a Time Dial Setting (TDS) in an overcurrent relay determines the operation time of the relay for a certain current value. The higher the TDS value, the longer it takes the relay to operate for a certain fault current. Overcurrent relays have four different curve types, namely, long time inverse, normal inverse time, very inverse time, and extremely inverse time [14]. Figure 1.6 shows the typical curves obtained for overcurrent relays.

Directional overcurrent relays are a type of overcurrent relays, which are used to protect non-radial power distribution systems. A directional overcurrent relay is a combination of an overcurrent relay unit with a directional unit. The directional unit detects and operates for a certain phase-angle and current magnitude. The relay sends a trip signal only for current flow in one direction and is insensitive to current flow in the opposite direction.

In overcurrent protection of power distribution systems several overcurrent relays are used as shown in Figure 1.7. In this figure, relays R1 to R6 protect the buses and the connected loads to the system when a fault occurs. Directional overcurrent relays, connected for the same direction, have to be coordinated. The most downstream

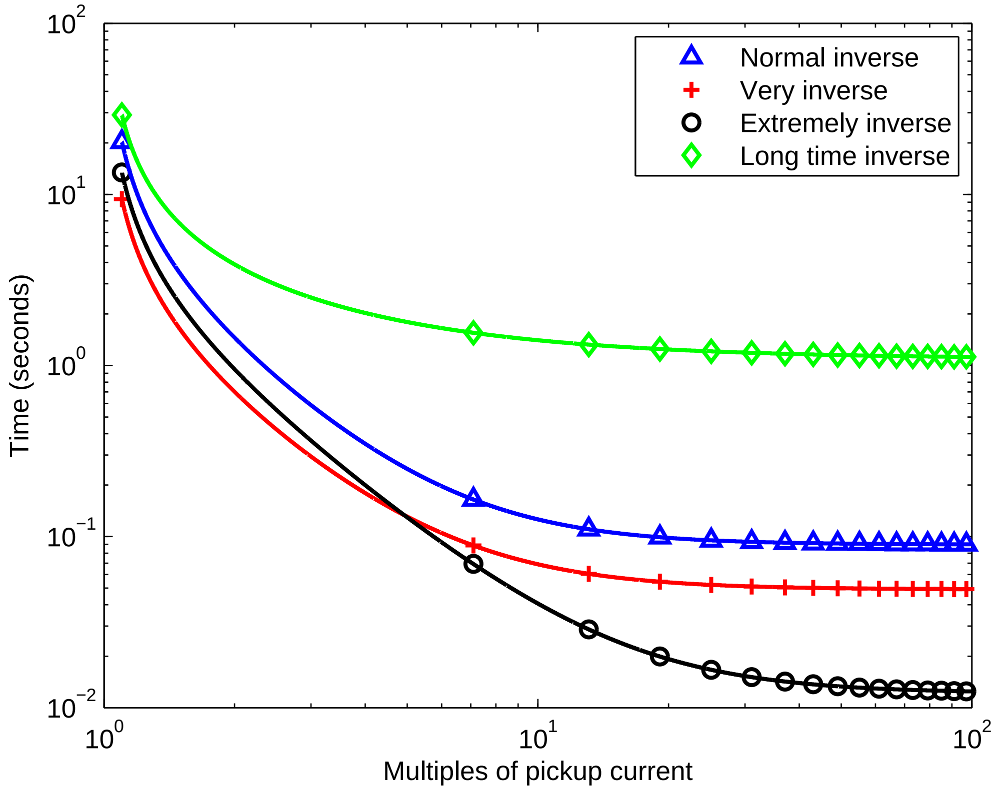

Figure 1.6: Different types of TDS curves.

relay, in each direction, is the fastest relay to clear a fault. On the other hand, the most upstream relay is slowest to clear a fault. The coordination problem can be solved using either a conventional topological technique or an optimization technique [19].

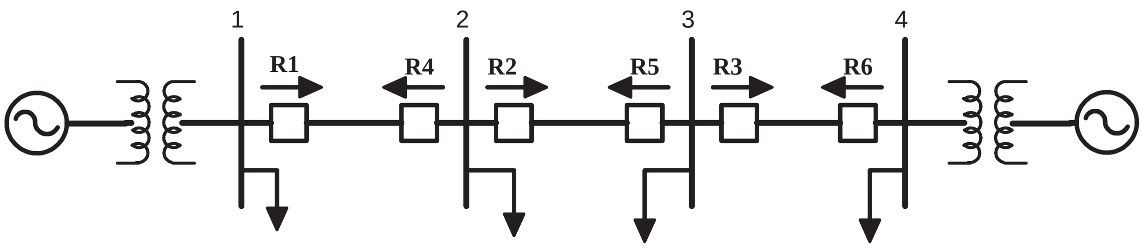

Figure 1.7: Relay coordination example.

1.2.3 Conventional Overcurrent Relay Coordination

In the conventional technique, overcurrent relays are coordinated according to a certain coordination time. An example of a typical relay coordination is given briefly in this section, where the directional overcurrent relays R1, R2, and R3 are to be coordinated. R3 is the most downstream relay and R1 is the most upstream relay as shown in Figure 1.7. The coordination is done by first calculating the minimum fault current at bus 4. Using this value, the CT ratio and tap setting are determined for the first relay. The TDS for the first relay is always chosen to be minimum, because it is the fastest acting relay. Also, the CT ratio and tap setting of the second relay are the same as the first relay. The maximum fault current at bus 4 is calculated to determine the operation time of the first relay, then the coordination time is added to determine the operation time of the second relay. Using the second relay's operation time and characteristics curves the TDS is determined. After that, the third relay is set by calculating the minimum fault current at bus 3 to determine the CT ratio and tap setting. Then, the maximum fault current at bus 3 is calculated to determine the operation time of the second relay. Using this time, the operation time of the third relay is calculated by adding the coordination time delay. Using relay characteristics curves, the TDS for the third relay is determined. Correct relay coordination is when the constraint given by

$$TDS_1 > TDS_2 > TDS_3 \tag{1.3}$$

is satisfied. Figure 1.8 shows TDS curves for a normal inverse relay having different TDS values.

1.2.4 Overcurrent Relay Coordination Using Linear and Nonlinear Optimization

In the optimization technique, the overcurrent relay coordination problem is stated as an optimization problem. Optimal coordination is performed to maintain all the directional overcurrent relays in the protection system properly coordinated and ready for fault occurrence. The coordination problem has a main objective function subject to coordination constraints, relay characteristics, and limits of the relay settings [19]. Optimal coordination computes the TDS value and the tap setting (pickup current) of the overcurrent relays, and the selection of these settings should satisfy the requirements of sensitivity, selectivity, reliability, and speed. Also, the TDS values and tap settings, of each relay, should minimize the overall operation time of the directional overcurrent relays, while maintaining the relay coordination requirements intact [20]. Several approaches exist to implement optimal coordination, such as Linear Program-

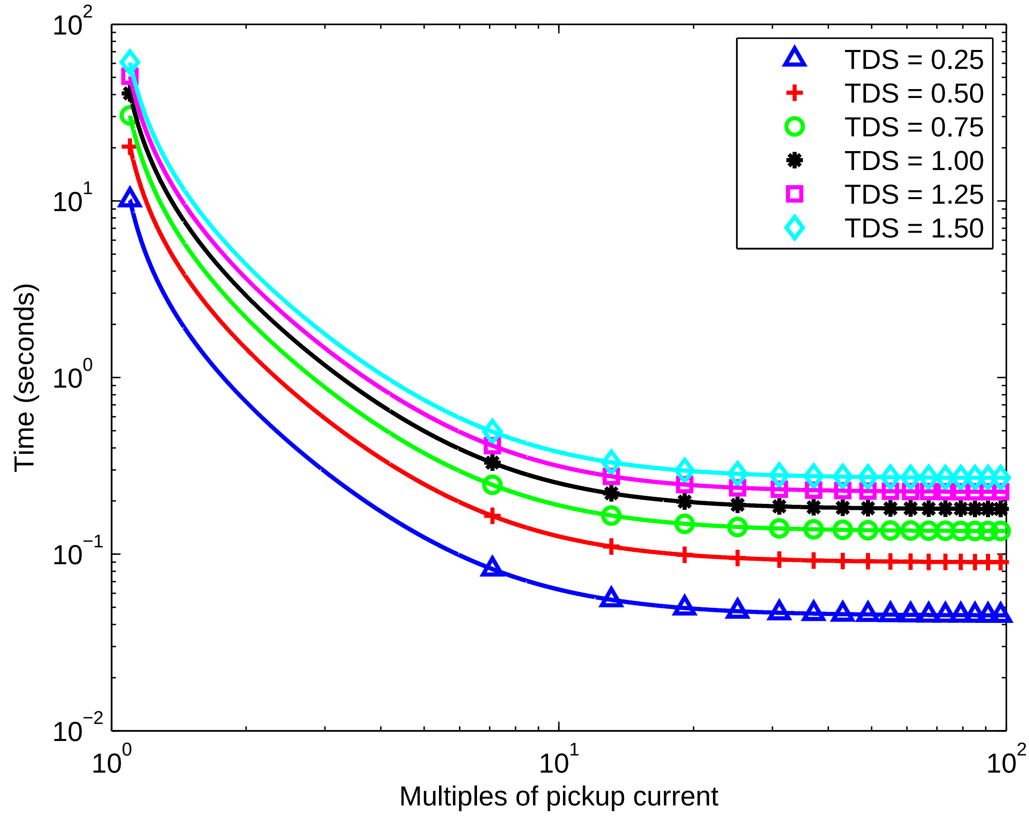

Figure 1.8: Relay characteristic curves for different TDS values.

ming (LP), Non-Linear Programming (NLP), and Mixed-Integer Non-Linear Programming (MINLP). In LP, the pickup current is fixed, whereas in NLP the pickup current is set as continuous values. On the other hand, in MINLP the pickup current is set as discrete values during optimal coordination [20]. In all the approaches the TDS values are initially set to the minimum and then gradually increased.

1.3 Problem Statement

Power distribution systems penetrated with DGs are always subject to changes in the system configuration. During fault clearance or maintenance, certain DGs might get disconnected. The changes in the configuration may lead to significant changes in the fault current level, which cause mis-coordination and mis-operation of the previously coordinated directional overcurrent relays. To maintain proper coordination, protection relays should change their settings automatically whenever a change in the power system configuration occurs. Therefore, to solve the problems associated with the protection system and the penetration of DGs into the power distribution network, an adaptive protection scheme is needed.

This adaptive protection system should perform real-time monitoring and provide changes in the protection accordingly [21]. This can be done by developing an algorithm that detects the system's topology, estimate the system's state, measure the fault currents, and determine the relays' settings. Different types of protection relays are used in adaptive protection systems, and the most commonly used are distance and overcurrent relays. Directional overcurrent relays are recommended in an adaptive protection system due to the reasons in Section 1.2. In the adaptive protection system, a proper communication system is needed to enable the exchange of information between the various devices in the power distribution system. Different solutions are proposed in the literature to solve the adaptive protection problem. Some of the solutions use local measurements to implement an adaptive protection system, which include power system state estimation and islanding detection [5, 22, 23]. Other methods use distance relays and Phasor Measurement Unit (PMU) in a communication-based adaptive protection system [24, 17, 25]. Also, multi-agent systems are used when DGs are present in the power distribution system to achieve adaptive protection [26, 27, 28, 29]. Using communication-based schemes for adaptive protection avoids uncertainty in determining the power system's configuration.

1.4 Thesis Objectives and Contribution

The objective of this thesis is to develop a communication-based adaptive protection system that efficiently utilizes communication techniques to update the relay settings based on the DG connection statuses. The proposed adaptive system considers a centralized communication system as well as a decentralized system. In the centralized approach, information about the connection status of the generators is communicated through the Central Relaying Unit (CRU). On the other hand, in the decentralized approach, the connection status is directly shared among all relays. In both approaches, a linear optimization algorithm is implemented to calculate the new coordination settings based on the received connection statuses of the DGs. In the centralized approach, the optimization algorithm is implemented at the CRU while in the decentralized approach it is implemented in each relay. In either case, the algorithm calculates the optimum

TDS for the downstream and upstream looking relays with respect to the transmission grid. As a result, the relays become ready to clear out any future fault in the network.

While the proposed communication-based adaptive approach assumes an intranet as the primary network, it is also designed such that the Internet could be used as a backup should the intranet fails. Several simulation scenarios are performed to validate the performance of the proposed adaptive protection system. These scenarios were carried for different fault locations, different fault types, and different power system configurations. Time delay calculations are also performed to evaluate the benefits of the communication-based system on the behavior of the adaptive protection system.

1.5 Thesis Outline

The rest of the thesis is organized as follows:

Chapter 2 provides a literature review for the work done in the area of adaptive protection in distribution systems. The different techniques are introduced and the key concepts are discussed along with their pros and cons. Chapter 3 focuses on the proposed techniques, where each technique is explained and their operations are discussed. Chapter 4 presents the system model, and shows the results. Also, it demonstrates the operation of the adaptive protection system for changing topology and for various fault conditions on the system. Chapter 5 concludes and summarizes the proposed techniques and results. Also, it includes recommendations for future work that can be implemented for further improvements.

Chapter 2

Literature Review

Traditional protection systems suffer from the lack of sensitivity and slow response times [30]. An Adaptive Distribution Protection Systems (ADPS) is needed to avoid the problems associated with classic protection systems. ADPSs have significant advantages over traditional protection systems. They increase the protection system's sensitivity, reliability, efficiency, safety, and flexibility. Furthermore, ADPSs enhance the protection system's security, account for Current Transformer (CT) ratio mismatches, and provide economical benefits [30].

ADPSs are classified as either non-communication based schemes or communication -based schemes. In addition, communication-based schemes include centralized communication-based schemes and multi-agent systems. In a communication-based ADPS communication is performed from the digital overcurrent relay to the substation computer, and from the substation computer to the central computer. Communication between the relay microprocessor and the substation microprocessor is performed over a communication link [30].

In the ADPS, each relay has a fixed relaying program existing in the Read-only Memory (ROM). Overcurrent relay's changeable settings exist in the Erasable and Writable ROM, and transient and intermediate results reside in Random-access Memory (RAM). Analog-to-digital (A/D) converters and signal conditioning filters are used to convert the signals obtained from the CT, Capacitor Voltage Transformer (CVT), and Potential Transformer (PT). Figure 2.1 shows a typical hardware architecture of an ADPS [30].

This chapter discusses some of the developed adaptive protection schemes over the past years. Also, it talks about the advantages of the different methods, and highlights the discrepancy in some of the proposed schemes.

2.1 Non-communication Based ADPS

Non-communication based ADPSs use local measurements to perform system estimation and islanding detection. The advantage of using non-communication based

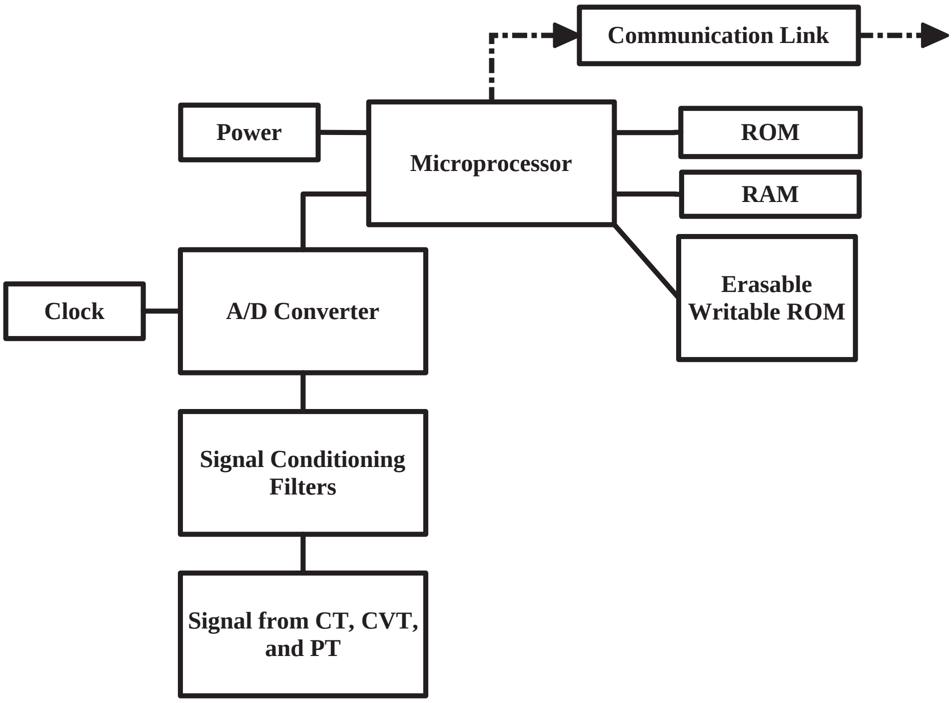

Figure 2.1: Typical ADPS hardware architecture.

ADPSs is their lower cost compared to communication-based ADPSs. A non- communication based adaptive protection system is discussed in [5]. The proposed system changes the value of the pickup current, where the pickup current is decreased as the value of the total power injected by the DGs is increased. Furthermore, the system estimates the fault current at the relay after taking into account the location of the DG and its output current. The fault current at the relay is estimated using Gauss-Newton method [5]. However, two approximations are made during simulations, the DG transients are ignored and calculations only account for the steady state current. Also, the fault current at the relay is assumed to be constant and equal to the steady state fault current.

Another Non-communication based adaptive protection system is implemented by continuously measuring the voltage and the frequency [22]. The measured values determine whether the DGs are connected or removed from the power distribution system. Also, the algorithm measures the current in the system to determine fault occurrence as shown in Figure 2.2 [22].

To perform adaptive protection, the relays that picked up the fault and operated the circuit breakers need to be determined. Therefore, all relays in the protection system store the settings of all other relays, and when a fault occurs a timer starts in each relay.

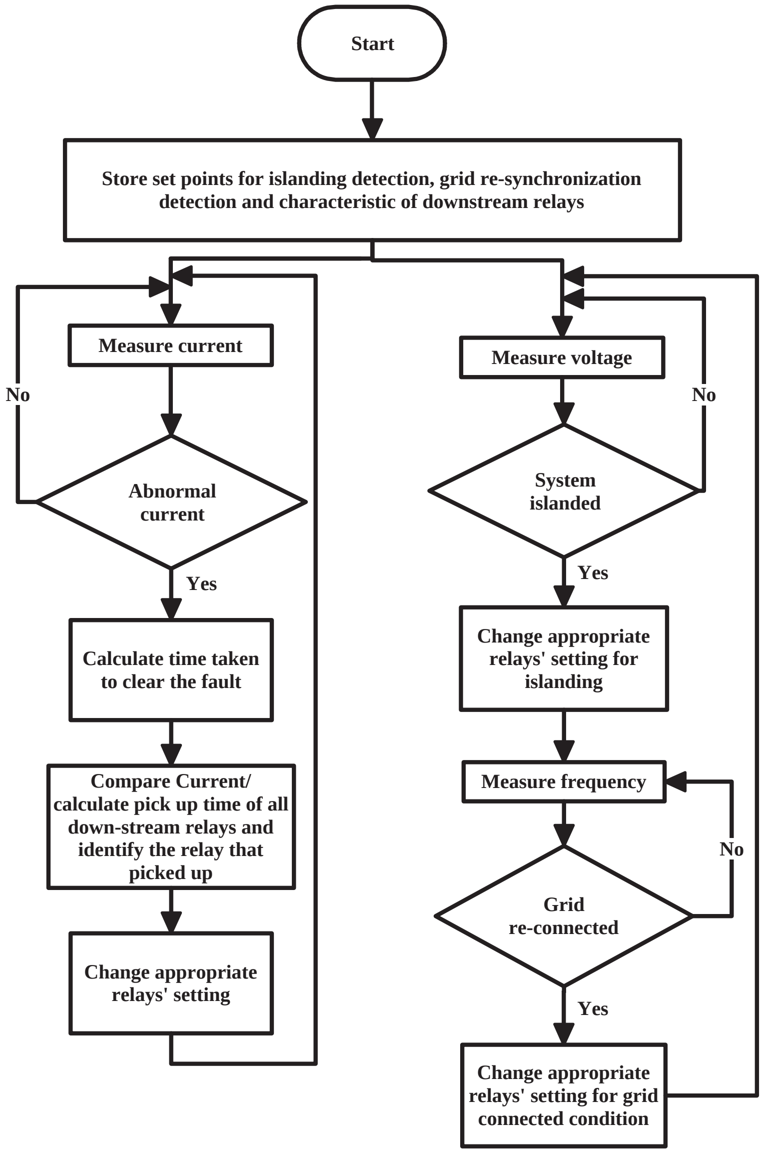

Figure 2.2: Adaptive protection system using voltage and frequency measurement.

If the measured current in a certain relay falls below the pickup current then one of the other relays in the protection system cleared the fault. The relay then subtracts the total time taken for the relay contact to close and the circuit breaker to open. The result is the time taken by the relay, which initiated the fault clearing, to pickup. Based on the current measurement during the fault and the time overcurrent characteristics of the downstream relays, the relay calculates the pickup time of all downstream relays. Using the calculated times, the relay that operated is determined. Then, the settings of the other relays are changed depending on the operation of the protection system during the fault. The fault current measured by the other relays is assumed to be the same as the current measured by the relay that operated, but this may not be the case [22]. The fault current changes from one section to another, which causes uncertainty in determining the faulted section.

An adaptive distance relay protection system is proposed in [6]. The protection zones of the distance relay are set in an adaptive manner. Zone II threshold setting of distance relay 2 is calculated using

$$Z_{set.2}^{II} = K_{rel}^{II}\left(Z_{BC} + K_b Z_{set.3}^{I}\right), \tag{2.1}$$

in the power system shown in Figure 2.3.

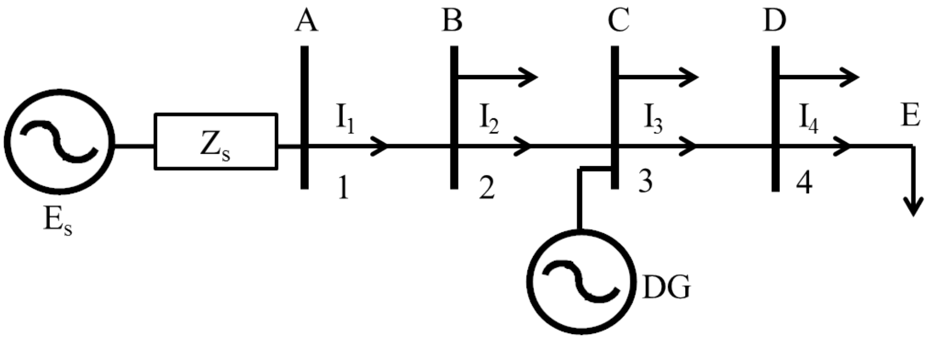

Figure 2.3: Adaptive distance relay protection system.

$Z_{set.3}^{I}$ is zone I setting of distance relay 3, and K_{rel}^{II} is zone II relay coefficient of distance relay 2. Two equations are used to calculate the branch coefficient K_b. If the fault is a line-to-line fault at phases BC, K_b is calculated using

$$K_b = 1 + \frac{\dot{I}_{DG.b} - \dot{I}_{DG.c}}{\dot{I}_{2.b} - \dot{I}_{2.c}}. \tag{2.2}$$

However, if a three-phase fault occurs, K_b is calculated using

$$K_b = 1 + \frac{\dot{I}_{DG}}{\dot{I}_2}. \tag{2.3}$$

Similar to the previous approach, mis-operation of the distance relays is avoided by adaptively setting the protection zone thresholds.

Finally, an approach to implement a non-communication based adaptive protection system is investigated in [31]. The adaptive protection system takes into account wind farms presence in a power distribution system. When wind farms are connected to the power distribution system, several conditions may occur during a fault. First, the

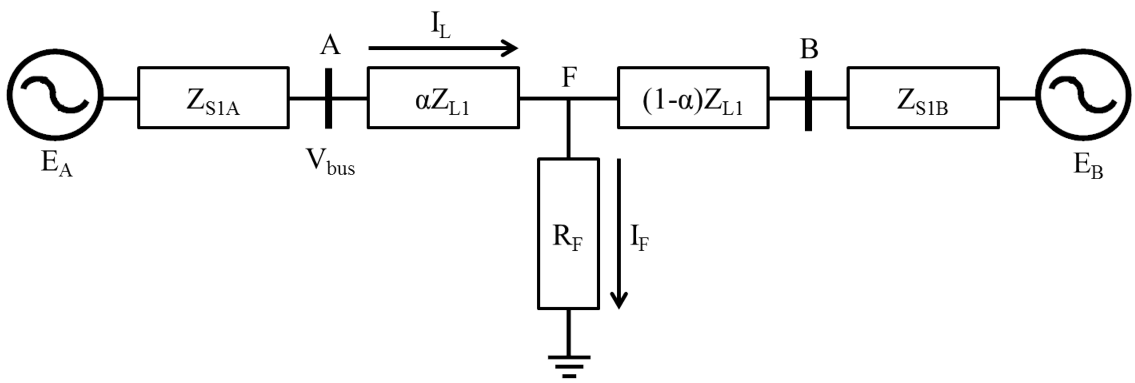

Figure 2.4: Adaptive distance relay protection system.

voltage in the dedicated power line drops, and the electromagnetic torque developed decreases. Then, the wind farm is accelerated due to deviation between the electromagnetic and mechanical torques. The stability of the wind farm depends on several factors which include the fault condition, the output power of the wind farm, and the fault position. The adaptive protection system, shown in Figure 2.5, continuously measures the current and voltage at the Point of Common Coupling (PCC) [31]. The measured values are used to calculate the output power of the wind farm, and to determine if a fault condition exists. During a fault, the fault type is classified using the measured current and voltage. After that, the system determines if the adaptive protection system is able to aid in clearing the fault, and the Time-Current Curve (TCC) is changed according to the output power of the wind farm.

2.2 Communication-based ADPS

Communication-based ADPSs use communication channels to transmit data between different devices in the power distribution system in order to perform adaptive protection. Protective devices used in communication-based ADPSs include PMUs and distance relays.

Distance protection relays perform calculations offline and keep them constant throughout the operation. Performed calculations are based on the maximum generation mode in the power system. In contrast, sensitivity of protection is checked in the minimum running mode of the system. Differences between the measured impedance by the relay and the actual impedance of the line, while taking into consideration the ground fault impedance, cause distance relays to malfunction [17]. Therefore, adaptive

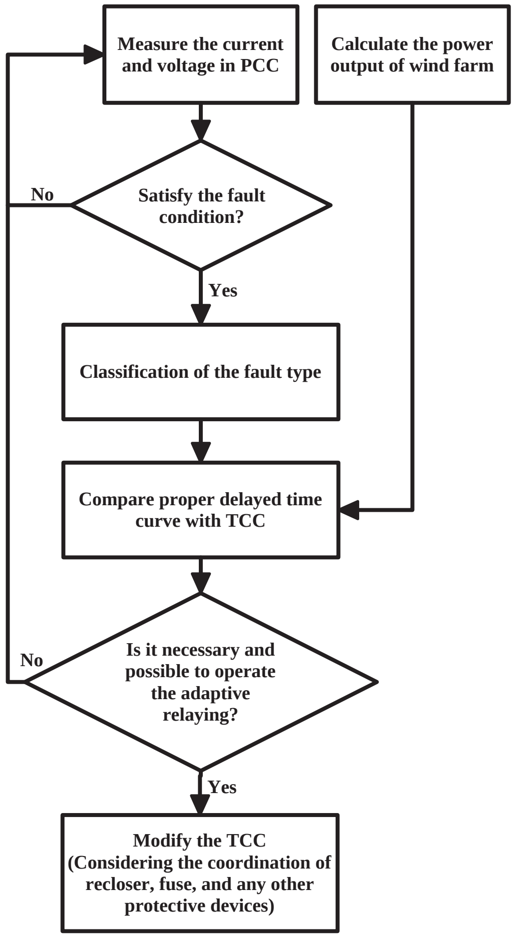

Figure 2.5: Adaptive protection system when wind farms are connected to the power distribution system.

distance protection systems are developed to overcome the shortcomings of distance protection systems.

Adaptive distance relay protection is implemented by changing the protection zones for ground faults. Protection zones are changed according to load deviations and changes in the system conditions. The calculated impedance in a distance relay varies with the variations in the load current and characteristics of the load. Variations create a difference between the impedance seen by distance relays and the actual impedance at the ground fault. Using a traditional distance relay, the impedance is calculated using

$$Z_A = \frac{V_A}{I_A + K_0 \times 3I_0}, \tag{2.4}$$

where Z_A, V_A, and I_A are the phase impedance, voltage, and current, respectively [17]. Also, K_0 and I_0 are the coefficient of zero phase sequence compensation and zero phase sequence current, respectively.

Equation 2.4 is adjusted to implement adaptability in the calculation of Z_A for the system model shown in Figure 2.4 [17]. The actual impedance seen by the relay is $\alpha Z_{L1} + R_F$, where

$$0 < \alpha < 1. \tag{2.5}$$

The apparent impedance of the adaptive distance relay is

$$Z_A = \alpha Z_{L1} + \frac{3R_F}{\frac{Z_T(1-Ph)}{Z_{1B}+Z_{1A}Ph} + \frac{2Z_{1B}}{Z_{1A}+Z_{1B}} + \frac{Z_{0B}}{Z_{0A}+Z_{0B}}(1+3K_0)}, \tag{2.6}$$

where Ph is the phase difference between the two buses A and B, and it is calculated using

$$Ph = 1 - \frac{I_L(Z_{1A}+Z_{1B})}{E_A}, (E_A = V_{bus} + I_L Z_{S1A}). \tag{2.7}$$

Any mis-operations are avoided in distance protection when both equations are utilized. Also, the issues involving under-reach and over-reach of distance relays are averted [17].

In communication-based adaptive protection systems, a PMU can utilize the power-angle, voltage, current, and power measurements to implement accurate fault detection for power lines. In adaptive protection using PMU for the system in Figure 2.6, the first zone of the distance relay calculates the line impedance, using the PMU's measurements, according to

$$Z = \frac{(U_1 - U_2)(U_1 + U_2)}{U_1 I_2 + U_2 I_1}. \tag{2.8}$$

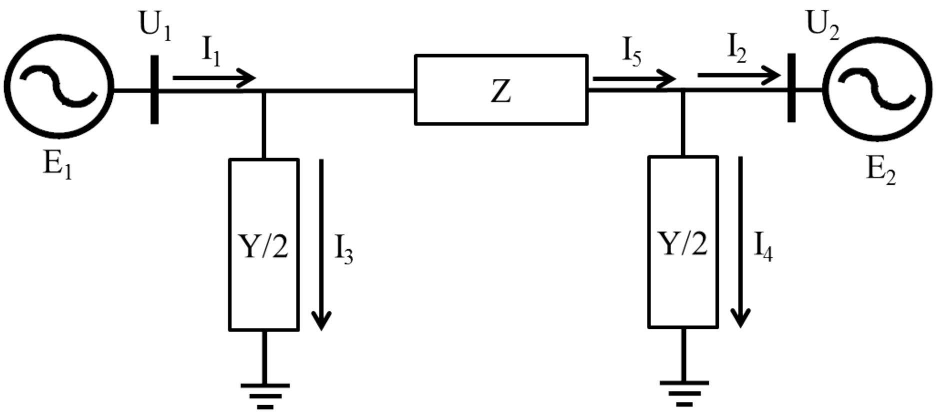

Figure 2.6: Adaptive PMU protection system.

The second zone of the distance relay is set by calculating the impedance of the transmission line. The influence of infeed current and parallel circuits are considered. In the third zone of the distance relay, the phase angle at each key point after clearing a fault is calculated. If the calculated power angles are small and the system is stable, the protection system is adaptively regulated online according to an online-calculated impedance. If the calculated power angles are close to the critical operation and unstable running of the system, backup protection is blocked until the overload is removed. The time to remove the overload should be less than the operation time of the zone backup protection [24].

A third approach to implement a communication-based adaptive protection system is discussed in [23]. When a fault is close to the source, the operating time of the relay might be long, and fast clearance is not achieved. A communication-based adaptive protection technique helps reduce the operating time of the relay [23]. Adaptive protection techniques can use integrated protection to protect the line. The functions implemented in each relay are Overcurrent (OC), Accelerated Overcurrent (AOC), Directional Under Voltage (DUV), and Accelerated Directional Under Voltage (ADUV). The operation of the relay functions depends on the system condition, whether the utility source or generator are connected or not. The information from the relays is received at a central protection relay from the substation. Then, the relay performs the necessary calculations to determine whether a fault occurred or not. The relay issues a trip command to the circuit breaker if a fault is detected [23].

2.3 Multi-Agent Systems

Multi-Agent Systems (MAS) are communication-based ADPSs that use decentralized communication schemes. A MAS is a collection of agents, which coordinate and collaborate to achieve a desired goal [29]. It has distributed artificial intelligence and the ability to resolve problems of the power system logically and physically [28]. Also, a MAS has to perform its local tasks, and interact with the other agents. Interaction and communication in a MAS is within the same society and different societies. For communication, a communication protocol is used to enable the agents exchange and understand the communicated messages [26].

In MASs, an agent is a software package that has knowledge, thought, and purpose [28]. Moreover, an agent is able to operate alone or under people's direction and has four characteristics:

- Autonomy: the agent has control over its own actions and internal states.
- Social ability: the agent has the ability to communicate with other agents.
- Reactivity: the agent has the ability to asses and evaluate the current situation and react accordingly.
- Pre-activeness: the agent shows a certain target behavior when startup information is received.

Each agent has four modules, and they include the setting calculation module which executes the setting and current calculations. Second, the knowledge base module, where all the data related to relay setting calculation is stored. Third, the knowledge analysis module, which performs knowledge verification and analysis. Finally, the communication module, which performs communication among the agents, and aids in transferring the knowledge between them [29].

Three types of agents are recognized by [28], shown in Figures 2.7, 2.8, and 2.9, and are as follows:

1. Deliberative agent
   It is an agent which has a preset circumstance model and the ability to freely function. Also, it has complete knowledge of the database.

2. Reactive agent
   It is an agent which lacks complete knowledge of the system along with complex reasoning. But a reactive agent is a condition-action agent, and it is used whenever a quick response is needed to the outside world.

3. Hybrid agent
   It is a combination of the deliberative agent and the reactive agent models, where the deliberative agent helps in the decision making process. On the other hand, the reactive agent model aids in responding quickly to any significant event faced.

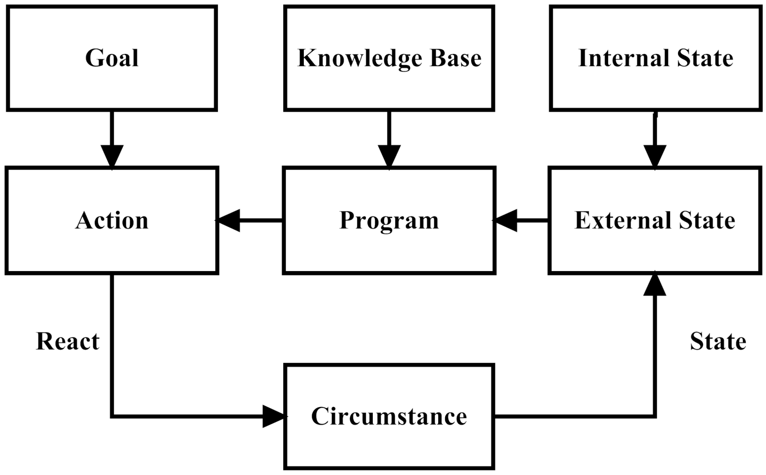

Figure 2.7: Deliberative Agent.

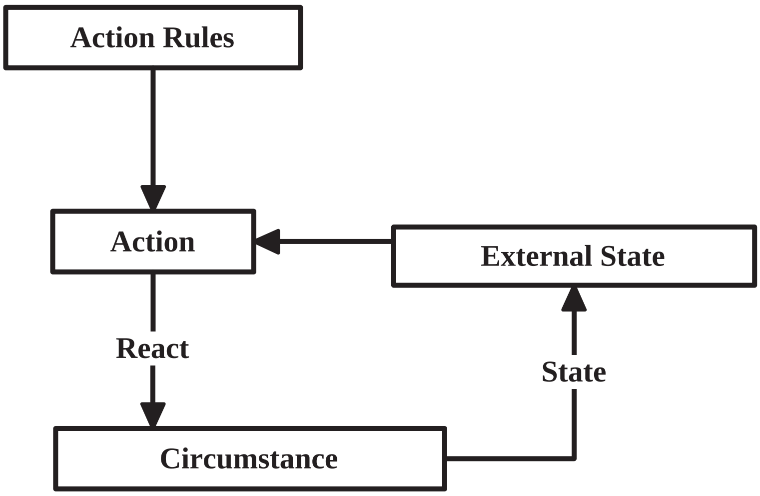

Figure 2.8: Reactive Agent.

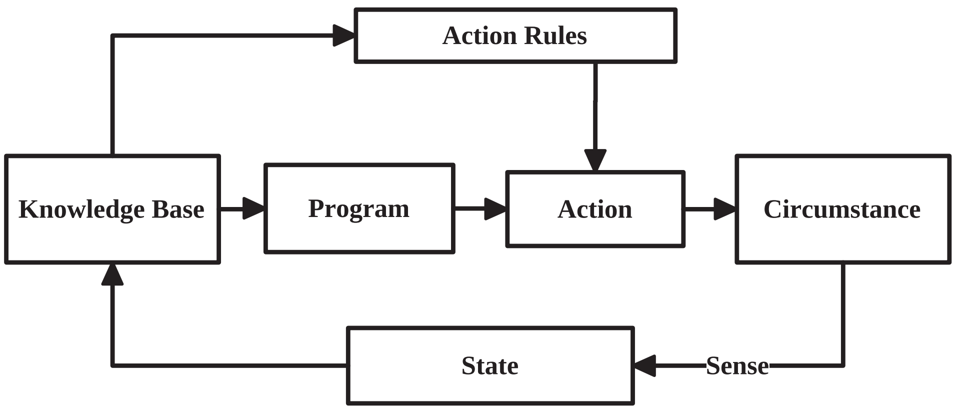

Figure 2.9: Hybrid Agent.

A multi-agent architecture can consist of agent communities that include relay agents, DG agent, and equipment agents. Relay agents search for relevant information by communicating with other agents. Also, they receive DG connection status, fault current, and breaker status. Then, the coordination strategy determines the resetting of the protection. The structure of the relay agent is shown in Figure 2.10 [26].

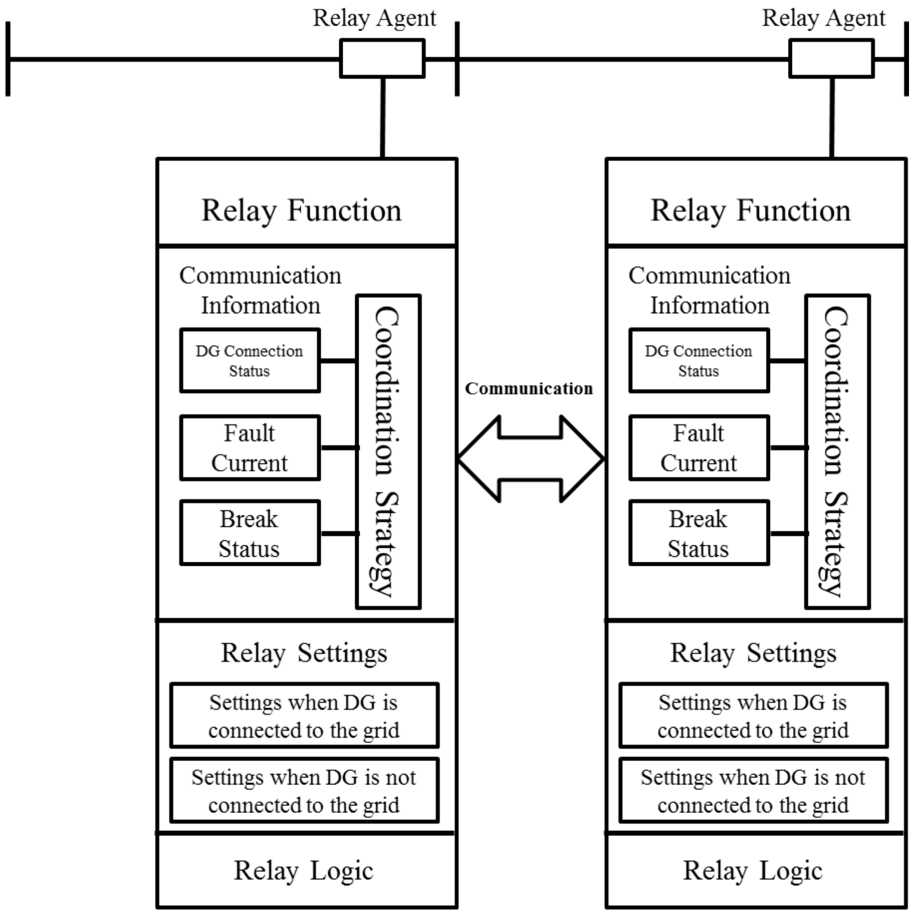

Figure 2.10: Structure of a relay agent.

DG agent considers each DG in the power distribution system as one agent and sends its connection status to relay agents. Equipment agents include CT agent and breaker agent. They perform local power measurements and communicate them to the relay agent to provide protection and coordination functions. In the MAS, all agents perform measurements of the current, voltage, and breaker status. Several output actions can take place depending on the measured and communicated values. The output actions include sending out a trip signal, adjusting the transformer tap, and switching signal in capacitor bank [26].

Another system organization of a MAS is proposed in [27], where a MAS is layered in structure and distributed in control. The adaptive protection system is divided into three layers as shown in Figure 2.11. First, the organizing layer is responsible for programming the adaptive protection from an overall system view. It has the responsibility to resolve the conflicts between the different agents. The organizing layer reorganizes the agents in case of changes in the power system due to the operation of breakers, and show them to the operators. Furthermore, it consists of a reorganizer agent which can layout the protection scheme of the whole system. Second, the cooperating layer is the middle layer, and it consists of a calculation agent, a real-time model agent, and a protection agent. Finally, the executing layer acts in response to any changes in the power system. If the power system condition is abnormal, a signal is received from the cooperating layer and a trip signal is sent out [27].

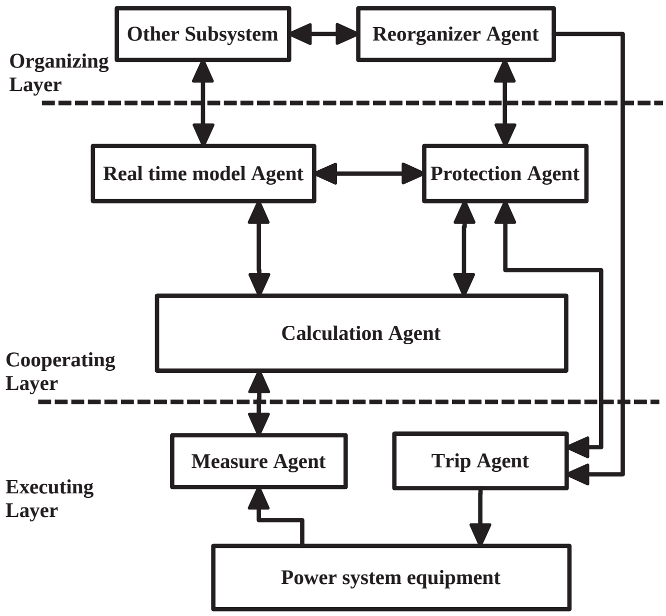

Figure 2.11: Adaptive protection MAS architecture.

In the MAS, the measuring agent in the executing layer communicates with the calculation agent. Then, the calculation agent calculates the essential values to evaluate the system's operating state. After that, the calculated values are communicated to the real-time model agent. Then, the real-time model agent communicates with the reorganizer agent in the organizing layer. The reorganizer agent changes the protective settings according to the system's operating state. After that, the reorganizer agent communicates the new settings to the protection agents. Protection agents include over-current agents, grounding agents, distance agents, and under-voltage agents. Finally, the measuring agents communicates with the calculation agent and trip agent, which decide whether or not to send a trip signal. The decision is made using the received information from the protection agents [27].

Chapter 3

Proposed Adaptive Protection System

The proposed communication-based adaptive overcurrent protection system is explained in this chapter. Section 3.1 describes the proposed communication scheme. Section 3.2 explains the operation of the proposed methodologies, and highlights the differences between them. Section 3.3 presents the developed backup technique used in case of communication failure and explains its operation. Section 3.4 highlights the differences between the proposed adaptive protection system and existing solutions.

3.1 Communication Network

Communication is a major activity in an adaptive protection system, and a communication network is needed to provide communication between DGs, relays, and a Central Relaying Unit (CRU) [25]. In the proposed adaptive protection system, intranet is used as a main communication network, and it is a collection of networks supporting a single site, and linked at the network layer of operation, using routers [32]. Moreover, intranet is a closed network, and can have a high cost of implementation. However, it has high reliability and security [33].

The Internet is used as a backup in case of communication failure using intranet. It has a cheaper cost of implementation and global access. However, the Internet has reliability issues because it is a best effort network, and timely delivery of information is not guaranteed. Also, it has security issues and can be hacked. When using the Internet, the connection is made between the DG, relay, or CRU to the Internet to transmit the data. The data reaches the receiving end after passing through hubs in the communication network. Communication for the adaptive protection system is assumed to be within the same subnetwork. Therefore, the longest path of a transmitted packet is limited to include a maximum of two hubs. Three data types are exchanged in the proposed adaptive protection system, and are as follows:

1. Connection status of the DG which indicates whether the DG is connected to the power distribution system or not.

2. Fault direction indication of the overcurrent relay. The fault direction is represented as a binary ‘1’ or ‘0’ when the fault is in the forward or reverse direction respectively.

3. Optimized TDS and tap setting values are sent to all the relays in the system when a change in the power distribution system’s configuration occurs.

3.1.1 DNP3

Distributed Network Protocol 3.0 (DNP3) is suggested as the communication protocol in the adaptive protection system. It is used to facilitate data exchange between DGs, relays, and CRU in the proposed adaptive protection system. DNP3 was first presented in 1993 by GE, and it is based on the IEC 60870-5 protocol [34]. It was created to perform Supervisory Control and Data Acquisition (SCADA) applications [34]. DNP3 is known for being robust, efficient, widely compatible, and reliable [35].

When DNP3 is used in an adaptive protection system, DNP3 processing time in the devices causes an increase in the communication time delay. Table 3.1 shows the time delay due to DNP3 processing [36]. The processing time delay is hardware dependent. Table 3.2 shows the specifications used in [36] to obtain the time delay results. Communication between two overcurrent relays is the longest processing time delay which is 22.7430 ms. The hardware for the relays and Circuit Breaker (CB) controllers need to be upgraded to obtain faster processing time.

Table 3.1: DNP3 processing delay.

Device	Transmission (ms)	Receiving (ms)
Relay	11.856	10.828
CB Controller	6.088	5.829
Control Center	0.501	0.489

Table 3.2: DNP3 hardware specifications.

Device	CPU	Memory	Kernel Version
CB Controller	ARM 200 MHz	64 MB	ARM Linux 2.4.26
Relay	ARM 500 MHz	128 MB	ARM Linux 2.4.21
Control Center	P4 1.66 GHz	64 GB	Linux 2.6.32

3.1.2 Fiber Optic Communication

In the proposed adaptive protection system, dedicated fiber optic cables are used as the physical communication medium to transmit data. Fiber optic communication helps in transferring large amounts of data with low latency which is a necessity in a protection system [37]. In fiber optic communication, the number of symbols is equal to 2^N, where N is the number of bits transmitted. Furthermore, the gross bit rate, R, and the number of bits are used to calculate the symbol rate, and it is given by

$$\text{Symbol Rate} = \frac{R}{N}. \tag{3.1}$$

Several factors are taken into account during fiber optic simulations. They help obtain an accurate representation of the communication time delay. These factors include:

1. Length of the fiber optic channel (m).
2. Attenuation (dB/m), which is a measure of the power loss of the signal along the distance of the fiber optic channel by absorption or scattering [38]. During the simulation, it is used to determine the amplification gain needed.
3. Effective area (μm^2), which is used to calculate the gamma index. Gamma index (1/W/m) are the fiber nonlinear coefficients [39].
4. Fiber nonlinear index (m^2/W) is described by the Kerr effect, where the refractive index changes in proportion to the optical intensity of the light as it propagates through the medium. The relationship between the fiber nonlinear index (n_2) and the nonlinear coefficient (γ) is given by

$$\gamma = \frac{2\pi n_2}{\lambda_0 A_{eff}}, \tag{3.2}$$

where A_{eff} and λ_0 are the fiber effective area and the laser beam's wavelength respectively.

5. Optical wavelength, represented by

$$\lambda = \frac{c}{v}, \tag{3.3}$$

is the wavelength of the laser beam. A wavelength of 1550 nm is used and it is considered a long wavelength [38].

6. Group Velocity Dispersion (GVD) has a unit of (ps/nm/km). An optical fiber having a positive GVD indicates that the frequency components spread out as the light propagates along the fiber. A negative GVD means that the frequency components move closer together as the light propagates.

7. Dispersion slope (ps/nm^2.km) causes different laser beams' wavelengths to experience different dispersions.

3.2 Proposed Adaptive Protection Strategy

Centralized and decentralized adaptive protection schemes were proposed in this thesis. The developed algorithms in the two schemes consist of several functions. Each function performs a task in the protection system. The tasks include:

- Current and voltage measurement
- Fundamental frequency phasor estimation using Fast Fourier Transform (FFT)
- Relay coordination using linear optimization
- Identification of current system topology
- Fault detection
- Fault direction estimation using negative-sequence directional element

3.2.1 Centralized Adaptive Protection System (CAPS)

In the CAPS, communication between the DGs and relays is always performed through a CRU as shown in Figure 3.1. First, current measurement is performed at each DG to determine the DG's connection status. Then, the generators' connection statuses are received at a CRU using a fiber optic communication channel utilizing the DNP3 protocol. The received analog signals are represented by a binary '1' or '0' in case the generator is connected or disconnected, respectively.

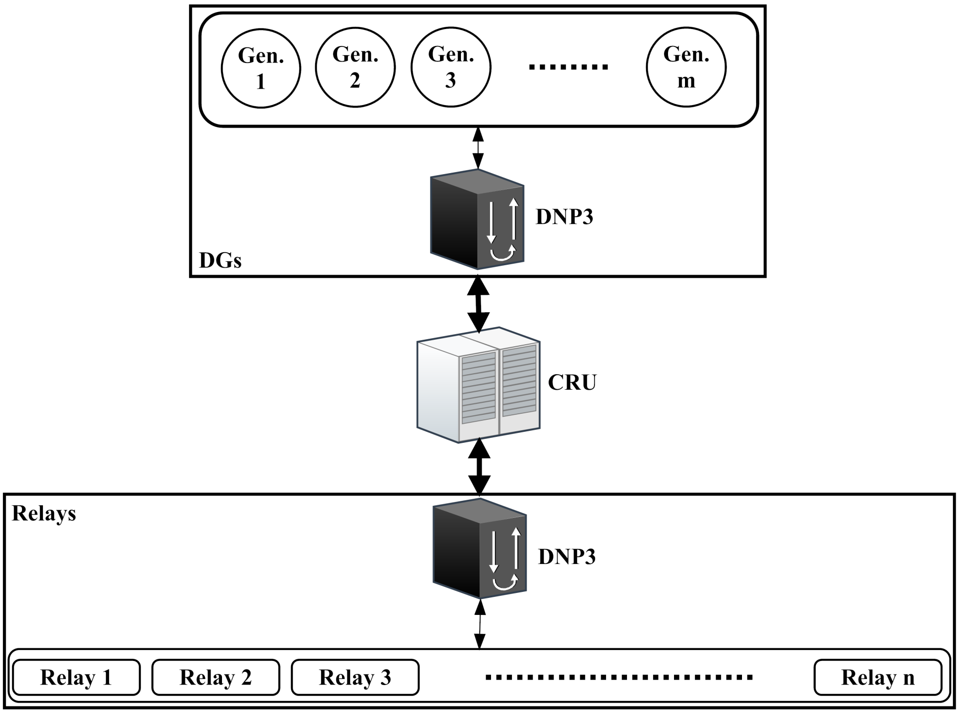

Figure 3.1: CAPS's communication topology.

The power distribution system's configuration is determined when all the connection signals are received at the CRU. After that, the determined configuration is compared to the stored system configuration. If the received configuration is changed, a database containing previously determined minimum and maximum fault currents measured by the relays during system fault analysis is used. The database provides the maximum load currents, maximum fault currents, and minimum fault currents for the existing system configuration. The fixed CT ratios are selected using 125% of the maximum load current at each relay. Also, the tap settings are changed based on the system configuration, and are selected using the load current at each relay.

Once the tap settings are determined, the objective function, given in Equation B.1, is formulated, and optimized based on the constraint equations B.4 and B.5. The coefficients of the objective equation are calculated using the tap setting values. Then, linear optimization, explained in Appendix B, is implemented to calculate the optimized TDS values for each relay. During linear optimization, the moderately inverse-time overcurrent relay characteristic is used. Then, the calculated TDS values and tap settings are communicated to the relays, using DNP3, to update their settings.

When a fault is close to the source, overcurrent relay protection systems may suffer from time delay in fault clearance due to relay coordination requirements. Therefore, a faulted section identification algorithm is proposed to speed up fault clearance. In the CAPS, the relays continuously check for fault occurrence. Once a fault is detected, the fault direction is identified using the negative sequence directional element explained in Appendix C and is implemented in the relays [40]. After that, the relays send their detected fault direction to the CRU using DNP3. The faulted section is identified when both relays at the beginning and end of that section see the fault in the forward direction. For example, the three line sections shown in Figure 3.2 are protected with directional relays at both ends, which can detect the direction of the fault in the second section. The relays in the first and third sections have different direction estimation. While only the relays in the second section see the fault in the forward direction.

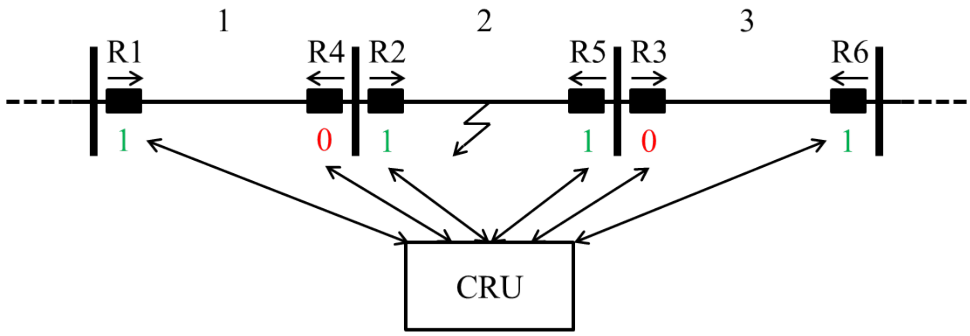

Figure 3.2: CAPS's faulted section identification.

Once the faulted section is identified, the CRU determines the optimal TDS values and tap settings for the faulted section and existing system configuration. The optimal settings are determined using previously constructed databases. The databases contain TDS values and tap settings for different combinations of fault locations and power system configurations. The determined TDS values and tap settings are sent to the relays, using DNP3, to update their protection settings, where the closest relays to the fault are prioritized. The new settings ensure that the closest relay is the fastest acting relay, and upstream relays have a minimum coordination time of 0.3 s. If ambiguity occurs during the faulted section detection, the system uses TDS values and tap settings determined prior to the faulted section identification algorithm. The flowchart of the proposed CAPS is shown in Figure 3.3.

The main advantage of a CAPS is simplicity of implementation. Also, there is no conflict in the decision taken. However, a CAPS has one point of failure. If the communication system between the DGs, relays, and CRU fails, the protection system does not get updates for any change in the power distribution system's configuration. But one solution is to mirror the central node.

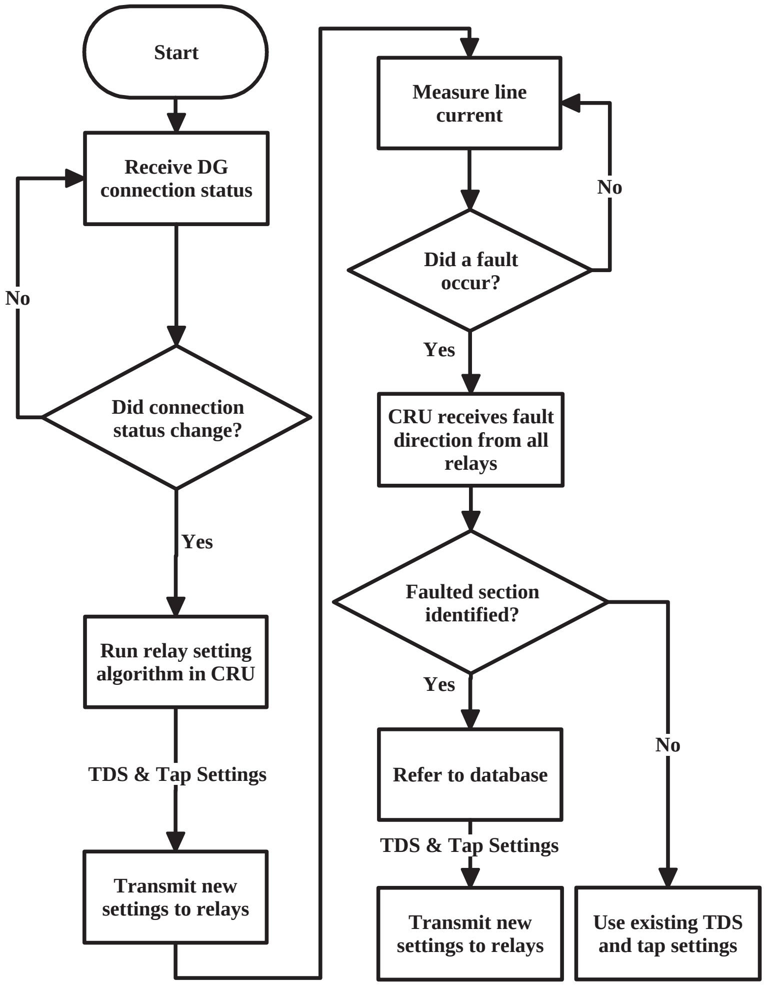

Figure 3.3: Flowchart of the CAPS.

3.2.2 Decentralized Adaptive Protection System (DAPS)

A decentralized communication-based adaptive protection system utilizing the DNP3 protocol is proposed. In the DAPS, data transmission of the tap settings, TDS values, and DG connection statuses is performed directly between all the devices in the power distribution system as shown in Figure 3.4.

3.2.2.1 Proposed MAS

A MAS is implemented in the decentralized adaptive protection technique as shown in Figure 3.5, where different agents handle different types of information.

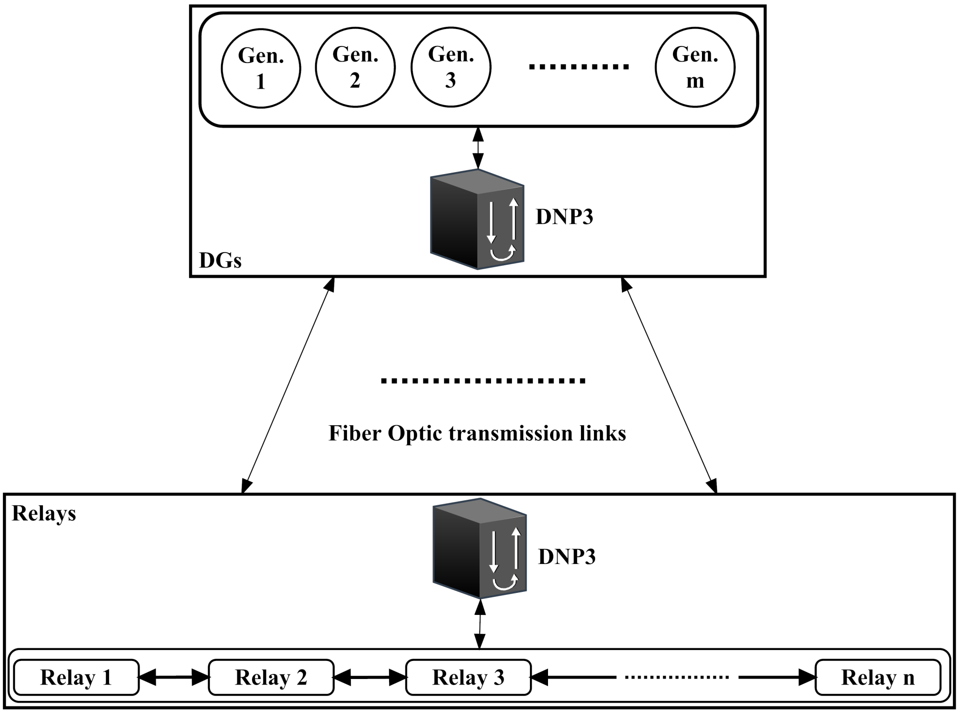

Figure 3.4: DAPS's communication topology.

The collaboration of the agents helps in coordinating the directional overcurrent relays. First, data measurement sub-agents are implemented in relays. Data measurement sub-agents measure the current and voltage at the relay location. The measured values are communicated to the protection sub-agent. Then, the protection sub-agent uses the currents and voltages to perform linear optimization. If a fault occurs, the protection sub-agent uses the optimal TDS values and tap settings to calculate the operation time delay. Then, the execution sub-agent sends a trip signal to the circuit breaker. In the DG agent, a DG connection sub-agent sends the DG's connection status to the relay agents. The communication sub-agents in relay and DG agents help facilitate the communication between the two agent communities.

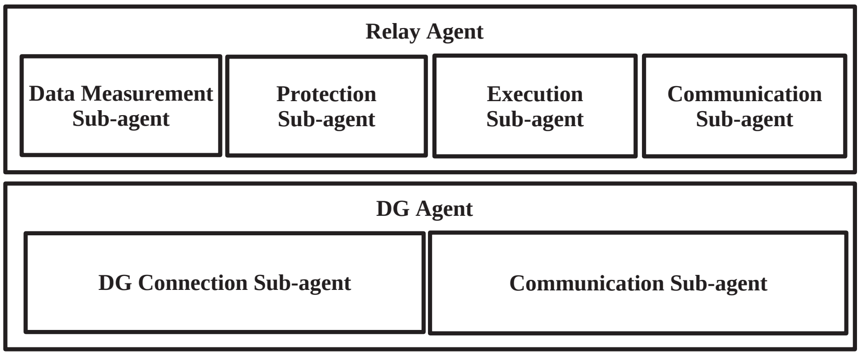

Figure 3.5: Proposed MAS.

3.2.2.2 Operation of the Proposed DAPS

In the DAPS, connection status signals from the Transmission Grid (TG) and DGs are transmitted to each relay present in the system using DNP3. Then, each relay determines the new configuration of the power distribution system. After that, the determined configuration is compared to the stored configuration. If the configuration is changed, each relay determines the tap setting value for the current configuration. Then, the calculation of the TDS values is performed at each relay using the linear optimization technique explained in Appendix B, and a 0.3 s coordination time is used. The calculated values are stored, and replace previous protection settings. As a result, the directional overcurrent relays become ready for new fault occurrence.

Similar to the CAPS, a faulted section identification algorithm is implemented in the DAPS to speed up fault clearance, and it is shown in Figure 3.6. During a fault, each downstream looking relay with respect to the TG sends a fault direction signal using the negative sequence impedance directional element to the previous downstream looking relay. Also, each upstream looking relay transmits the fault direction to the previous upstream looking relay. The relay that receives a reverse fault signal and has a forward fault direction is the closest relay to the fault. Then, the TDS values and tap settings are determined using a database for that relay and the two backup relays. The determined TDS values and tap settings are sent to the backup relays, using DNP3, through fiber optic communication. These values determine the clearance time of the backup relays in case the closest relay does not operate. Therefore, during a fault six relays are coordinated to minimize fault clearance time. The two closest relays to the fault (downstream and upstream looking) and two backup relays for each primary relay. Figure 3.7 shows the flowchart of the DAPS.

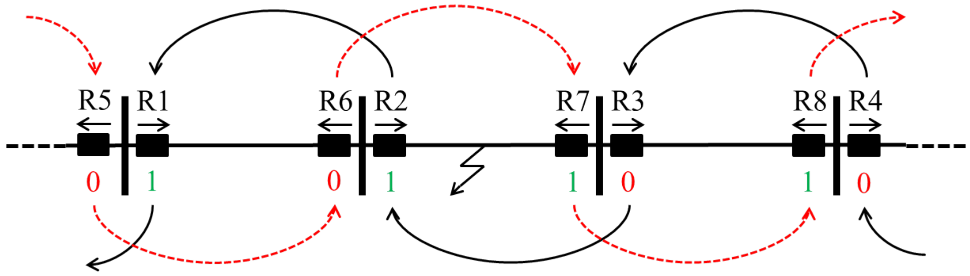

Figure 3.6: DAPS's faulted section identification.

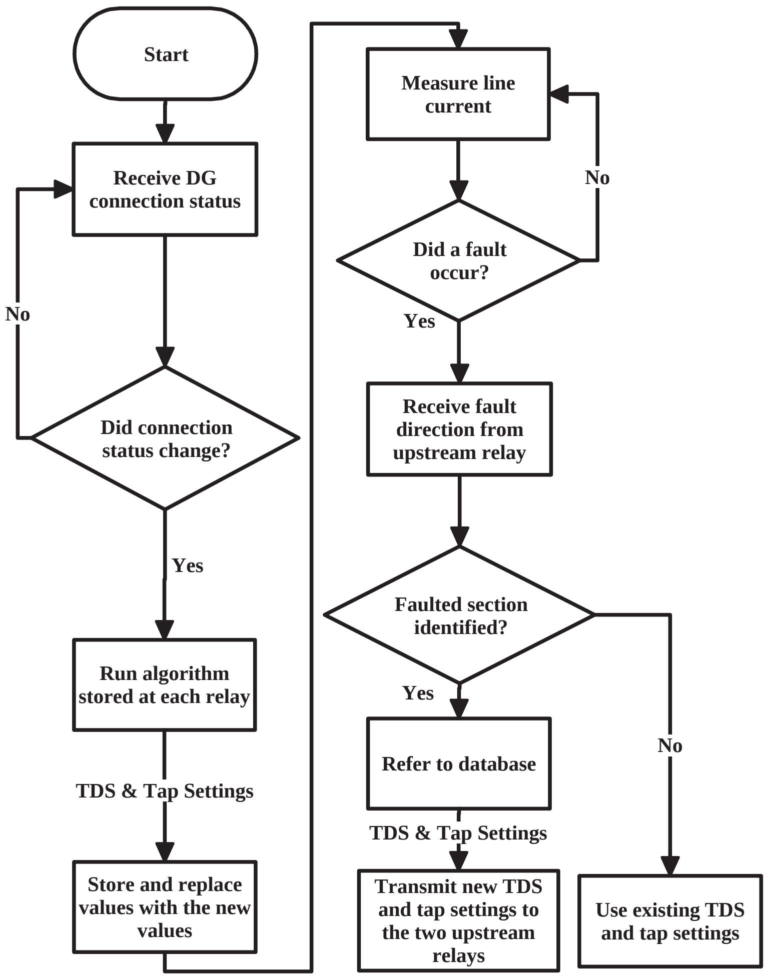

Figure 3.7: Flowchart of the DAPS.

If a communication failure occurs in a decentralized system, the system is able to partially perform adaptive protection. However, this technique requires higher traffic compared to a centralized technique, and more involvement for the communication protocol. Also, a decentralized technique requires a higher cost, because smarter units have to be employed in the system.

3.3 Backup Adaptive Protection System

The proposed adaptive protection system techniques are very communication dependent. If a communication failure occurs, the protection system can no longer be coordinated in the CAPS. While in the DAPS, the directional overcurrent relays are partially coordinated.

A backup non-communication based adaptive protection system is proposed. The flow chart of the backup technique is shown in Figure 3.8. The backup protection system operates only for a change in the power distribution system's configuration. Therefore, it does not utilize a faulted section identification algorithm. In the backup protection system, the power distribution system's configuration is determined using state detection algorithms utilizing local measurements [22]. Only two states are detected, which are normal and islanded operation modes because is a significant difference in the fault current between these two operation modes [22]. The backup protection system serves as a last line of defense, to limit the damage in case of a fault, until the communication network is back online.

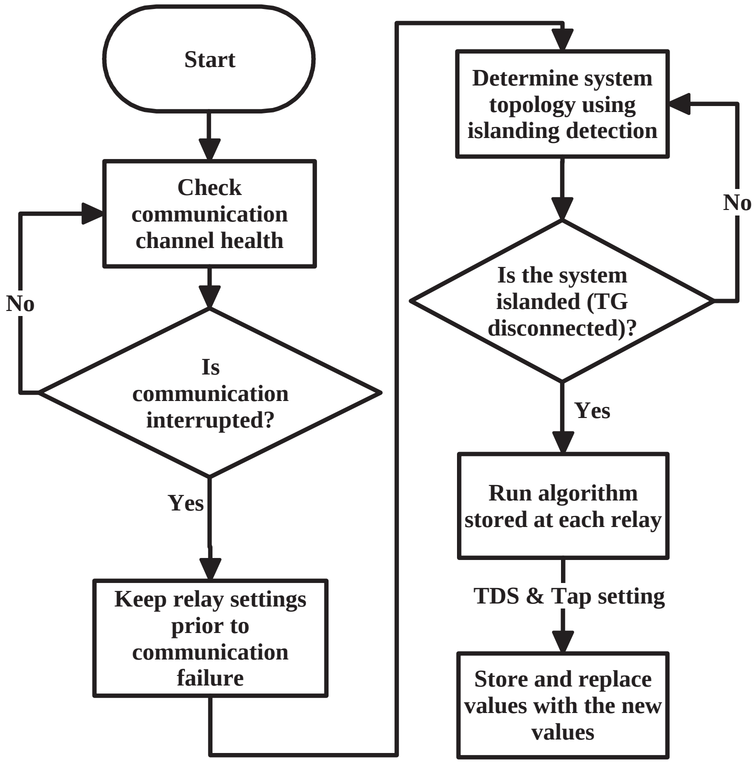

Figure 3.8: Flowchart of the backup adaptive protection system.

In the backup adaptive protection system, the communication channel's health is checked using DNP3 [41]. If communication is interrupted, protection settings prior to communication failure remain unchanged. Then, the configuration of the power distribution system is determined using islanding detection. After that, the backup protection system compares the detected configuration to the stored configuration. If the power system's configuration changes, the tap settings are changed and the TDS values at each relay are calculated using linear optimization. Finally, the calculated values are stored and replace previous protection settings.

3.4 Differences Between The Proposed Work and Existing Solutions

Previously proposed non-communication protection based systems use local measurements to estimate the state of the power distribution system [5, 6, 22, 31]. Therefore, they suffer from uncertainties when required to update the settings of protection relays. These adaptive protection systems take several assumptions into account such as neglecting the transients in the DG response during a fault, considering the fault current at the relay to be constant and equal to the steady state fault current value, and assuming the fault current seen by all relays protecting a feeder to be equal [5, 22]. These assumptions may affect the operation of the protection negatively. Thus, the introduction of communication based adaptive protection systems avoids uncertainties when determining the configuration of the power distribution system. Also, it increases the accuracy and reliability of the adaptive protection system.

Similar to non-communication based protection systems, most of the previously proposed communication-based adaptive protection systems use either distance or overcurrent relays [25, 23]. However, overcurrent relays are preferred in an adaptive protection system for their lower cost, wide range of characteristics, and simplicity of operation as previously discussed in Section 1.2.2.3. Also, some of the communication-based adaptive protection systems implement a multi-agent system [28, 27, 26]. In the multi-agent system, adaptive protection in the power distribution system is performed in a decentralized manner. The previously proposed multi-agent systems only present ideas on how to build a communication-based adaptive protection system. The communication simulations in [26] show that adaptive protection in power distribution systems penetrated with DGs can be achieved using communication. The communication based adaptive protection system proposed in this thesis is based on this assumption.

In this thesis, overcurrent relay coordination is performed according to the current configuration of the power distribution system. Also, centralized and decentralized communication techniques are proposed, and the advantages and disadvantages of each technique during fault clearance are demonstrated in Chapter 4. Moreover, using communication-based techniques enable the identification of the faulted section which can speed up the fault clearance process. The effectiveness of the faulted section identification is investigated in Chapter 4 when centralized or decentralized adaptive protection systems are used. Furthermore, in both techniques a simple linear optimization algorithm is implemented, where during faulted section identification the objective function and constraints are modified to ensure that the closest relays to the fault are the fastest acting relays. In addition, this thesis proposes a backup protection system that can be used during emergency situations when there is a communication failure.

Chapter 4

Results

The proposed centralized and decentralized adaptive protection strategies have been extensively tested under different operating conditions. This chapter has three main sections. The components of the system model used and its computer simulation are given in Section 4.1. The estimated communication time delay encountered in the proposed protection strategies is given in Section 4.2. The results of the proposed methodologies are given in Sections 4.3 and 4.4.

4.1 System Model

The power distribution system in [42] is used to test the proposed adaptive protection system. It is part of an existing distribution network, owned by Himmerlands Elforsyning, in Aalborg, Denmark. The single line diagram of the system is given in Figure 4.1 and its data in Tables 4.1, 4.2, 4.3, and 4.4. The power distribution system consists of ten buses connecting nine line sections, six loads, three Wind Turbine Generators (WTG), one TG, and one Combined Heat and Power (CHP) plant.

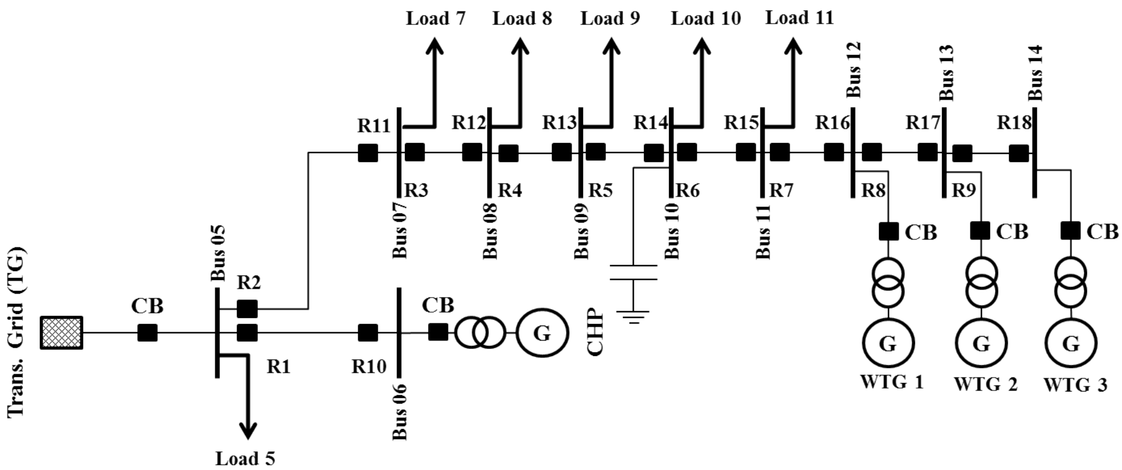

Figure 4.1: System Model.

Table 4.1: Transmission grid data.

Parameters	Value
Maximum short circuit power	10000 MVA
Minimum short circuit power	8000 MVA
Maximum R/X ratio	0.1
Maximum Z2/Z1 ratio	1.0
Maximum X0/X1 ratio	1.0
Maximum R0/X0 ratio	0.1

Table 4.2: Line data for the modeled system.

From Bus	To Bus	Resistance (Ω)	Reactance (Ω)
5	6	0.1256	0.1404
5	7	0.1344	0.0632
7	8	0.1912	0.0897
8	9	0.4874	0.2284
9	10	0.1346	0.0906
10	11	1.4555	1.1130
11	12	0.6545	0.1634
12	13	0.0724	0.0181
13	14	0.7312	0.3114

Table 4.3: Generators data.

Parameters	CHP	WTG
Type of generator	Synchronous	Asynchronous
Number of Parallel Machine	3	1
Transformer to connect to grid	3.3 MVA 20/6.3 kV	630 kVA 20/0.4 kV
Individual generator's rating		
Rated Power	3.3 MW	630 kW
Rated Voltage	6.3 kV	0.4 kV
Stator resistance	0.0504 pu	0.018 pu
Stator Reactance	0.1 pu	0.015 pu
Synchronous reactance d-axis	1.5 pu	
Synchronous reactance q-axis	0.75 pu	
Transient reactance d-axis	0.256 pu	
Sub-transient reactance d-axis	0.168 pu	
Sub-transient reactance q-axis	0.184 pu	
Transient time constant d-axis	0.53 s	
Sub-transient time constant d-axis	0.03 s	
Sub-transient time constant q-axis	0.03 s	
Mag. Reactance		4.42 pu
Rotor Resistance		0.0108 pu
Rotor Reactance		0.128 pu
Inertia Time Constant	0.54 s	0.38 s

Table 4.4: Load and generation data.

Bus	PG (MW)	QG (Mvar)	PL (MW)	QL (Mvar)
05	0.00	0.00	3.87	0.85
06	6.00	0.00	0.00	0.00
07	0.00	0.00	0.56	0.11
08	0.00	0.00	0.56	0.11
09	0.00	0.00	0.55	0.10
10	0.00	1.50	0.85	0.20
11	0.00	0.00	0.51	0.13
12	0.31	0.00	0.00	0.00
13	0.31	0.00	0.00	0.00
14	0.31	0.00	0.00	0.00
Total	6.93	1.5	6.9	1.5

The power distribution system is modeled in PSCAD/EMTDC, and it is shown in Figures A.1, A.2, and A.3. Also, the transformer model used to connect the CHP plant and WTGs to the system is shown in Figure 4.2 and its data in Table 4.5. In the adaptive protection system, eighteen directional overcurrent relays are used, where each line section is protected by two directional overcurrent relays. Furthermore, fault analysis for different fault locations, fault types, and connection statuses of the DGs is performed using PSCAD/EMTDC. During fault analysis, PSCAD/EMTDC's multiple run component, shown in Figure 4.3, is used to vary the fault location and the DGs' connection statuses. In addition, the fault type is varied manually by specifying an integer corresponding to the 'fault type' in the fault module shown in Figure 4.4. Afterwards, fault currents measured by the relays are saved using PSCAD/EMTDC's Real Time Playback (RTP) and Common format for Transient Data Exchange for power systems (COMTRADE) recorder shown in Figure 4.5. Finally, fault analysis data is stored in databases which are used in MATLAB to develop the proposed adaptive protection system.

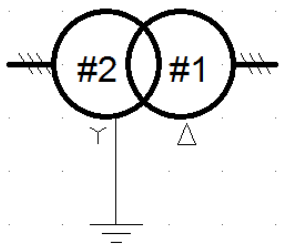

Figure 4.2: Transformer model.

Table 4.5: Transformer model data.

Base operating frequency	50 Hz
Primary winding type	Delta
Secondary winding type	Wye
Positive sequence leakage reactance	0.1 pu
No load losses	0.001 pu
Copper losses	0.002 pu
Air core reactance	0.2 pu
In rush delay time constant	1 s
Knee voltage	1.25 pu
Time to release flux clipping	0.1 s

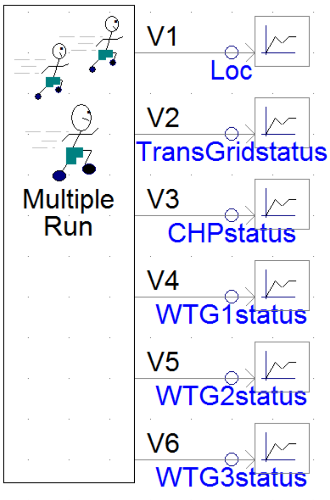

Figure 4.3: Multiple run module.

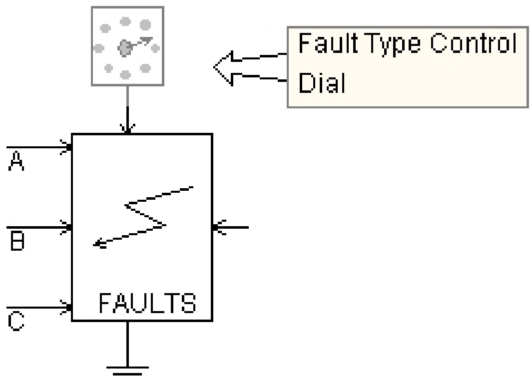

Figure 4.4: Fault module.

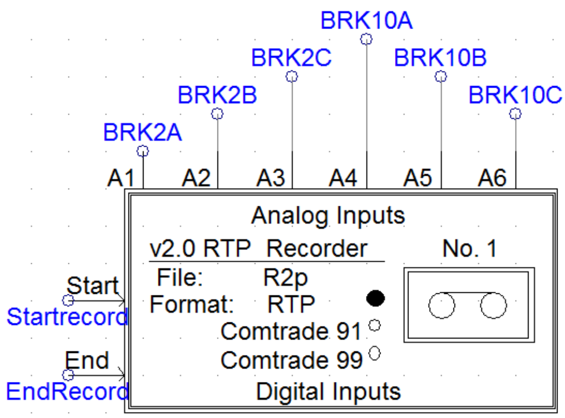

Figure 4.5: RTP and COMTRADE recorder.

4.2 Communication Time Delay

In what follows, we describe the simulation setup and the computation of time-delay using Optilux, a MATLAB optical fiber simulation toolbox [39]. Table 4.6 shows the parameters used during the simulations.

Table 4.6: Fiber simulation parameters.

Parameter	
Data size	64 bytes
Attenuation	$0.2\,\mathrm{dB\,km^{-1}}$
Effective area	$80\,\mu\mathrm{m}^2$
Fiber nonlinear index	$2.7 \times 10^{-20}\,\mathrm{m^2\,W^{-1}}$
optical wavelength	1550 nm
GVD	17 ps/nm/km
Dispersion slope	$0\,\mathrm{ps/nm^2.km}$

The proposed adaptive protection system includes 18 directional overcurrent relays and 5 generators. The addresses of DGs, relays, and CRU in the protection system were defined using a 16-bit address for each device. The addresses of the relays start from 6 to 23, and the first five addresses are reserved for the generators.

4.2.1 Centralized Adaptive Protection System (CAPS)

In the CAPS, the transmitted data is formatted using DNP3 by applying the operation guidelines in [41]. Furthermore, the data transmitted between the CRU and the relays includes fault direction signals, TDS values, and relay tap settings. For instance, the formatting of the communicated data using DNP3 at the application layer is as follows:

- Application Request Header
  - Application Control (1 octet): E0
  - Function Code (1 octet): 02
- Object Header (4 bytes)
  - Object Type Field - Group (1 octet): 42
  - Object Type Field - Variation (1 octet): 01
  - Qualifier Field (1 octet): 01
  - Range Field (1 octet): 11
- DNP3 Objects
  - 32-bit data

Afterwards, the information is passed to the transport layer and a transport header having a value 'C0' is added. At the data link layer, a header block and a 16-bit Cyclic Redundancy Check (CRC) are added to the user data. The formation of the data at the transport and data link layers is as follows:

- Header Block
  - Start (2 octets): 05 64
  - Length (1 octet): 80
  - Control (1 octet): D3
  - Destination (2 octets): 06 00
  - Source (2 octets): 00 00
  - CRC (2 octets)
- User data
  - CRC (2 octets)

After formatting the data, the average communication time delay to transmit one fault direction signal from a relay to the CRU is calculated by varying the relay's address and fault direction signal, and it was computed to be 1.6384 µs. The average communication time delay for TDS and tap settings transmission, from the CRU to the relay, is calculated by varying the relay's address, TDS values, and tap settings. The average time delay was calculated to be 1.6400 µs.

In the CAPS, when a fault occurs each relay transmits the detected fault direction to the CRU as shown in Figure 4.6. At the CRU, the fault direction signals are received in sequence. As a result, the time delay due to a fault direction signal transmission during a fault occurs at eighteen instances.

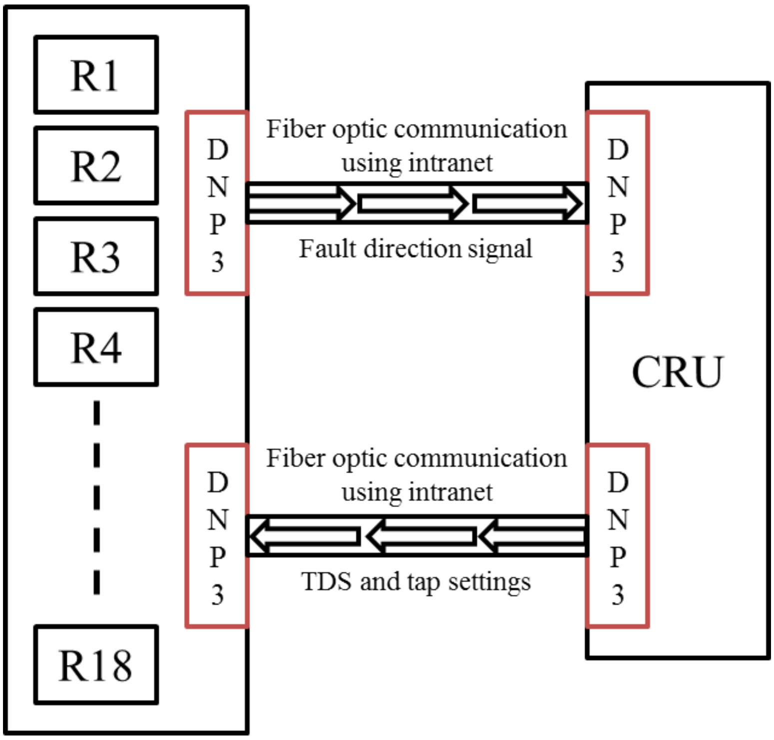

Figure 4.6: CAPS communication model.

Once all the fault direction signals are received and the faulted section is identified, the tap settings and TDS values are transmitted from the CRU to the relays. As a result, this process adds another time delay to the faulted section identification algorithm. The total communication time delay is computed to be 59.0112 µs.

4.2.2 Decentralized Adaptive Protection System (DAPS)

In the DAPS, the communication between the DGs and the overcurrent relays is trigger-based. The DGs send their statuses whenever a change occurs to their own connection. Furthermore, the DG's connection status is transmitted to the nearest relay. At the relay, the received data is stored and transmitted to the next relay along the transmission line. In this case, only transmission time delay is taken into account, and the time to store and transmit the data in the relay is assumed to be negligible.

During the faulted section identification algorithm, two communication possibilities can be used. First, the closest relay to the fault transmits the TDS values and tap settings to both backup relays. Second, the closest relay to the fault transmits the values to the first backup relay. Then, the first backup relay passes the TDS values and tap settings to the secondary backup relay.

During a fault, each downstream looking relay with respect to the TG transmits a fault direction signal to the previous downstream looking relay as shown in Figure 4.7. Also, each upstream looking relay with respect to the TG transmits a fault direction signal to the previous upstream looking relay. At the same time, each relay receives a direction signal from the next relay in their respective directions. The time delay due to fault direction signal transmission occurs twice during a fault. Therefore, a time delay of 6.5472 µs is added during the faulted section identification algorithm.

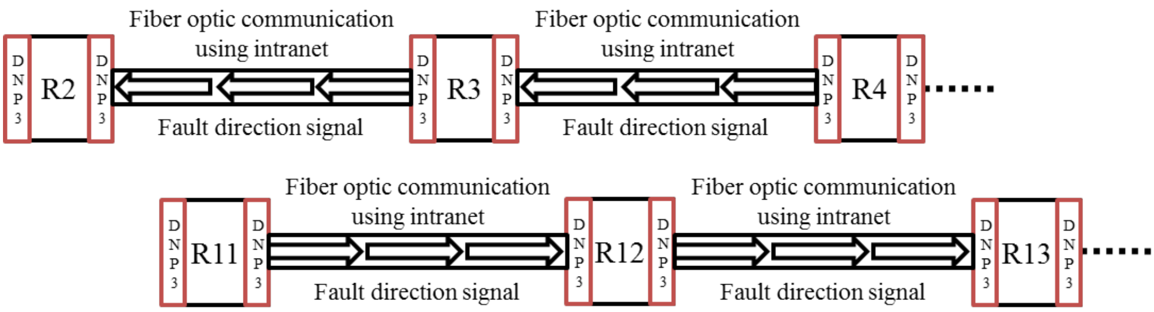

Figure 4.7: DAPS communication model.

Once the faulted section is identified, the TDS values and tap setting transmission is simulated after formatting the data using DNP3. The user data contains the new protection settings to be stored in the relays. The data is transmitted from the primary relay to the first backup relay, and then it is forwarded to the second backup relay. The communication delay is calculated to be 3.2736 µs. Therefore, the total communication time delay in a decentralized adaptive protection system, during a fault, is 9.8208 µs.

4.2.3 DNP3 Processing Time

When DNP3 processing time is taken into account, the total communication time delay in the centralized adaptive protection system during the faulted section identification is 244.9270 ms. Whereas the total communication time delay in the decentralized adaptive protection system during the faulted section identification is 22.6938 ms.

4.2.4 Internet Communication Delay

If communication using intranet fails, as demonstrated in Figure 4.8, then the Internet could be used as a backup for communication between DGs, relays, and the CRU. Consequently, the worst case Round-Trip Time (RTT) using the Internet is calculated. The RTT calculates the longest time taken for data transmission over the Internet. It ensures that the adaptive protection system responds in a timely manner during fault occurrence. Also, it helps justify implementing a faulted section detection algorithm when intranet is not functional.

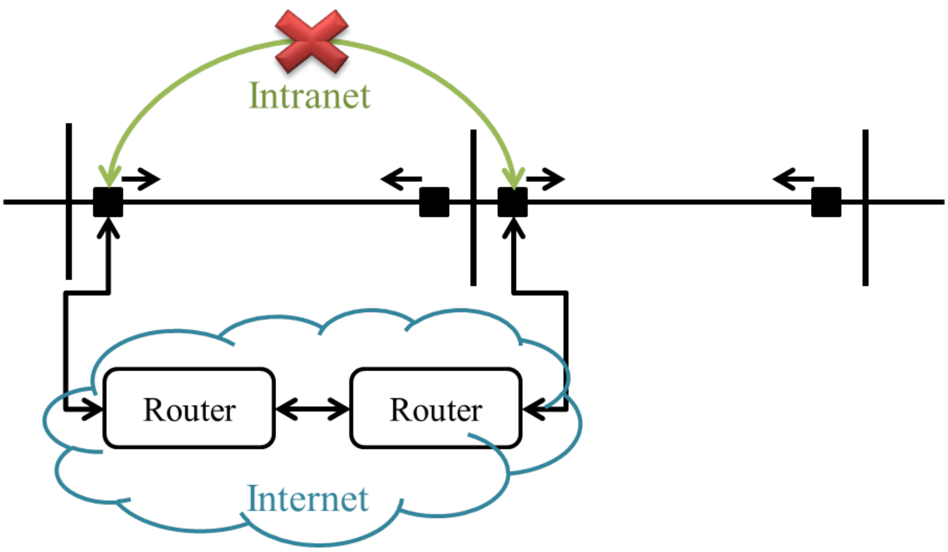

Figure 4.8: Disruption in intranet communication.

The RTT calculations are performed for the network shown in Figure 4.9. The network follows the IEEE803.2 standard, and consists of three 100Base-FX segments each of length 2 km and two Class II repeaters with all ports TX/FX. The RTT calculations are performed according to the guidelines provided in [32].

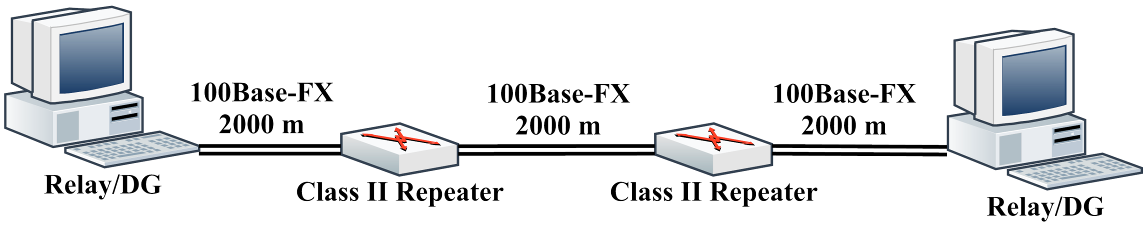

Figure 4.9: Internet communication network.

Table 4.7 shows the end-to-end delay in bit time, and a safety margin of 4 bit times is added. The safety margin adds an extra headroom to make sure the communication time delay is still acceptable even if an unexpected delay in the network occurs. From the table, the total RTT is converted from bit times to seconds. First, the calculated total RTT is multiplied by 64 bytes, which is the minimum transmission unit over the Internet. Then, it is divided by the channel speed, which is 100 Mbps. The total RTT and the channel propagation delay introduce a communication time delay of 0.9779 ms. Therefore, the total communication time delay using the Internet for the CAPS during faulted section identification is 264.4264 ms. Also, the total communication time delay for the DAPS during faulted section identification is 25.6178 ms.

Table 4.7: RTT delay calculation.

Equipment	RT delay
Class II Repeater with all ports TX/FX	92
Class II Repeater with all ports TX/FX	92
Safety margin	4
Total	188 bit times

4.3 Simulation of the Proposed Adaptive Protection Systems

Different simulation cases were performed to test the performance of the proposed adaptive protection schemes. Simulations include relay setting update for system configuration change, faulted section identification, and safe islanding operation. The simulations cases were performed to test both centralized and decentralized techniques, and are as follows:

- Case 1: CHP plant is disconnected from the power distribution system.
- Case 2: Single-Line to Ground (SLG) on line 8-9 when CHP is disconnected.
- Case 3: SLG fault on line 8-9 when all generators are connected.
- Case 4: Line-to-Line (LL) fault on line 8-9 when all generators are connected.
- Case 5: SLG fault on line 11-12 when all generators are connected.
- Case 6: Double-Line to Ground (DLG) fault on line 8-9 when WTG1 is disconnected.
- Case 7: DLG on line 11-12 when CHP is disconnected.
- Case 8: SLG fault on line 8-9 when all WTGs are disconnected.
- Case 9: SLG fault on line 8-9 when TG is disconnected (islanded mode).
- Case 10: SLG fault on line 11-12 when TG is disconnected (islanded mode).

4.3.1 Centralized Adaptive Protection System (CAPS)

4.3.1.1 CHP Plant is Disconnected from the Power Distribution System

In the first simulation case, the system was operating under normal power system conditions where all the generators are connected to the power distribution system. Then, the CHP plant, which is connected to bus 6, is disconnected. Consequently, the CHP sends its connection status signal to the CRU. The transmitted connection status signal is formatted using DNP3. After that, the CRU determines the new power distribution system configuration, and the new tap settings and TDS values are computed using the linear optimization technique explained in Appendix B. Finally, the new protection settings are transmitted to the relays after being formatted using DNP3. Table 4.8 shows the TDS values and tap settings before and after the power system configuration change. In the table, the TDS values are adjusted to maintain fast fault clearance during the new power system configuration. Therefore, the TDS values are decreased to account for the decrease in the fault current level when the CHP plant is disconnected.

Table 4.8: Centralized: CHP is disconnected.

	Before configuration change		After configuration change	
Relay	Tap setting	TDS	Tap setting	TDS
1	4.9	0.2494	0.1	0.3469
2	0.5	3.8172	0.5	3.8143
3	2.4	3.0920	2.4	3.0897
4	2.0	2.6085	2.0	2.6068
5	1.9	2.1294	1.9	2.1280
6	2.1	1.5741	2.1	1.5731
7	4.0	1.0191	4.0	1.0184
8	2.7	0.6228	2.7	0.6224
9	1.8	0.1307	1.8	0.1307
10	4.9	0.1471	10.0	9.7920
11	3.2	0.1146	3.2	0.1146
12	2.9	0.4713	2.9	0.4709
13	2.6	0.9086	2.6	0.9078
14	2.2	1.4129	2.2	1.4118
15	3.2	1.8697	3.2	1.8682
16	4.0	2.2438	4.0	2.2420
17	3.6	2.7216	3.6	2.7194
18	2.7	3.2696	2.7	3.2699

4.3.1.2 SLG Fault at Line 8-9 with CHP Disconnected

When a SLG fault occurs on line 8-9 while the CHP is disconnected, the relays determine the fault direction, using the negative sequence directional element explained in Appendix C, and transmit the signals to the CRU using DNP3. The CRU determines the faulted section, as previously explained in Section 3.2.1, once all the fault direction signals are received. Then, the new relay settings are retrieved from databases containing TDS values and tap settings for various fault locations and power system configurations. Finally, the new protection settings are formatted using DNP3, and are sent to the overcurrent relays to speed up fault clearance. Furthermore, overcurrent relays R4 and R13 are the first to receive the new protection settings. Table 4.9 shows the relays' TDS values, tap settings, and operation times for a SLG fault on line 8-9 when CHP is disconnected. The table gives the TDS and operating time with and without faulted section identification algorithm. In this table, the TDS values and tap settings are adjusted to maintain the operation times as small as possible without violating the coordination constraints specified.

The faulted section identification algorithm reduces the operation times of relays R4 and R13 from 1.3922 s and 0.7414 s to 0.0947 s and 0.1019 s, respectively. Furthermore, the backup relays, R3 and R2, for the downstream looking relay with respect to the TG, R4, are coordinated using a minimum coordination time of 0.3 s. Similarly, the backup relays, R14 and R15, for the upstream looking relay with respect to the TG, R13, are also coordinated using a minimum coordination time of 0.3 s.

Table 4.9: Centralized: SLG fault at line 8-9 with CHP disconnected.

		Faulted section is not identified		Faulted section is identified	
Relay	Tap setting	TDS	Operation time (s)	TDS	Operation time (s)
1	0.1	0.3469	No operation	10.9677	No operation
2	0.5	3.8142	2.2013	1.5978	0.9222
3	2.4	3.0897	1.7476	0.8149	0.4609
4	2.0	2.6068	1.3922	0.1773	0.0947
5	1.9	2.1280	Blocked	5.5500	Blocked
6	2.1	1.5731	Blocked	5.5500	Blocked
7	4.0	1.0184	Blocked	5.5500	Blocked
8	2.7	0.6224	Blocked	5.5500	Blocked
9	1.8	0.1307	Blocked	5.5500	Blocked
10	10.0	9.7920	No operation	0.1000	No operation
11	3.2	0.1146	Blocked	5.5500	Blocked
12	2.9	0.4709	Blocked	5.5500	Blocked
13	2.6	0.9078	0.7414	0.1247	0.1019
14	2.2	1.4118	1.0673	0.5410	0.4090
15	3.2	1.8682	1.4026	0.9369	0.7034
16	4.0	2.2420	1.7721	1.2831	1.0142
17	3.6	2.7194	2.1634	1.7025	1.3545
18	2.7	3.2699	2.6155	2.2214	1.7785

'No operation' indicates that the current seen by the relay is less then the pickup current. In this case, R1 and R10 show 'No operation' since the CHP plant is disconnected. In addition, 'Blocked' indicates that the current seen by the overcurrent relay is above the pickup current but the negative sequence directional element detects a reverse fault.

4.3.1.3 SLG Fault at Line 8-9 with All Generators Connected

The operation of the CAPS is investigated under normal operation. Table 4.10 shows the relays' TDS values, tap settings, and operation times for a SLG fault on line 8-9 when all the generators are connected.

Table 4.10: Centralized: SLG fault at line 8-9 with all generators connected.

		Faulted section is not identified		Faulted section is identified	
Relay	Tap setting	TDS	Operation time (s)	TDS	Operation time (s)
1	4.9	0.2494	Blocked	0.2494	Blocked
2	0.5	3.8172	1.9111	1.5026	0.8665
3	2.4	3.0920	1.5816	0.7900	0.4465
4	2.0	2.6085	1.2811	0.1675	0.0894
5	1.9	2.1294	Blocked	5.5500	Blocked
6	2.1	1.5741	Blocked	5.5500	Blocked
7	4.0	1.0191	Blocked	5.5500	Blocked
8	2.7	0.6228	Blocked	5.5500	Blocked
9	1.8	0.1307	Blocked	5.5500	Blocked
10	4.9	0.1471	No operation	0.3307	No operation
11	3.2	0.1146	Blocked	5.5500	Blocked
12	2.9	0.4713	Blocked	5.5500	Blocked
13	2.6	0.9086	0.6908	0.1245	0.1015
14	2.2	1.4129	0.9938	0.5699	0.4304
15	3.2	1.8697	1.3003	1.0228	0.7672
16	4.0	2.2438	1.6308	1.4377	1.1354
17	3.6	2.7216	1.9642	1.9222	1.5278
18	2.7	3.2696	2.2998	2.4774	1.9816

From the table, it is noticed that the faulted section identification algorithm speeds up the fault clearing process. This helps further minimize damage to equipment connected to the power distribution system. Hence, the operation times for relays R4 and R13 are reduced from 1.2811 s and 0.6908 s to 0.0894 s and 0.1015 s, respectively. Figure 4.10 shows that the fault current is cleared after 0.3465 s including a communication time delay of 0.2449 s, where the fault is applied at 0.4 s and the breaker for R13 opens at 0.7465 s. Additionally, Figure 4.11 shows the change in the TDS curves when the faulted section is identified and the relays' settings are updated. In the figure, the TDS curves with the solid lines are the relay settings during normal fault clearance operation. The TDS curves with the dashed lines are the relay settings when the faulted section identification algorithm is used.

4.3.1.4 LL Fault at Line 8-9 with All Generators Connected

A LL fault is applied on line 8-9 when all the generators are connected. Compared to Section 4.3.1.3, this case highlights the effect of changing the fault type on the CAPS under normal operation. Table 4.11 illustrates the relays' TDS values, tap settings, and operation times.

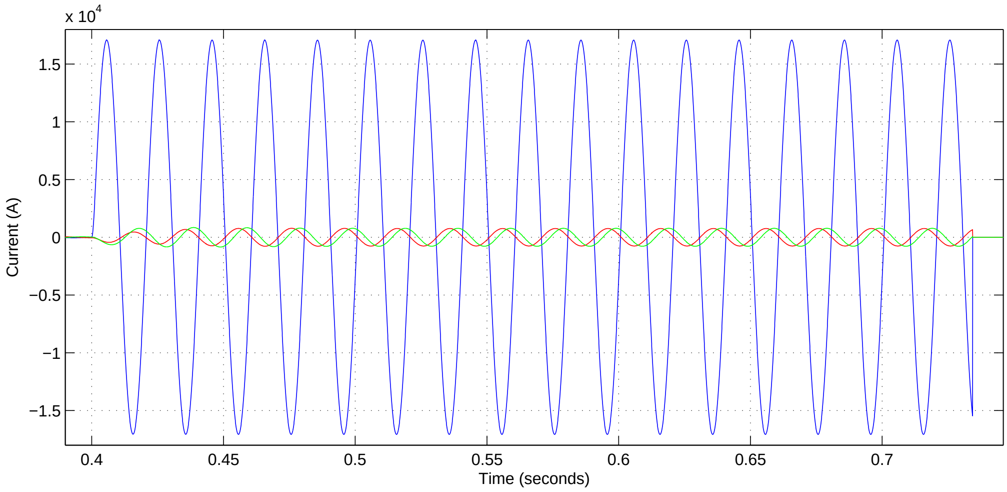

Figure 4.10: Fault current at relay R4 for a SLG fault on line 8-9 when all generators are connected.

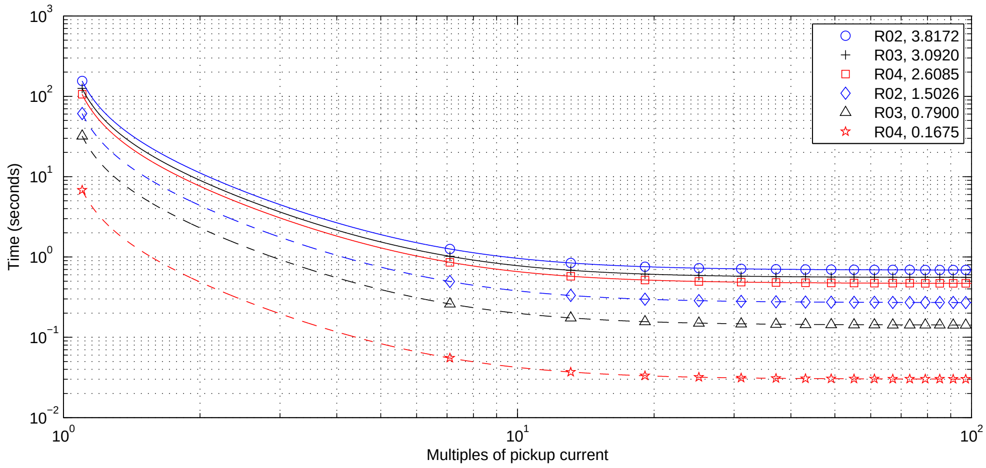

(a) Downstream looking relays' TDS curves.

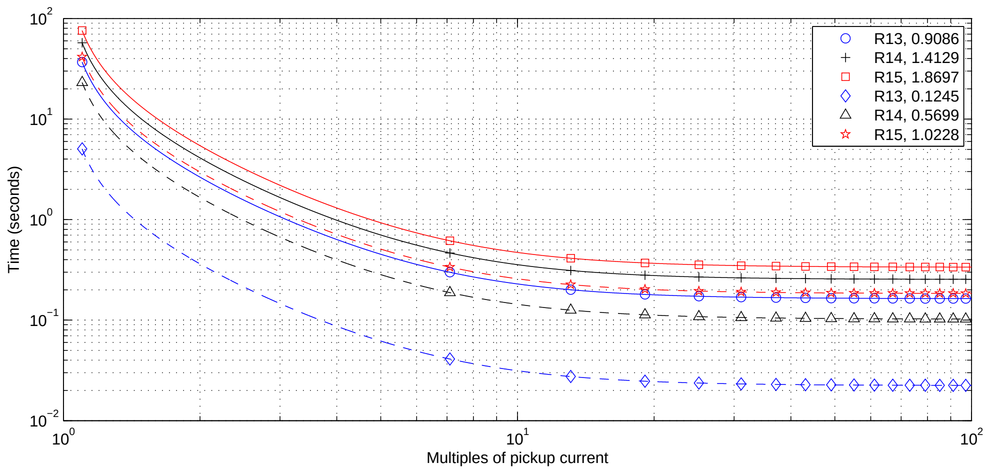

(b) Upstream looking relays' TDS curves.

Figure 4.11: Upstream and downstream TDS curves for a SLG fault on line 8-9 with all generators connected.

Table 4.11: Centralized: LL fault at line 8-9 with all generators connected.

		Faulted section is not identified		Faulted section is identified	
Relay	Tap setting	TDS	Operation time (s)	TDS	Operation time (s)
1	4.9	0.2494	Blocked	0.2494	Blocked
2	0.5	3.8172	2.2514	1.5026	0.8862
3	2.4	3.0919	1.7863	0.7900	0.4564
4	2.0	2.6085	1.4207	0.1675	0.0912
5	1.9	2.1294	Blocked	5.5500	Blocked
6	2.1	1.5741	Blocked	5.5500	Blocked
7	4.0	1.0191	Blocked	5.5500	Blocked
8	2.7	0.6228	Blocked	5.5500	Blocked
9	1.8	0.1307	Blocked	5.5500	Blocked
10	4.9	0.1471	No operation	0.3307	No operation
11	3.2	0.1146	Blocked	5.5500	Blocked
12	2.9	0.4713	Blocked	5.5500	Blocked
13	2.6	0.9086	0.8298	0.1245	0.1137
14	2.2	1.4129	1.1837	0.5699	0.4774
15	3.2	1.8697	1.5605	1.0228	0.8536
16	4.0	2.2438	1.9901	1.4377	1.2751
17	3.6	2.7216	2.4277	1.9222	1.7146
18	2.7	3.2696	2.9271	2.4774	2.2179

In the table, overcurrent relay operation times are slightly longer compared to Section 4.3.1.3 because a larger fault current flow in the power distribution system during a SLG fault. However, the operation time for the faulted section detection algorithm is much faster compared to regular operation during the LL fault.

4.3.1.5 SLG Fault at Line 11-12 with All Generators Connected

In this simulation case, the effect of changing the fault location, during normal operation, on the CAPS is illustrated. The relays' TDS values, tap settings, and operation times for a SLG fault on line 11-12 when all the generators are connected are recorded in Table 4.12.

Table 4.12: Centralized: SLG fault at line 11-12 with all generators connected.

		Faulted section is not identified		Faulted section is identified	
Relay	Tap setting	TDS	Operation time (s)	TDS	Operation time (s)
1	4.9	0.2494	Blocked	0.2494	Blocked
2	0.5	3.8172	2.8723	2.9247	2.2007
3	2.4	3.0920	2.2635	2.2558	1.6514
4	2.0	2.6085	1.7645	1.7392	1.1765
5	1.9	2.1294	1.3604	1.2204	0.7797
6	2.1	1.5741	0.9955	0.6533	0.4132
7	4.0	1.0191	0.6739	0.1319	0.0872
8	2.7	0.6228	Blocked	5.5500	Blocked
9	1.8	0.1307	Blocked	5.5500	Blocked
10	4.9	0.1471	No operation	0.5049	No operation
11	3.2	0.1146	Blocked	5.5500	Blocked
12	2.9	0.4713	Blocked	5.5500	Blocked
13	2.6	0.9086	Blocked	5.5500	Blocked
14	2.2	1.4129	Blocked	5.5500	Blocked
15	3.2	1.8697	Blocked	5.5500	Blocked
16	4.0	2.2438	1.6276	0.1532	0.1111
17	3.6	2.7216	1.9860	0.6565	0.4791
18	2.7	3.2696	2.3995	1.2304	0.9030

Using the faulted section identification algorithm, the faulted section is identified and the directional overcurrent relays' settings are adjusted. Furthermore, the closest relays to the fault are the first to react and clear the fault. In Section 4.3.1.3, relays R4 and R13 are the fastest relays, whereas in Section 4.3.1.5 relays R7 and R16 are the fastest relays. Figure 4.12 shows fault current clearance by the closest relays, R7 and R16, after 0.3560 s including a communication time delay of 0.2449 s. In addition, Figure 4.13 shows the TDS curves during normal fault clearance operation and when the faulted section identification algorithm is used.

4.3.1.6 DLG Fault at Line 8-9 with WTG1 Disconnected

Also, the effect of disconnecting WTG1 on the CAPS is investigated. A DLG fault is applied on line 8-9, and Table 4.13 presents the relays' TDS values , tap settings, and operation times. The table shows only the settings of the primary and the two backup relays in both directions. The omitted relays are either not operating or blocked.

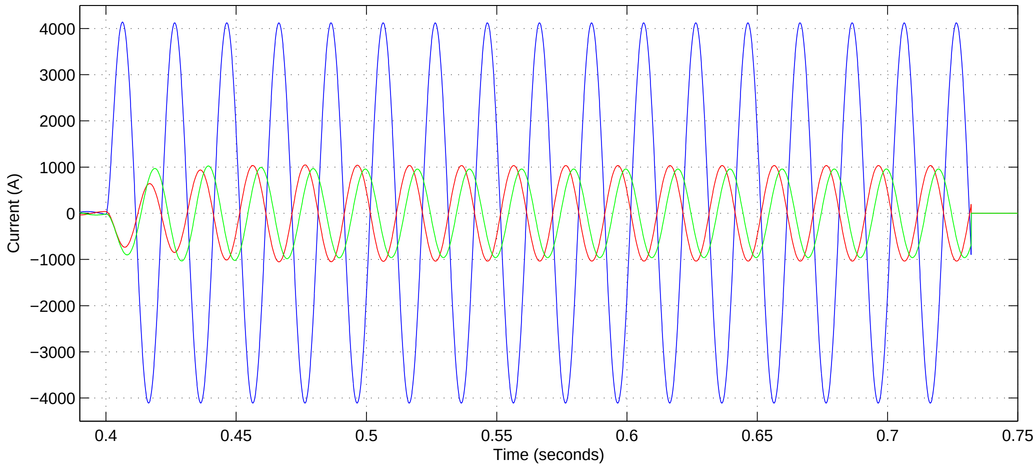

Figure 4.12: Fault current at relay R7 for a SLG fault on line 11-12 when all generators are connected.

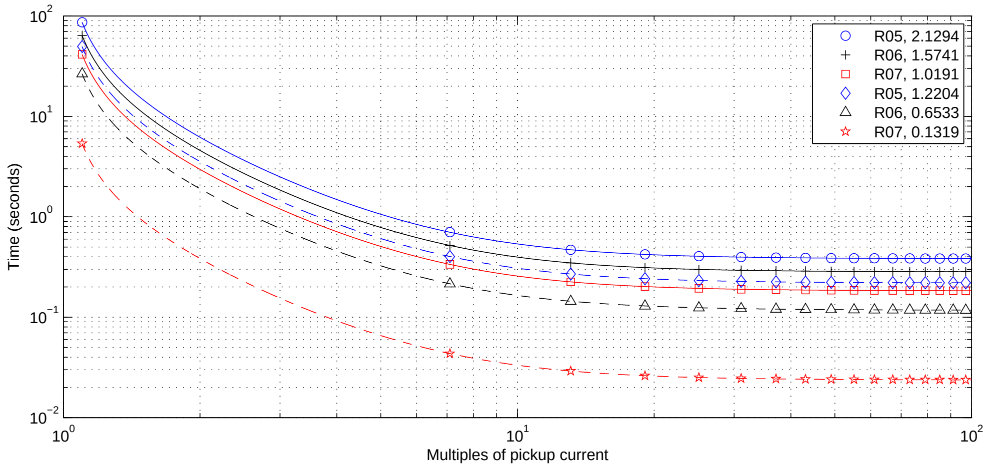

(a) Downstream looking relays' TDS curves.

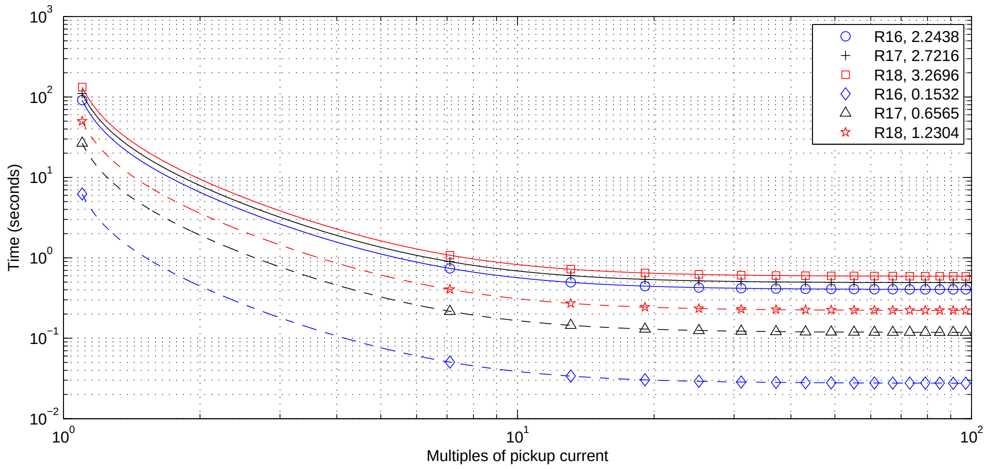

(b) Upstream looking relays' TDS curves.

Figure 4.13: Upstream and downstream TDS curves for a SLG fault on line 11-12 with all generators connected.

Table 4.13: Centralized: DLG fault at line 8-9 with WTG1 disconnected.

		Faulted section is not identified		Faulted section is identified	
Relay	Tap setting	TDS	Operation time (s)	TDS	Operation time (s)
2	0.6	3.2202	1.9131	1.5786	0.9378
3	2.9	2.7169	1.5824	0.8044	0.4685
4	2.6	2.3108	1.2820	0.1746	0.09684
13	3.4	0.7520	0.7425	0.1209	0.1194
14	3.1	1.1538	1.0571	0.5054	0.4630
15	2.2	1.7980	1.3591	1.0633	0.8038

This simulation case reveals the algorithm's behavior for another system configuration change followed by a fault. In the table, the tap settings are adjusted for the new configuration to maintain an optimized and coordinated protection system. Moreover, the TDS values are changed according to the identified faulted section to speed up the fault clearance.

4.3.1.7 DLG Fault at Line 11-12 with CHP Disconnected

In this simulation case, the effect of changing the fault location is investigated during DG disconnection. The relays' TDS values, tap settings, and operation times for a DLG fault on line 11-12 when CHP is disconnected are shown in Table 4.14. Furthermore, the table shows only the settings of the primary and the two backup relays in both directions. The omitted relays are either not operating or blocked.

Table 4.14: Centralized: DLG fault at line 11-12 with CHP disconnected.

		Faulted section is not identified		Faulted section is identified	
Relay	Tap setting	TDS	Operation time (s)	TDS	Operation time (s)
5	1.9	2.1280	1.3602	1.2368	0.7906
6	2.1	1.5730	0.9953	0.6608	0.4181
7	4.0	1.0184	0.6738	0.1342	0.0888
16	4.0	2.2420	1.6992	0.1531	0.1160
17	3.6	2.7194	2.0667	0.6561	0.4986
18	2.7	3.2669	2.4855	1.2294	0.9354

In the table, the tap settings change due to the change in the power distribution system's configuration. In addition, the TDS values are changed during the faulted section identification algorithm to speed up fault clearance. Hence, faulted section identification reduces long operation times caused by coordination time constraint between the directional overcurrent relays.

4.3.1.8 SLG Fault at Line 8-9 with All WTGs Disconnected

When all the WTGs are disconnected, part of the power distribution system becomes radial. Furthermore, the operation of the CAPS during radial operation between buses 5 and 14 is simulated. Table 4.15 shows the relays' TDS values, tap settings, and operation times for a SLG fault on line 8-9 when all the WTGs are disconnected. Moreover, the table shows only the settings of the primary and the two backup relays in both directions. The omitted relays are either not operating or blocked.

Table 4.15: Centralized: SLG fault at line 8-9 with all WTGs disconnected.

		Faulted section is not identified		Faulted section is identified	
Relay	Tap setting	TDS	Operation time (s)	TDS	Operation time (s)
2	0.8	2.1898	1.3670	1.5164	0.9466
3	3.8	1.7546	1.0692	0.7762	0.4730
4	3.8	1.4553	0.8573	0.1707	0.1005
13	1.9	0.1825	No operation	5.5500	No operation
14	1.9	0.2325	No operation	5.5500	No operation
15	0.9	0.2652	No operation	5.5500	No operation

In the table, the tap settings are changed according to the new configuration. Also, TDS values during the faulted section identification algorithm are changed to employ faster fault clearance. However, the upstream looking relays take no action because no fault is detected. Figure 4.14 shows the TDS curves for the downstream looking relays during normal fault clearance operation and when the faulted section identification algorithm is used.

4.3.1.9 SLG Fault at Line 8-9 with TG Disconnected (Islanded Mode)

The centralized adaptive protection system's behavior is looked into during islanding operation. Table 4.16 presents the relays' TDS values, tap settings, and operation times for a SLG fault on line 8-9 when TG is disconnected. The table shows only

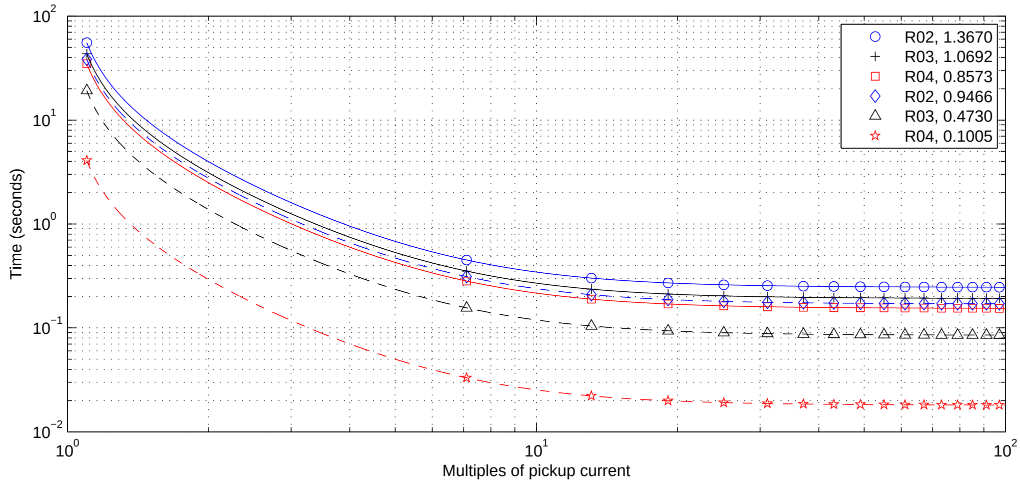

Figure 4.14: Downstream looking relays' TDS curves for a SLG fault at line 8-9 with all WTGs disconnected.

the settings of the primary and the two backup relays in both directions. The omitted relays are either not operating or blocked.

Table 4.16: Centralized: SLG fault at line 8-9 with TG disconnected (islanded mode).

		Faulted section is not identified		Faulted section is identified	
Relay	Tap setting	TDS	Operation time (s)	TDS	Operation time (s)
2	0.5	2.4360	2.0656	0.9512	0.8066
3	2.3	2.1699	1.7610	0.5479	0.4447
4	2.0	1.9520	1.4608	0.1386	0.1037
13	2.6	0.8348	0.6941	0.1238	0.1030
14	2.2	1.2974	0.9969	0.5614	0.4314
15	3.0	1.7322	1.3017	1.0200	0.7665

During islanded operation, the overcurrent relays' settings are adjusted to keep operation times to a minimum, while maintaining the coordination time between the relays. To illustrate, Figure 4.15 shows the TDS curves during normal fault clearance operation and when the faulted section identification is used.

4.3.1.10 SLG Fault at Line 11-12 with TG Disconnected (Islanded Mode)

After that, the fault location is changed during islanding operation to demonstrate the effect of varying the fault location when the TG is disconnected. Table 4.17 shows the relays' TDS values, tap settings, and operation times for a SLG fault on line 11-12 when TG is disconnected. The table shows only the settings of the primary and

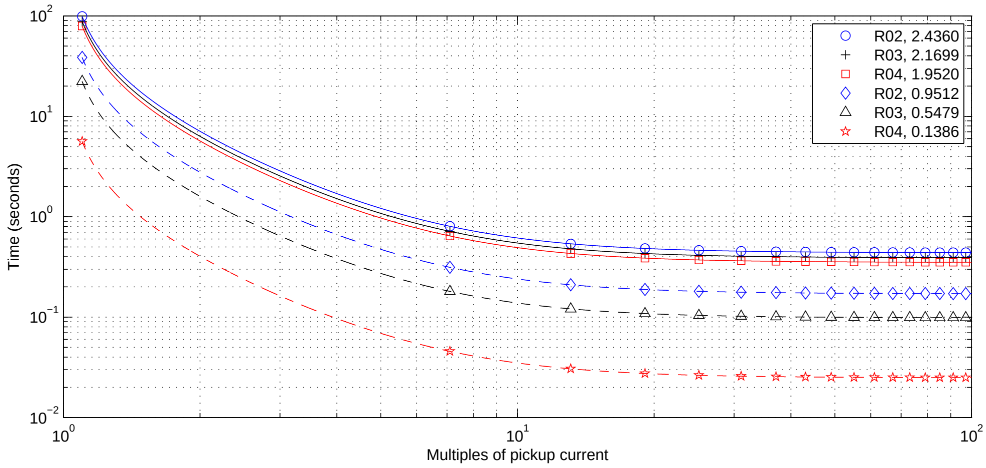

(a) Downstream looking relays' TDS curves

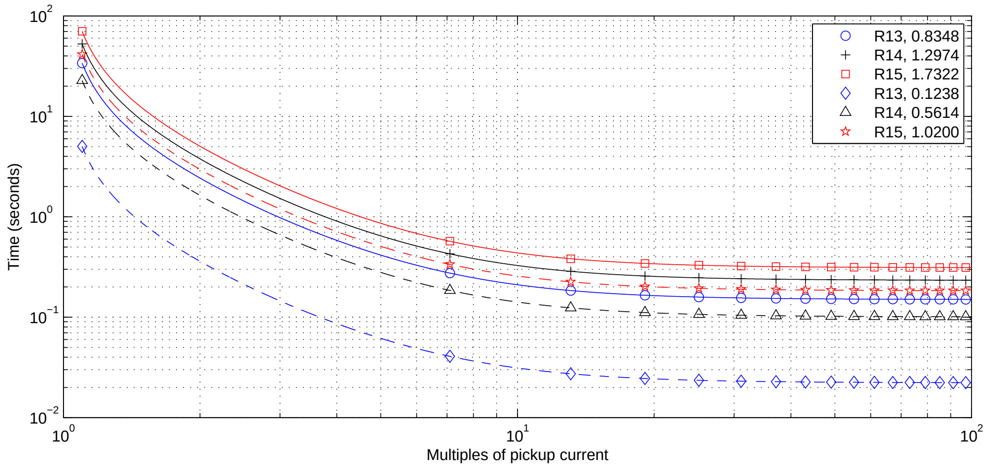

(b) Upstream looking relays' TDS curves

Figure 4.15: Upstream and downstream TDS curves for a SLG fault on line 8-9 with TG disconnected (islanded mode).

the two backup relays in both directions. The omitted relays are either not operating or blocked.

Table 4.17: Centralized: SLG fault at line 11-12 with TG disconnected (islanded mode).

		Faulted section is not identified		Faulted section is identified	
Relay	Tap setting	TDS	Operation time (s)	TDS	Operation time (s)
5	1.6	1.6668	1.2589	0.9995	0.7549
6	2.0	1.2770	0.9423	0.5629	0.4154
7	3.8	0.8245	0.6422	0.1217	0.0948
16	3.8	2.0522	1.5101	0.1523	0.1121
17	3.4	2.4562	1.8148	0.6488	0.4794
18	2.6	2.8446	2.1212	1.2100	0.9023

When the fault location is changed, the tap settings remain unchanged when compared to Section 4.3.1.9 because the power system's configuration is the same for the two cases. However, the TDS values are changed depending on the location of the fault to reduce the operation time of the closest relays. Figure 4.16 demonstrates the change in the TDS values when the faulted section identification algorithm is used.

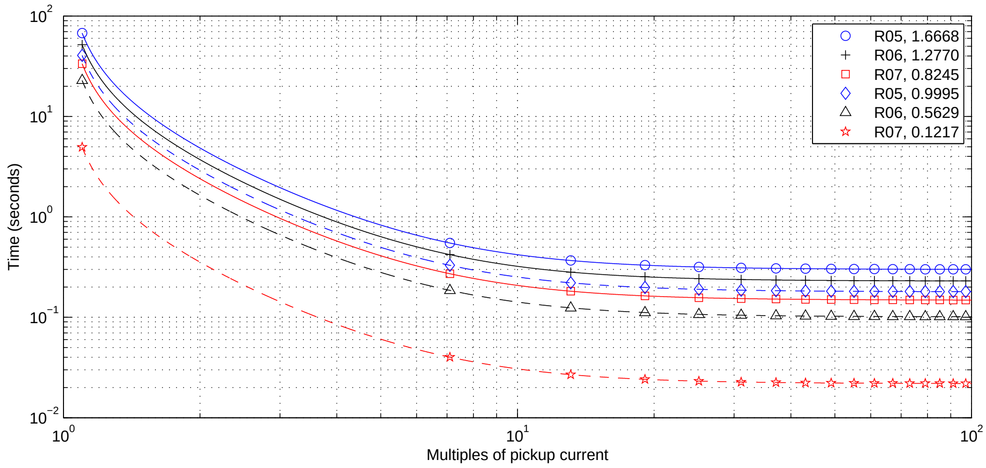

(a) Downstream looking relays' TDS curves

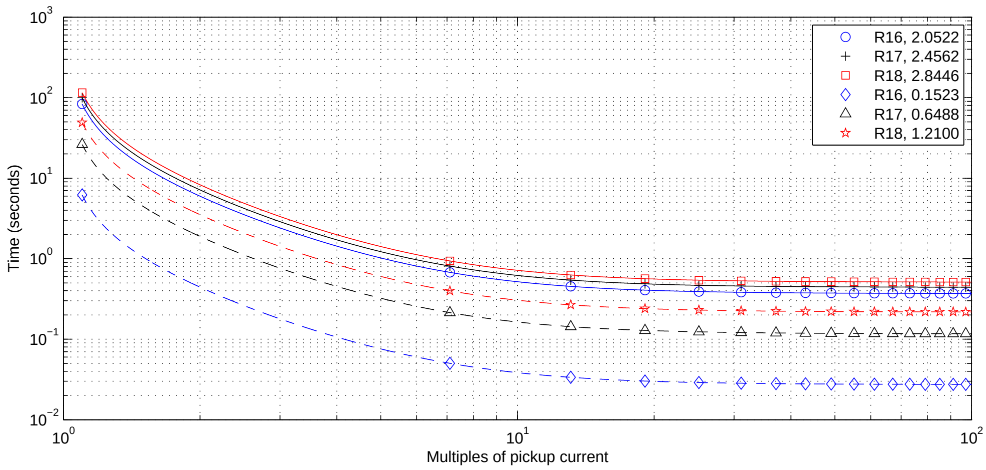

(b) Upstream looking relays' TDS curves

Figure 4.16: Upstream and downstream TDS curves for a SLG fault on line 11-12 with TG disconnected (islanded mode).

4.3.2 Decentralized Adaptive Protection System (DAPS)

The previous simulation cases are repeated for the DAPS. However, the operation of the decentralized technique differs from the CAPS during fault occurrence. In the DAPS, during a configuration change, each relay receives the connection statuses of the DGs. Then, the tap settings are changed and the TDS values are computed using the linear optimization algorithm at each relay. When a fault occurs, the relay settings are changed according to the fault location using a faulted section identification algorithm to speed up fault clearance.

4.3.2.1 CHP Plant is Disconnected from the Power Distribution System

In the first simulation case, the system was operating under normal conditions where all the generators are connected to the power distribution system. Then, the CHP plant, shown in Figure 4.1, is disconnected, and it sends a connection status signal to all the overcurrent relays in the system. The transmitted connection status signal is formatted using DNP3. Then, each relay determines the new power distribution system configuration. As a consequence, the new tap settings and TDS values are computed in each relay using the linear optimization technique explained in Appendix B. That is, the TDS value in each relay is adjusted to maintain fast fault clearance for the new system configuration. Finally, the new relay settings replace the previous protection settings. Table 4.18 shows the TDS values and tap settings before and after the power system configuration change.

Table 4.18: Decentralized: CHP is disconnected.

	Before configuration change		After configuration change	
Relay	Tap setting	TDS	Tap setting	TDS
1	4.9	0.2494	0.1	0.3469
2	0.5	3.8172	0.5	3.8143
3	2.4	3.0920	2.4	3.0897
4	2.0	2.6085	2.0	2.6068
5	1.9	2.1294	1.9	2.1280
6	2.1	1.5741	2.1	1.5731
7	4.0	1.0191	4.0	1.0184
8	2.7	0.6228	2.7	0.6224
9	1.8	0.1307	1.8	0.1307
10	4.9	0.1471	10.0	9.7920
11	3.2	0.1146	3.2	0.1146
12	2.9	0.4713	2.9	0.4709
13	2.6	0.9086	2.6	0.9078
14	2.2	1.4129	2.2	1.4118
15	3.2	1.8697	3.2	1.8682
16	4.0	2.2438	4.0	2.2420
17	3.6	2.7216	3.6	2.7194
18	2.7	3.2696	2.7	3.2699

4.3.2.2 SLG Fault at Line 8-9 with CHP Disconnected

After that, a SLG fault is applied on line 8-9 when the CHP is disconnected. Table 4.19 shows the obtained results, and it shows the operation of the DAPS with and without the faulted section identification algorithm.

Table 4.19: Decentralized: SLG fault at line 8-9 with CHP disconnected.

		Faulted section is not identified		Faulted section is identified	
Relay	Tap setting	TDS	Operation time (s)	TDS	Operation time (s)
1	0.1	0.3469	No operation	10.9677	No operation
2	0.5	3.8143	2.2013	1.6161	0.9327
3	2.4	3.0897	1.7476	0.8235	0.4658
4	2.0	2.6068	1.3922	0.1771	0.0946
5	1.9	2.1280	Blocked	5.5500	Blocked
6	2.1	1.5731	Blocked	5.5500	Blocked
7	4.0	1.0184	Blocked	5.5500	Blocked
8	2.7	0.6224	Blocked	5.5500	Blocked
9	1.8	0.1307	Blocked	5.5500	Blocked
10	10	9.7920	No operation	5.5500	No operation
11	3.2	0.1146	Blocked	5.0289	Blocked
12	2.9	0.4709	Blocked	5.0289	Blocked
13	2.6	0.9078	0.7414	0.1000	0.0817
14	2.2	1.4118	1.0673	0.5102	0.3857
15	3.2	1.8682	1.4026	0.9222	0.6923
16	4.0	2.2420	1.7721	8.0059	No operation
17	3.6	2.7194	2.1634	5.0289	No operation
18	2.7	3.2699	2.6155	5.0289	No operation

During the fault, each downstream looking overcurrent relay detects and transmits the fault direction signal to the previous downstream looking relay. Similarly, each upstream looking overcurrent relay detects and transmits the fault direction signal to the previous upstream looking relay. Once the faulted section is identified, the closest relays determine and transmit the TDS values and tap settings to the backup relays in both directions. Hence, the protection system's response time to the fault is reduced.

When the configuration is changed, the TDS values and tap settings are adjusted to account for the change in the fault current. This helps maintain fast clearance time even when the fault current is reduced due to CHP disconnection from the power distribution system. Compared to Section 4.3.1.2, in the DAPS R4 and R13 achieve faster fault clearance by having operation times of 0.0946 s and 0.0817 s, respectively. In the CAPS, R4 and R13 clear the fault after 0.0947 s and 0.1019 s, respectively. Also, the

DAPS achieves a much faster operation during the faulted section identification algorithm, due to a shorter communication time delay of 0.0227 s, compared to the CAPS.

4.3.2.3 SLG Fault at Line 8-9 with All Generators Connected

In this simulation case, the performance of the DAPS is studied during normal power system operation. Therefore, a SLG to ground fault is simulated on line 8-9 when all the generators are connected, and the TDS values, tap settings, and operation times are calculated.

Table 4.20: Decentralized: SLG fault at line 8-9 with all generators connected.

		Faulted section is not identified		Faulted section is identified	
Relay	Tap setting	TDS	Operation time (s)	TDS	Operation time (s)
1	4.9	0.2494	Blocked	0.2494	Blocked
2	0.5	3.8172	1.9111	1.6174	0.9328
3	2.4	3.0920	1.5816	0.8241	0.4658
4	2.0	2.6085	1.2811	0.1772	0.0946
5	1.9	2.1294	Blocked	5.5500	Blocked
6	2.1	1.5741	Blocked	5.5500	Blocked
7	4.0	1.0191	Blocked	5.5500	Blocked
8	2.7	0.6228	Blocked	5.5500	Blocked
9	1.8	0.1307	Blocked	5.5500	Blocked
10	4.9	0.1471	No operation	5.500	No operation
11	3.2	0.1146	Blocked	4.5608	Blocked
12	2.9	0.4713	Blocked	4.5608	Blocked
13	2.6	0.9086	0.6908	0.1000	0.0816
14	2.2	1.4129	0.9938	0.5106	0.3856
15	3.2	1.8697	1.3003	0.9229	0.6923
16	4.0	2.2438	1.6308	7.5101	No operation
17	3.6	2.7216	1.9642	4.5608	No operation
18	2.7	3.2696	2.2998	4.5608	No operation

Table 4.20 shows the operation of the DAPS during the fault. In the table, overcurrent relays R2, R3, and R4 are coordinated for the downstream direction, and R13, R14, and R15 are coordinated for the upstream direction. Furthremore, Figure 4.17 shows the change in the TDS values using the faulted section identification algorithm. The fault is cleared by relays R4 and R13 after an operation time delay of 0.0946 s and a communication time delay of 0.0227 s. The operation of the decentralized technique is faster than the centralized technique during the faulted section identification. To illustrate, Figure 4.18 shows the fault current cleared after 0.1173 s from fault occurrence.

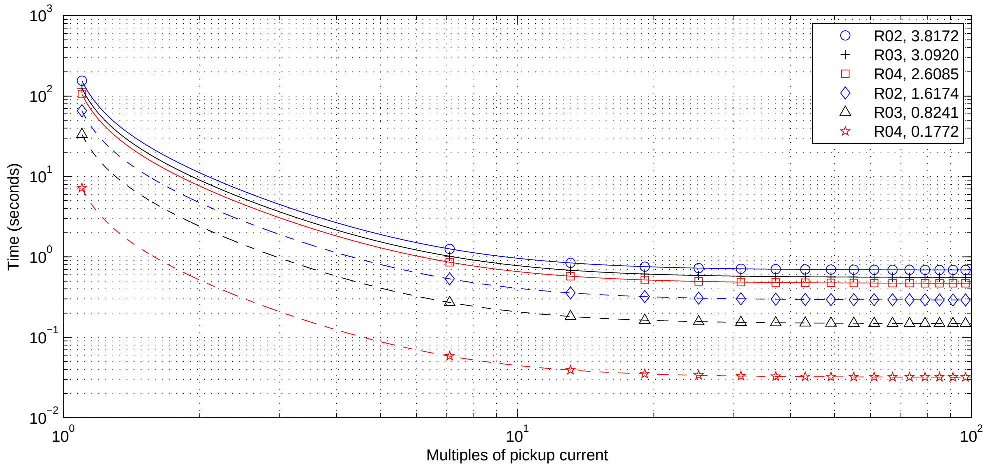

(a) Downstream looking relays' TDS curves

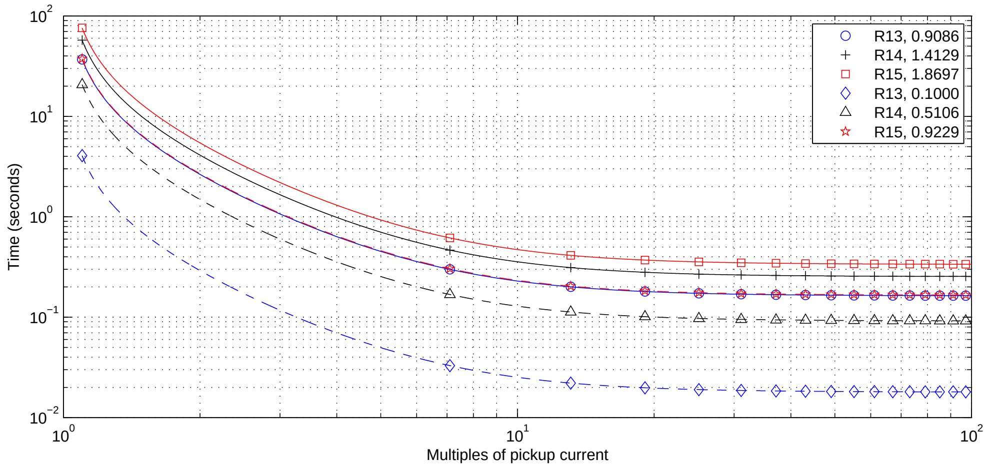

(b) Upstream looking relays' TDS curves

Figure 4.17: Upstream and downstream TDS curves for a SLG fault on line 8-9 with all generators connected.

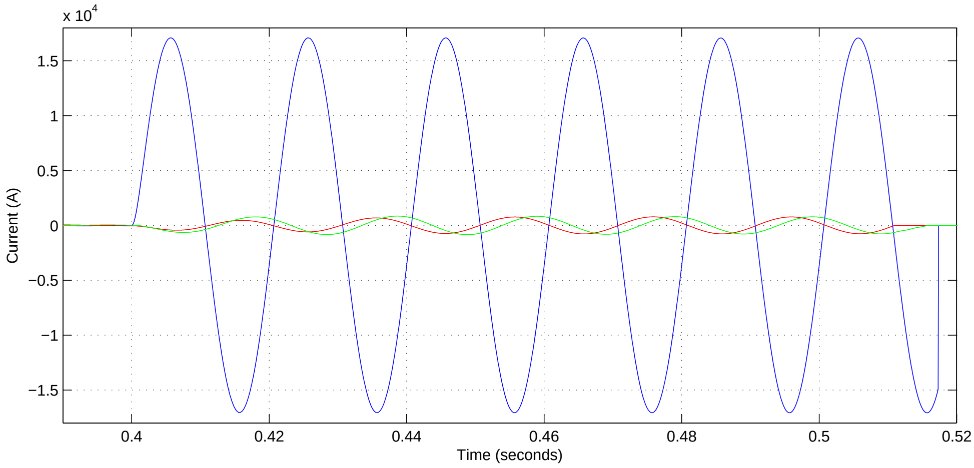

Figure 4.18: Fault current for a SLG fault on line 8-9 when all generators are connected.

4.3.2.4 LL Fault at Line 8-9 with All Generators Connected

After that, the fault type is changed during normal operation, and a LL fault is applied on line 8-9. The behavior of the DAPS is displayed in Table 4.21.

Table 4.21: Decentralized: LL fault at line 8-9 with all generators connected.

		Faulted section is not identified		Faulted section is identified	
Relay	Tap setting	TDS	Operation time (s)	TDS	Operation time (s)
1	4.9	0.2494	Blocked	0.2494	Blocked
2	0.5	3.8172	2.2514	1.6174	0.9540
3	2.4	3.0920	1.7863	0.8241	0.4761
4	2.0	2.6085	1.4207	0.1771	0.0965
5	1.9	2.1294	Blocked	5.5500	Blocked
6	2.1	1.5741	Blocked	5.5500	Blocked
7	4.0	1.0191	Blocked	5.5500	Blocked
8	2.7	0.62278	Blocked	5.5500	Blocked
9	1.8	0.1307	Blocked	5.5500	Blocked
10	4.9	0.1471	No operation	5.5500	No operation
11	3.2	0.1146	Blocked	4.5608	Blocked
12	2.9	0.4713	Blocked	4.5608	Blocked
13	2.6	0.9086	0.8298	0.1000	0.0913
14	2.2	1.4129	1.1837	0.5106	0.4278
15	3.2	1.8697	1.5605	0.9229	0.7703
16	4.0	2.2438	1.9901	7.5101	No operation
17	3.6	2.7216	2.4277	4.5608	No operation
18	2.7	3.2696	2.9271	4.5608	No operation

It is noted that the DAPS's settings are not affected by the fault type. Thus, the existing fault type is not taken into account when performing linear optimization. The linear optimization technique is performed for maximum fault currents only, which are determined during power system fault analysis. Therefore, the operation times of the relays are slightly slower for the downstream and upstream looking relays compared to Section 4.3.2.3.

4.3.2.5 SLG Fault at Line 11-12 with All Generators Connected

The fault location is changed, and a SLG fault is simulated on line 11-12. The simulation shows the effect of changing the fault location on the DAPS during normal power system operation. Moreover, Table 4.22 shows the tap settings, TDS values, and operation times.

Table 4.22: Decentralized: SLG fault at line 11-12 with all generators connected.

		Faulted section is not identified		Faulted section is identified	
Relay	Tap setting	TDS	Operation time (s)	TDS	Operation time (s)
1	4.9	0.2494	Blocked	0.2494	Blocked
2	0.5	3.8172	2.8723	5.5500	No operation
3	2.4	3.0920	2.2635	5.5500	No operation
4	2.0	2.6085	1.7645	7.7104	No operation
5	1.9	2.1294	1.3604	1.4676	0.9376
6	2.1	1.5741	0.9955	0.7510	0.4750
7	4.0	1.0191	0.6739	0.1611	0.1065
8	2.7	0.6228	Blocked	5.5500	Blocked
9	1.8	0.1307	Blocked	5.5500	Blocked
10	4.9	0.1471	No operation	5.5500	No operation
11	3.2	0.1146	Blocked	5.3470	Blocked
12	2.9	0.4713	Blocked	5.3470	Blocked
13	2.6	0.9086	Blocked	5.3470	Blocked
14	2.2	1.4129	Blocked	5.3470	Blocked
15	3.2	1.8697	Blocked	5.3470	Blocked
16	4.0	2.2438	1.6276	0.1000	0.0725
17	3.6	2.7216	1.9860	0.5180	0.3780
18	2.7	3.2696	2.3995	0.9333	0.6850

In the table, changing the fault location causes the DAPS to change the TDS values. Also, the three closest relays for each direction (R7, R6, and R5 for the downstream direction and R16, R17, and R18 for the upstream direction) are coordinated to perform fast fault clearance. Figure 4.19 shows the TDS curves during normal protection system fault clearance and when the faulted section identification algorithm is used.

4.3.2.6 DLG Fault at Line 8-9 with WTG1 Disconnected

In this case, the DAPS's behavior is illustrated when one WTG is disconnected. Hence, a DLG fault is applied on line 8-9 when WTG1 is disconnected from the power distribution system.

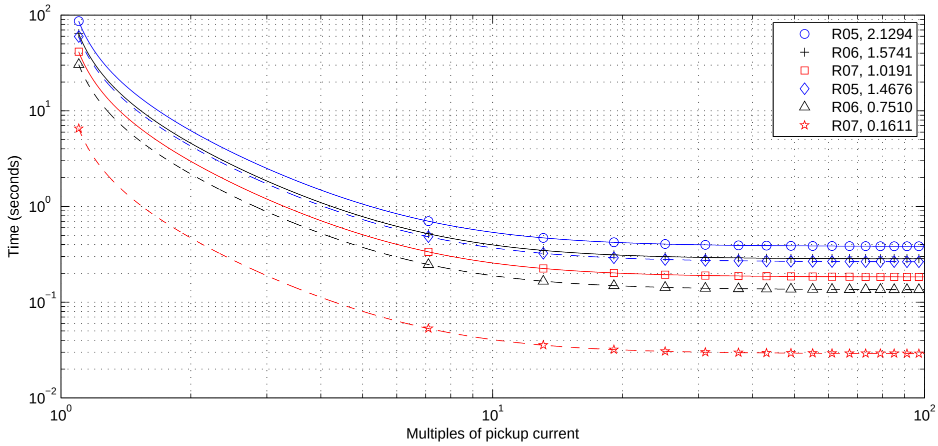

(a) Downstream looking relays' TDS curves

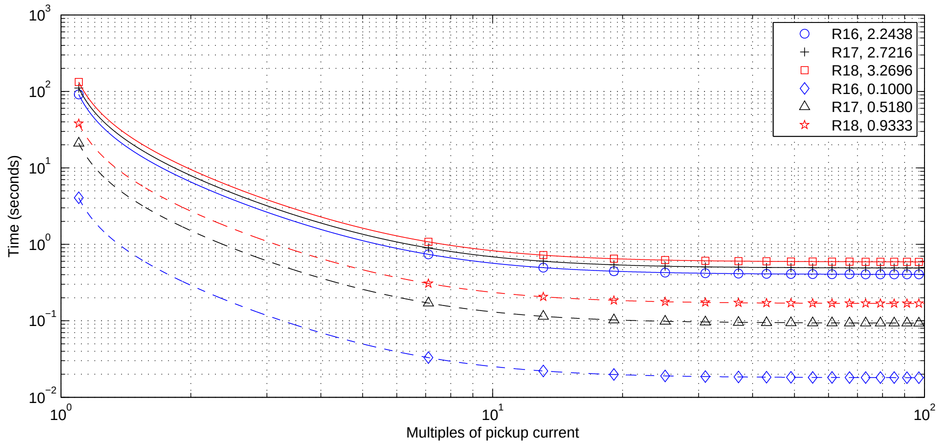

(b) Upstream looking relays' TDS curves

Figure 4.19: Upstream and downstream TDS curves for a SLG fault on line 11-12 with all generators connected.

Table 4.23: Decentralized: DLG fault at line 8-9 with WTG1 disconnected.

		Faulted section is not identified		Faulted section is identified	
Relay	Tap setting	TDS	Operation time (s)	TDS	Operation time (s)
2	0.6	3.2202	1.9131	1.5786	0.9378
3	2.9	2.7169	1.5824	0.8044	0.4685
4	2.9	2.3108	1.2820	0.1746	0.0968
13	3.4	0.7520	0.7425	0.10000	0.0987
14	3.1	1.1538	1.0571	0.4552	0.4170
15	2.2	1.7980	1.3591	0.9630	0.7279

Compared to Section 4.3.2.2, the results in Table 4.23 show that the TDS values are slightly modified to account for the new power system configuration. Also, the new TDS values maintain the coordination time between the relays intact. The table shows only the settings of the primary and the two backup relays in both directions. The omitted relays are either not operating or blocked.

4.3.2.7 DLG Fault at Line 11-12 with CHP Disconnected

The operation of the DAPS is investigated when the fault location is changed and a DG is disconnected. Therefore, a DLG fault is applied on line 11-12, and the CHP is disconnected.

Table 4.24: Decentralized: DLG fault at line 11-12 with CHP disconnected.

		Faulted section is not identified		Faulted section is identified	
Relay	Tap setting	TDS	Operation time (s)	TDS	Operation time (s)
5	1.9	2.1280	1.3602	1.4666	0.9375
6	2.1	1.5730	0.9953	0.7504	0.4749
7	4.0	1.0184	0.6738	0.1610	0.1065
16	4.0	2.2420	1.6992	0.1000	0.0758
17	3.6	2.7194	2.0067	0.5177	0.3934
18	2.7	3.2699	2.4855	0.9326	0.7096

In Table 4.24, the TDS values are adjusted for the current power distribution system configuration. The table shows only the settings of the primary and the two backup relays in both directions. The omitted relays are either not operating or blocked. Compared to Section 4.3.2.2, the faulted section detection algorithm ensures that overcurrent relays R7 and R16 are the fastest relays to operate.

4.3.2.8 SLG Fault at Line 8-9 with All WTGs Disconnected

The performance of the DAPS is investigated when all the WTGs are disconnected. For this reason, a SLG fault is simulated on line 8-9, and Table 4.25 shows the tap settings, TDS values, and operation times. The table shows only the settings of the primary and the two backup relays in both directions. The omitted relays are either not operating or blocked.

Table 4.25: Decentralized: SLG fault at line 8-9 with all WTGs disconnected.

		Faulted section is not identified		Faulted section is identified	
Relay	Tap setting	TDS	Operation time (s)	TDS	Operation time (s)
2	0.8	2.1898	1.3670	1.5164	0.9466
3	3.8	1.7546	1.0692	0.7762	0.4730
4	3.8	1.4553	0.8573	0.1707	0.1005
13	1.9	0.1825	No operation	5.5885	No operation
14	1.9	0.2325	No operation	5.5885	No operation
15	0.9	0.2652	No operation	5.5885	No operation

During radial operation between buses 5 and 14 both the decentralized and centralized techniques perform exactly the same. Also, in both cases fault clearance by relay R4 is performed after 0.1005 s. However, the operation of the DAPS is faster when taking communication time delay into account.

4.3.2.9 SLG Fault at Line 8-9 with TG Disconnected (Islanded Mode)

The decentralized adaptive protection system is tested during islanding mode. Therefore, the TG is disconnected from the power distribution system and the DGs remain connected. Then, a SLG fault is applied on line 8-9, and the results are shown in Table 4.26. The table shows only the settings of the primary and the two backup relays in both directions. The omitted relays are either not operating or blocked.

Table 4.26: Decentralized: SLG Fault at Line 8-9 with TG Disconnected (Islanded Mode).

		Faulted section is not identified		Faulted section is identified	
Relay	Tap setting	TDS	Operation time (s)	TDS	Operation time (s)
2	0.5	2.4360	2.0656	1.0551	0.8947
3	2.3	2.1699	1.7610	0.5854	0.4751
4	2.0	1.9520	1.4608	0.1509	0.1129
13	2.6	0.8348	0.6941	0.1000	0.0831
14	2.2	1.2974	0.9969	0.5036	0.3869
15	3.0	1.7322	1.3017	0.9212	0.6923

During islanding operation, the DAPS is able to adapt the relays' settings for the new power system configuration. The fault clearance time is reduced using faulted section identification algorithm. To illustrate, Figure 4.20 shows the change in the TDS values when the faulted section identification algorithm is used.

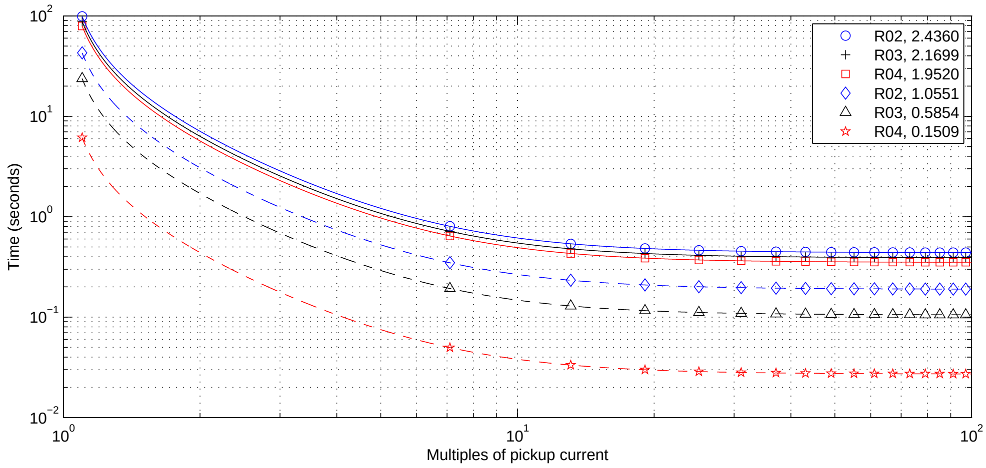

(a) Downstream looking relays' TDS curves

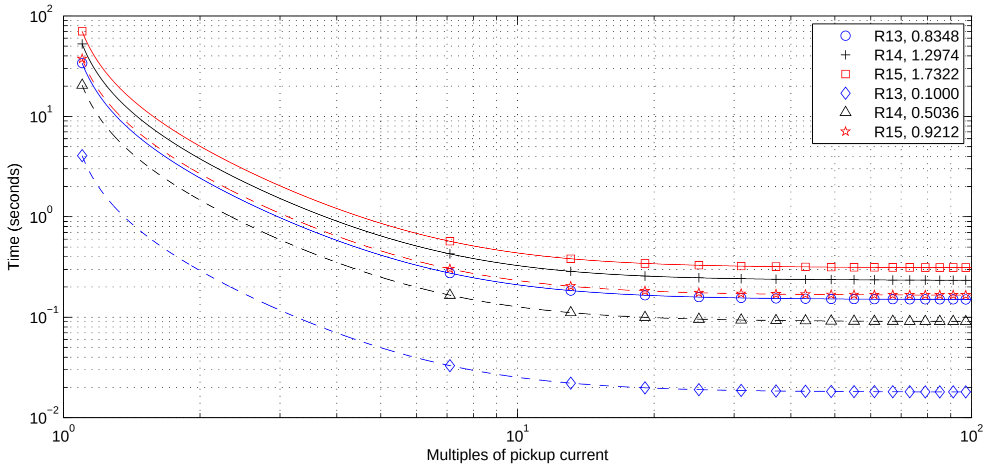

(b) Upstream looking relays' TDS curves

Figure 4.20: Upstream and downstream TDS curves for a SLG fault on line 8-9 with TG disconnected (islanded mode).

4.3.2.10 SLG Fault at Line 11-12 with TG Disconnected (Islanded Mode)

After that, the DAPS's operation is demonstrated during islanding mode for a different fault location. Hence, a SLG fault is applied on line 11-12 when the TG is disconnected. Furthermore, Table 4.27 shows the tap settings, TDS values, and operation times. The table shows only the settings of the primary and the two backup relays in both directions. The omitted relays are either not operating or blocked.

Table 4.27: Decentralized: SLG fault at line 11-12 with TG disconnected (islanded mode).

		Faulted section is not identified		Faulted section is identified	
Relay	Tap setting	TDS	Operation time (s)	TDS	Operation time (s)
5	1.6	1.6668	1.2589	1.2081	0.9124
6	2.0	1.2770	0.9423	0.6506	0.4801
7	3.8	0.8245	0.6422	0.1496	0.1165
16	3.8	2.0522	1.5101	0.1000	0.0736
17	3.4	2.4562	1.8148	0.5123	0.3785
18	2.6	2.8446	2.1212	0.9184	0.6849

It is noticed that when the fault location is varied the TDS values are changed during the faulted section identification. As a result, overcurrent relays R7 and R16 become the fastest acting relays. Therefore, faulted section identification is possible during islanding operation, which is demonstrated in Figure 4.21.

4.4 Backup Technique

During a communication failure, the adaptive protection scheme is degraded and the power distribution system's configuration can only be detected using an islanding detection technique utilizing local measurements [22]. For that reason, there are only two configurations that the system will work with. The first is when the TG is connected and the second is when the TG is disconnected (islanding mode). Therefore, the communication failure backup adaptive protection system does not detect DGs' disconnection.

In this section, the backup protection system will be tested based on local measurements only to detect the connection of the TG. If the TG is connected, the TDS values and tap settings are fixed for the configuration when the power system is operating normally. During this operation mode of the protection system, a SLG to ground fault is applied on line 10-11 and the power distribution system's configuration is varied by disconnecting some of the DGs. Tables 4.28 and 4.29 shows the effect of varying the power system's configuration on the operation times of the overcurrent relays.

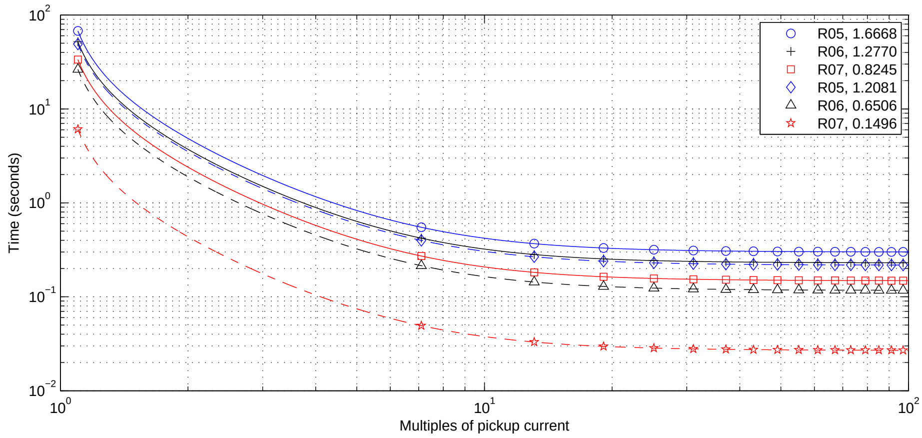

(a) Downstream looking relays' TDS curves

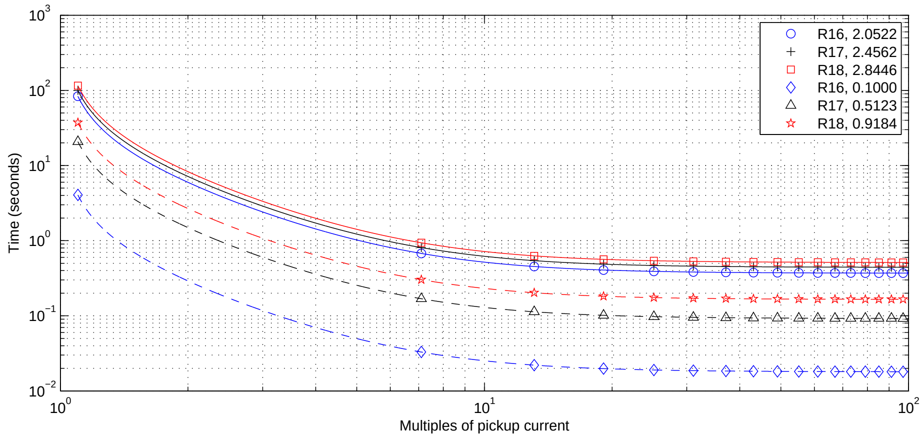

(b) Upstream looking relays' TDS curves

Figure 4.21: Upstream and downstream TDS curves for a SLG fault at line 11-12 with TG disconnected (islanded mode).

Table 4.28: Backup: varying DG connection during normal operation.

Relay	Operation time (s)
TG = 1, CHP = 1, WTG1 = 1, WTG2 = 1, WTG3 = 1	
4	1.4393
5	1.1274
6	0.8272
15	1.2668
16	1.5865
17	1.9104
TG = 1, CHP = 0, WTG1 = 1, WTG2 = 1, WTG3 = 1	
4	1.4404
5	1.1282
6	0.8278
15	1.2678
16	1.5879
17	1.9122

Table 4.29: Backup: varying DG connection during normal operation.

Relay	Operation time (s)
TG = 1, CHP = 1, WTG1 = 0, WTG2 = 0, WTG3 = 1	
4	1.4392
5	1.1273
6	0.8271
15	1.5335
16	1.9483
17	2.0875
TG = 1, CHP = 0, WTG1 = 0, WTG2 = 0, WTG3 = 1	
4	1.4402
5	1.1281
6	0.8277
15	1.5352
16	1.9506
17	2.0897

Furthermore, the second part of the test involves the TG being disconnected, and the islanding detection technique in the relays detects an islanding operation. Then, the settings of the relays are changed for islanding operation mode. During this mode, the power system's configuration is varied to observe its effect on the operation time of the relays. Tables 4.30 and 4.31 show the operation times of the relays for a SLG to ground fault on line 10-11.

Table 4.30: Backup: varying DG connection during islanded operation.

Relay	Operation time (s)
TG = 0, CHP = 1, WTG1 = 1, WTG2 = 1, WTG3 = 1	
4	1.5016
5	1.1982
6	0.8981
15	1.2730
16	1.5913
17	1.9127
TG = 0, CHP = 1, WTG1 = 0, WTG2 = 1, WTG3 = 1	
4	1.8458
5	1.4194
6	1.0276
15	1.3596
16	1.7171
17	1.8653

Table 4.31: Backup: varying DG connection during islanded operation.

Relay	Operation time (s)
TG = 0, CHP = 1, WTG1 = 0, WTG2 = 0, WTG3 = 1	
4	1.8450
5	1.4188
6	1.0272
15	1.5553
16	1.9863
17	2.1197
TG = 0, CHP = 1, WTG1 = 0, WTG2 = 0, WTG3 = 0	
4	1.8442
5	1.4183
6	1.0268
15	No operation
16	No operation
17	No operation

In both operation modes, no mis-coordination occurs when the power system's configuration is varied. However, some of the overcurrent relays violate the specified coordination time. Also, the operation time of the relays becomes longer when more DGs are disconnected. Using the backup adaptive protection system is an effective tool when communication is interrupted. Nevertheless, this approach lacks the accuracy of the centralized and decentralized adaptive protection systems. Therefore, communication between the CRU, DGs, and relays should be enabled to ensure the power system's protection.

Chapter 5

Conclusions and Future Work

Several schemes exist to protect power distribution systems. However, conventional methods are becoming outdated as more DGs are incorporated into the power system. That is, DGs connected to a power distribution system can have a significant effect on the fault current. Therefore, protection systems must account for changes in the power distribution system's configuration. Also, they should protect the power system during intentional islanding because it increases the power system's reliability. Moreover, adaptive protection systems account for the shortcomings of conventional protection systems. Adaptive protection systems are implemented using non-communication based techniques, centralized communication-based techniques, and multi-agent systems.

This thesis proposed centralized and decentralized adaptive protection systems. Also, a faulted section identification algorithm was developed to speed up fault clearance. Furthermore, intranet was proposed as the primary communication network, and the Internet as a backup. In both communication networks, fiber optic cables are used as the physical communication medium. In addition, DNP3 was suggested as the communication protocol between DGs, relays, and the CRU. In both schemes, linear optimization was implemented to calculate the optimal TDS values during the protection system's operation. Also, a backup adaptive protection system was proposed in case of communication failure.

The communication time delays for the adaptive protection systems were calculated. Then, the operation of the centralized and decentralized adaptive protection systems was verified through several simulation cases. Both protection systems were able to cope with different power distribution system's configurations, fault types, and fault locations. Furthermore, the effectiveness of the faulted section detection algorithm was demonstrated in the adaptive protection systems. That is, fault section identification can reduce the operation times of the overcurrent relays significantly with the communication time delay taken into account. Also, it was determined that the decentralized adaptive protection system gives a shorter communication time delay than the centralized one. Although the centralized adaptive protection system has a simple structure, it has a one point of failure. On the other hand, the decentralized adaptive protection system is complex but it is reliable and faster. Finally, the backup adaptive protection system that can be used during communication failure was tested. However, the coordination time delay during communication failure is uncontrolled and therefore in some cases the 0.3 s coordination time was not satisfied.

There are two areas that could be researched to improve the operation of the adaptive protection system. The new IEC 61850 communication protocol could be used for communication between the protective devices in the adaptive protection system because it has more features compared to other protocols. Also, nonlinear programming or mixed integer nonlinear programming can be used for better optimization.

References

[1] A. Bergen and V. Vittal, *Power Systems Analysis*. Prentice Hall, 2000.

[2] N. Mithulananthan, "Distributed generator placement to maximize the loadability of a distribution system," *International Journal of Electrical Engineering Education*, vol. 43, pp. 107 –118, april 2006.

[3] S. Chowdhury, S. Chowdhury, C. F. Ten, and P. Crossley, "Islanding protection of distribution systems with distributed generators; a comprehensive survey report," in *Power and Energy Society General Meeting - Conversion and Delivery of Electrical Energy in the 21st Century, 2008 IEEE*, pp. 1 –8, july 2008.

[4] K. Butler-Purry and M. Marotti, "Impact of distributed generators on protective devices in radial distribution systems," in *Transmission and Distribution Conference and Exhibition, 2005/2006 IEEE PES*, pp. 87 –88, may 2006.

[5] M. Baran and I. El-Markabi, "Adaptive over current protection for distribution feeders with distributed generators," in *Power Systems Conference and Exposition, 2004. IEEE PES*, pp. 715 – 719 vol.2, oct. 2004.

[6] J. Ma, J. Li, and Z. Wang, "An adaptive distance protection scheme for distribution system with distributed generation," in *Critical Infrastructure (CRIS), 2010 5th International Conference on*, pp. 1 –4, sept. 2010.

[7] R. Best, D. Morrow, and P. Crossley, "Out-of-phase synchronization of a small alternator," in *Power Engineering Society General Meeting, 2007. IEEE*, pp. 1 –7, june 2007.

[8] "IEEE application guide for IEEE std 1547, IEEE standard for interconnecting distributed resources with electric power systems," *IEEE Std 1547.2-2008*, pp. 1 –207, 15 2009.

[9] D. Popovic and E. Boskov, "Advanced fault management as a part of smart grid solution," in *SmartGrids for Distribution, 2008. IET-CIRED. CIRED Seminar*, pp. 1 –4, june 2008.

[10] B. Ram and D. Vishwakarma, *Power System Protection and Switchgear*. McGraw-Hill, 2001.

[11] "American national standard for for high voltage expulsion and current-limiting type power class fuses and fuse disconnecting switches," *ANSI C37.46-2000 (Revision of ANSI C37.46-1981)*, pp. c1 –22, 2000.

[12] A. Thumann and H. Franz, *Efficient Electrical Systems Design Handbook*. Taylor and Francis, 2009.

[13] C. Mason, *The art and science of protective relaying*. General Electric series, Wiley, 1956.

[14] J. Blackburn and T. Domin, *Protective Relaying: Principles and Applications*. Power engineering, CRC Press, 2006.

[15] J. G. Andrichak and G. Alexander, "Distance relays fundamentals." Document.

[16] H. Shateri and S. Jamali, "Over-reaching factor for distance relay with mho characteristic," in *Universities Power Engineering Conference, 2007. UPEC 2007. 42nd International*, pp. 333 –337, sept. 2007.

[17] C.-H. Jung, D.-J. Shin, and J.-O. Kim, "Adaptive setting of digital relay for transmission line protection," in *Power System Technology, 2000. Proceedings. PowerCon 2000. International Conference on*, vol. 3, pp. 1465 –1468 vol.3, 2000.

[18] Electricity Training Association and Institution of Electrical Engineers, *Power System Protection: Digital protection and signalling*. Power System Protection, Institution of Electrical Engineers, 1995.

[19] A. Urdaneta, L. Perez, and H. Restrepo, "Optimal coordination of directional overcurrent relays considering dynamic changes in the network topology," *Power Delivery, IEEE Transactions on*, vol. 12, pp. 1458 –1464, oct 1997.

[20] H. Zeineldin, E. El-Saadany, and M. Salama, "Optimal coordination of directional overcurrent relay coordination," in *Power Engineering Society General Meeting, 2005. IEEE*, pp. 1101 – 1106 Vol. 2, june 2005.

[21] M. Sachdev, B. Chattopadhyay, and T. Sidhu, "A new approach to distribution system protection-adaptive relaying," in *Developments in Power System Protection, 1993., Fifth International Conference on*, pp. 165 –168, 1993.

[22] P. Mahat, Z. Chen, B. Bak-Jensen, and C. Bak, "A simple adaptive overcurrent protection of distribution systems with distributed generation," *Smart Grid, IEEE Transactions on*, vol. 2, pp. 428 –437, sept. 2011.

[23] D. Yuan, N. Zhang, X. Dong, Z. Bo, and A. Klimek, "An adaptive noncommunication protection for distribution systems," in *Universities Power Engineering Conference, 2007. UPEC 2007. 42nd International*, pp. 257 –261, sept. 2007.

[24] F. Chunju, L. Shengfang, Y. Weiyong, and K. Li, "Study on adaptive relay protection scheme based on phase measurement unit (PMU)," in *Developments in Power System Protection, 2004. Eighth IEE International Conference on*, vol. 1, pp. 36 – 39 Vol.1, april 2004.

[25] J. Ma, C. Mi, T. Wang, J. Wu, and Z. Wang, "An adaptive protection scheme for distributed systems with distributed generation," in *Power and Energy Society General Meeting, 2011 IEEE*, pp. 1 –6, july 2011.

[26] H. Wan, K. Li, and K. Wong, "An adaptive multiagent approach to protection relay coordination with distributed generators in industrial power distribution system," *Industry Applications, IEEE Transactions on*, vol. 46, pp. 2118 –2124, sept.-oct. 2010.

[27] J.-H. Chen, S.-H. Chen, and Y.-M. Yang, "Study on adaptive protection relay system based on multi-agetn," in *Machine Learning and Cybernetics, 2005. Proceedings of 2005 International Conference on*, vol. 1, pp. 114 –118, aug. 2005.

[28] Q. Zhao and S. Liu, "Relay protection based on multi-agent system," in *Electrical and Control Engineering (ICECE), 2011 International Conference on*, pp. 286 –289, sept. 2011.

[29] F. Yang, D. Zhao, X. Zhang, and J. Wu, "Research of relay protection setting calculation system for power plant based on multi-agent," in *Power and Energy Engineering Conference (APPEEC), 2010 Asia-Pacific*, pp. 1 –4, march 2010.

[30] K. Shah, E. Detjen, and A. Phadke, "Feasibility of adaptive distribution protection system using computer overcurrent relaying concept," *Industry Applications, IEEE Transactions on*, vol. 24, pp. 792 –797, sep/oct 1988.

[31] S. Jang, J. Choi, J. Kim, and D. Choi, "An adaptive relaying for the protection of a wind farm interconnected with distribution networks," in *Transmission and Distribution Conference and Exposition, 2003 IEEE PES*, vol. 1, pp. 296 – 302 Vol.1, sept. 2003.

[32] C. Spurgeon, *Ethernet: the definitive guide*. Definitive Guide Series, O'Reilly, 2000.

[33] B. Qiu, H. B. Gooi, Y. Liu, and E. K. Chan, "Internet-based SCADA display system," *Computer Applications in Power, IEEE*, vol. 15, pp. 14 –19, jan. 2002.

[34] S. Mohagheghi, J. Stoupis, and Z. Wang, "Communication protocols and networks for power systems-current status and future trends," in *Power Systems Conference and Exposition, 2009. PSCE '09. IEEE/PES*, pp. 1 –9, march 2009.

[35] G. Clarke, D. Reynders, and E. Wright, *Practical modern SCADA protocols: DNP3, 60870.5 and related systems*. Engineering instrumentation & control, Elsevier, 2004.

[36] X. Lu, Z. Lu, W. Wang, and J. Ma, "On network performance evaluation toward the smart grid: A case study of DNP3 over TCP/IP," in *Global Telecommunications Conference (GLOBECOM 2011), 2011 IEEE*, pp. 1 –6, dec. 2011.

[37] A. Phadke and J. Thorp, "Communication needs for wide area measurement applications," in *Critical Infrastructure (CRIS), 2010 5th International Conference on*, pp. 1 –7, sept. 2010.

[38] C. DeCusatis, *Fiber optic data communication: technological trends and advances*. Referex Engineering, Academic, 2002.

[39] P. Serena, M. Bertolini, and A. Vannucci, *Optilux toolbox*. University of Parma, Italy, March 2009.

[40] B. Fleming, "Negative-sequence impedance directional element," (Pasadena, California), 1998.

[41] "IEEE standard for electric power systems communications – distributed network protocol (DNP3)," *IEEE Std 1815-2010*, pp. 1 –775, jan. 2010.

[42] P. Mahat, Z. Chen, and B. Bak-Jensen, “A hybrid islanding detection technique using average rate of voltage change and real power shift,” *Power Delivery, IEEE Transactions on*, vol. 24, pp. 764 –771, april 2009.

[43] G. Benmouyal, M. Meisinger, J. Burnworth, W. Elmore, K. Freirich, P. Kotos, P. Leblanc, P. Lerley, J. McConnell, J. Mizener, J. Pinto de Sa, R. Ramaswami, M. Sachdev, W. Strang, J. Waldron, S. Watansiriroch, and S. Zocholl, “IEEE standard inverse-time characteristic equations for overcurrent relays,” *Power Delivery, IEEE Transactions on*, vol. 14, pp. 868 –872, jul 1999.

[44] B. Chattopadhyay, M. Sachdev, and T. Sidhu, “An on-line relay coordination algorithm for adaptive protection using linear programming technique,” *Power Delivery, IEEE Transactions on*, vol. 11, pp. 165 –173, jan 1996.

[45] H. Abyaneh, M. Al-Dabbagh, H. Karegar, S. Sadeghi, and R. Khan, “A new optimal approach for coordination of overcurrent relays in interconnected power systems,” *Power Delivery, IEEE Transactions on*, vol. 18, pp. 430 – 435, april 2003.

[46] A. Ukil, B. Deck, and V. Shah, “Current-only directional overcurrent relay,” *Sensors Journal, IEEE*, vol. 11, pp. 1403 –1404, june 2011.

[47] M. Sanaye-Pasand and O. Malik, “Power transmission lines fault direction estimation using artificial neural networks,” in *Electrical and Computer Engineering, 1996. Canadian Conference on*, vol. 2, pp. 758 –761 vol.2, may 1996.

[48] T. Sidhu, L. Mital, and M. Sachdev, “A comprehensive analysis of an artificial neural-network-based fault direction discriminator,” *Power Delivery, IEEE Transactions on*, vol. 19, pp. 1042 – 1048, july 2004.

Appendix A

System Model in PSCAD

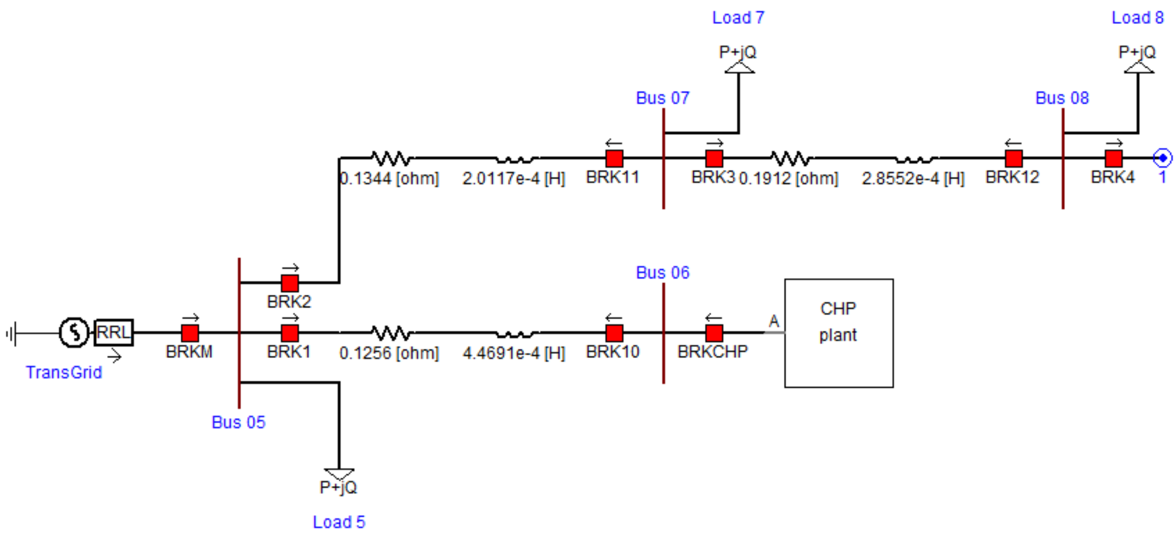

Figure A.1: PSCAD system model buses 5-8.

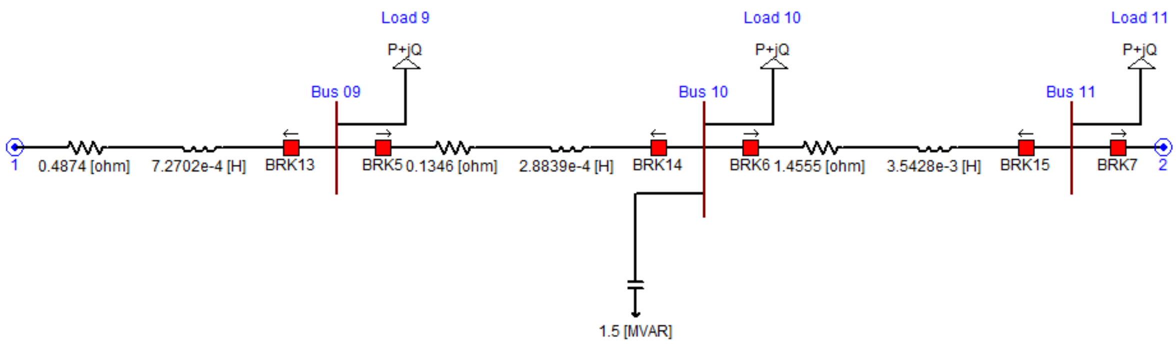

Figure A.2: PSCAD system model buses 9-11.

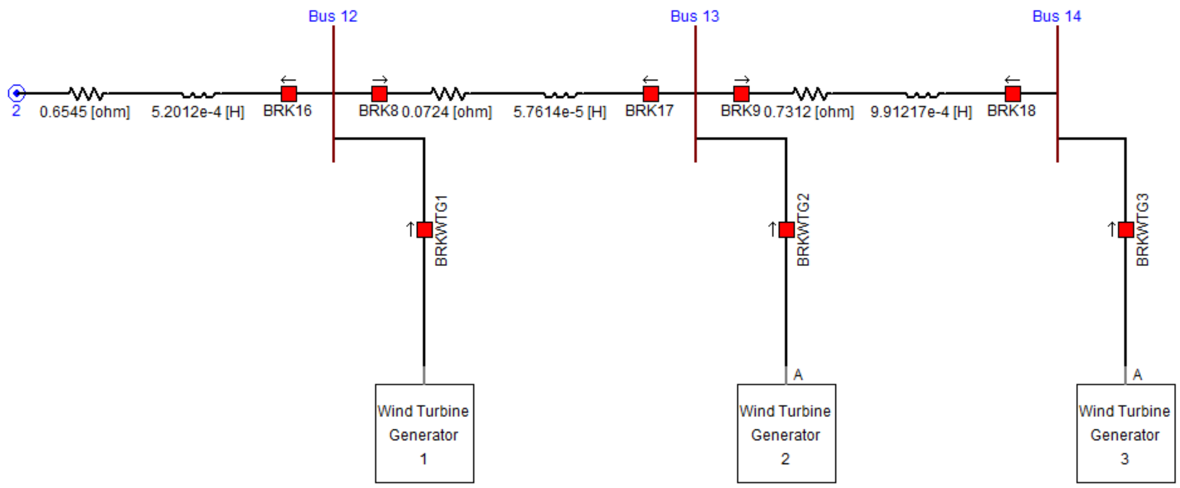

Figure A.3: PSCAD system model buses 12-14.

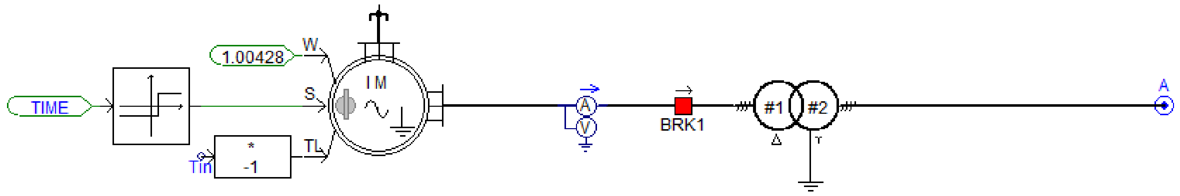

Figure A.4: PSCAD WTG model

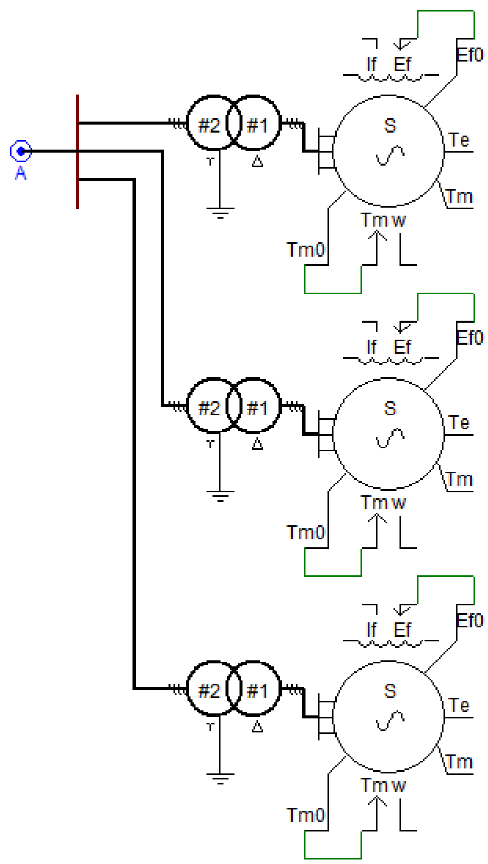

Figure A.5: PSCAD CHP model

Appendix B

Linear Optimization

In the proposed adaptive protection system, a simple linear optimization technique is used to coordinate the directional overcurrent relays. An objective function, constraints, and boundaries are formulated to coordinate the overcurrent relays in the protection system. The objective function, given by

$$objective = min \sum W_i' T_{ik}, \tag{B.1}$$

is the sum of all relay operation times [20]. The weights, W_i', are usually set to 1. T_{ik} is the operation time of the i^{th} relay R_i for a fault in zone k. The operation time of the relay T_{ik} is given by

$$T_{ik} = TDS_i \left(\frac{A}{(\frac{I_{ik}}{I_{pi}})^p - 1} + B \right), \tag{B.2}$$

where I_{ik} is the fault current passing through the relay, and A, B, and p vary according to the relay type used as shown in Table B.1 [43].

Table B.1: Model A type CO induction relay.

	Moderately Inverse	Very Inverse	Extremely inverse
A	0.047	18.92	28.08
B	0.183	0.492	0.130
p	0.02	2.00	2.00

When formulating the objective function, not knowing the values of the pickup current, I_{pi}, introduces nonlinearity to Equation B.2. Therefore, in LP the pickup current values are assumed, and Equation B.2 is simplified into

$$T_{ik} = a_i \times TDS_i, \tag{B.3}$$

where a_i is a constant value that varies from one relay to another depending on the pickup current value selected [20, 44].

In linear optimization, constraints relate the operation times of the primary and backup relays. They ensure relays are properly coordinated by maintaining a minimum coordination time. The coordination time prevents a backup relay from taking an action before the operation of the primary relay. The coordination time constraint equation is given by

$$T_{nk} - T_{ik} \geq \Delta T, \tag{B.4}$$

where T_{nk} is the operation time of the first backup relay for relay R_i in zone k, and ΔT is the coordination time between the primary and backup relays.

Finally, boundaries are set to limit the TDS values and pickup currents. Boundary constraints are given by

$$TDS_{imin} \leq TDS_i \leq TDS_{imax}, \tag{B.5}$$

and

$$I_{pimin} \leq I_{pi} \leq I_{pimax}. \tag{B.6}$$

The pickup current's lower limit is set equal to the maximum load current after being multiplied by 1.3. The upper limit is set equal to the minimum fault current at the far end of the faulted bus [45].

Appendix C

Negative Sequence Impedance Directional Element

The power distribution system becomes non-radial when DGs are connected. During a fault, current contribution will be from all the connected sources. Overcurrent relays should detect the direction of the fault current. Several schemes exist to detect fault direction such as voltage polarization, Artificial Neural Networks (ANN), and negative sequence impedance. Voltage polarization becomes unreliable when the fault is too close to the relay because the relay is almost grounded [46]. On the other hand, ANN can be provide several advantages when used for fault detection such as robustness, speed, and generalization capability [47]. But ANNs are black boxes and there is no information on how the solution is obtained. Also, there is no theory to specify the optimum structure of the ANN, which is determined through trial-and-error and experience [48].

In the proposed adaptive protection system, the direction of the fault is determined using a negative sequence impedance directional element. Negative sequence is one of the three symmetrical components used in fault analysis. It simplifies the process of calculating voltages and currents during a fault condition. Negative sequence component is a measure of the amount of unbalance in a power system [40]. Negative sequence impedance (Z_2) is determined by calculating the negative component of the voltage (V_2) and the current (I_2) during a fault, and it is given by

$$Z_2 = \frac{V_2}{I_2}. \tag{C.1}$$

Moreover, the negative components of the voltage and current are determined by first using FFT to obtain the fundamental frequency component of the measured current and voltage at the relay location. Then, the transformation matrix, given by

$$\begin{bmatrix} 1 & 1 & 1 \\ 1 & a & a^2 \\ 1 & a^2 & a \end{bmatrix}, \tag{C.2}$$

is used to obtain V_2 and I_2.

During a forward fault the negative sequence current leads the negative sequence voltage, which causes the negative sequence impedance to be negative. For a reverse fault, the opposite occurs where the negative sequence current is 180^{o} out-of-phase compared to the negative sequence current for a forward fault, this causes the negative sequence impedance to be positive [40].

Vita

Mohamad Youssef Sulaiman was born in 1989 in Abu Dhabi, United Arab Emirates. He received his Bachelor's degree with magna cum laude in Electrical Engineering from the American University of Sharjah in 2010. In 2010, he joined the Electrical Engineering master's program in the American University of Sharjah as a graduate teaching assistant. He was awarded the Master of Science degree in Electrical Engineering in 2012. During his master's study, he co-authored one paper to be presented in an international conference. His research interests are in power protection, power distribution, renewable energy, and smart grids.